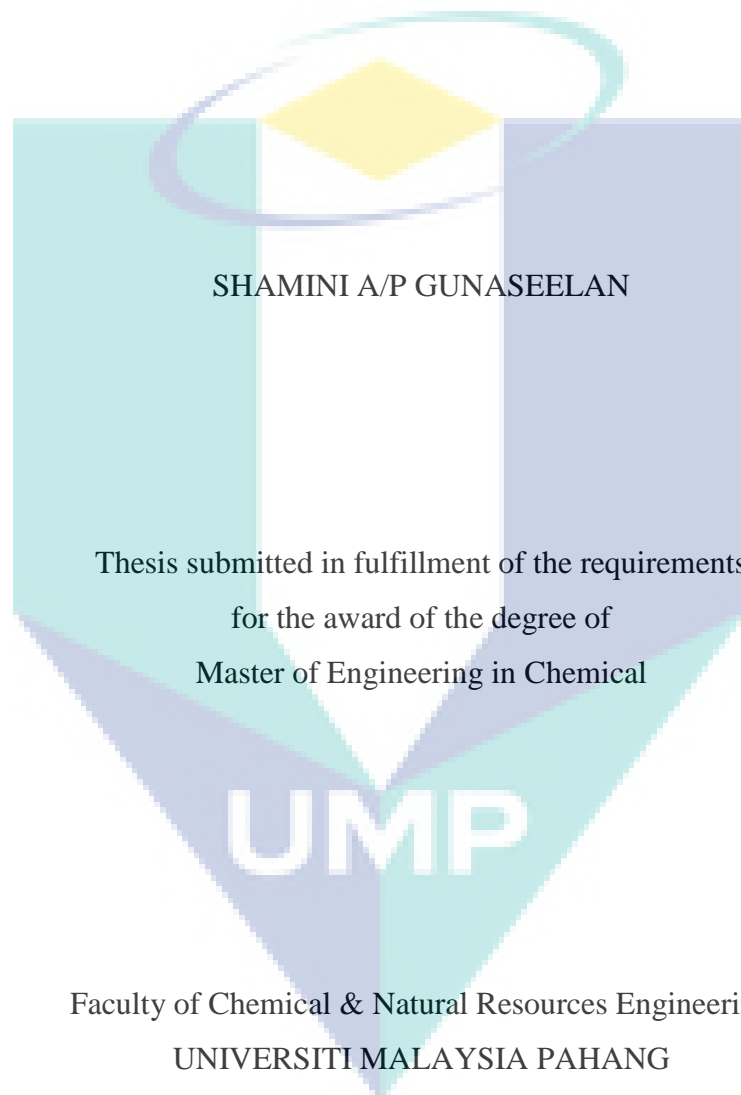


BARRIER, THERMAL AND MECHANICAL PROPERTIES OF  
POLYURETHANE-MODIFIED CLAY NANOCOMPOSITES FOR THERMAL  
INSULATION MATERIAL



SHAMINI A/P GUNASEELAN

Thesis submitted in fulfillment of the requirements  
for the award of the degree of  
Master of Engineering in Chemical

UMP

Faculty of Chemical & Natural Resources Engineering  
UNIVERSITI MALAYSIA PAHANG

SEPTEMBER 2014

**THESIS CONFIDENTIAL STATUS****UNIVERSITI MALAYSIA PAHANG****DECLARATION OF THESIS AND COPYRIGHT**

Author's full name : SHAMINI A/P GUNASEELAN

Date of birth : 28<sup>TH</sup> AUGUST 1988

Title : BARRIER, THERMAL AND MECHANICAL  
PROPERTIES OF POLYURETHANE-MODIFIED  
CLAY NANOCOMPOSITES FOR THERMAL  
INSULATION MATERIAL

Academic Session : SEMESTER 2 SESSION 2013/2014

I declare that this thesis is classified as :

**CONFIDENTIAL** (Contains confidential information under the Official Secret Act 1972)\*

**RESTRICTED** (Contains restricted information as specified by the organization where research was done)\*

**OPEN ACCESS** I agree that my thesis to be published as online open access (Full text)

I acknowledge that Universiti Malaysia Pahang reserve the right as follows:

1. The thesis is the Property of Universiti Malaysia Pahang
2. The library of Universiti Malaysia Pahang has the right to make copies for the purpose of research only.
3. The library has the right to make copies of the thesis for academic exchange.

Certified By:

\_\_\_\_\_  
(Student's Signature)

Shamini A/P Gunaseelan

Date: 02<sup>nd</sup> September 2014

\_\_\_\_\_  
(Signature of Supervisor)

Dr. Kamal Bin Yusoh

Date: 02<sup>nd</sup> September 2014

### SUPERVISOR'S DECLARATION

I hereby declare that I have checked this thesis and in my opinion, this thesis is adequate in terms of scope and quality for the award of the degree of Master of Engineering in Chemical.

Signature :  
Name of Supervisor : DR KAMAL BIN YUSOH  
Position : SENIOR LECTURER OF FACULTY OF CHEMICAL AND  
NATURAL RESOURCES ENGINEERING, UMP  
Date : 02<sup>ND</sup> SEPTEMBER 2014



## STUDENT'S DECLARATION

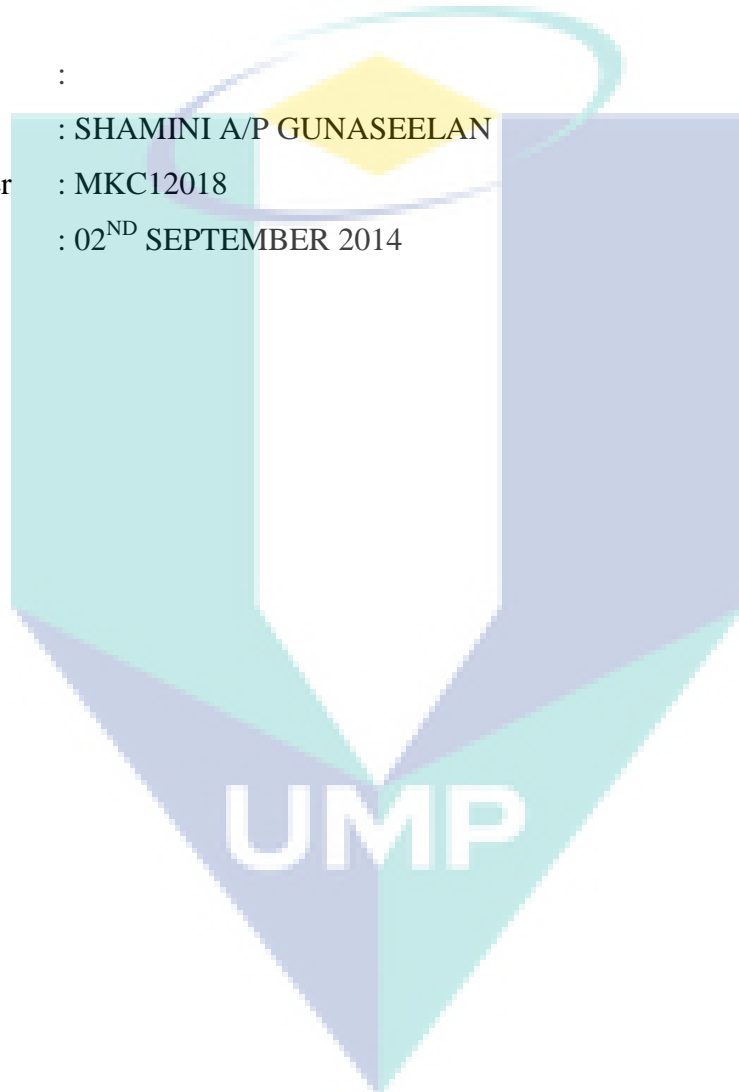
I hereby declare that the work in this thesis is my own except for quotations and summaries which have been duly acknowledged. This thesis has not been accepted for any degree and is not concurrently submitted for award of other degree.

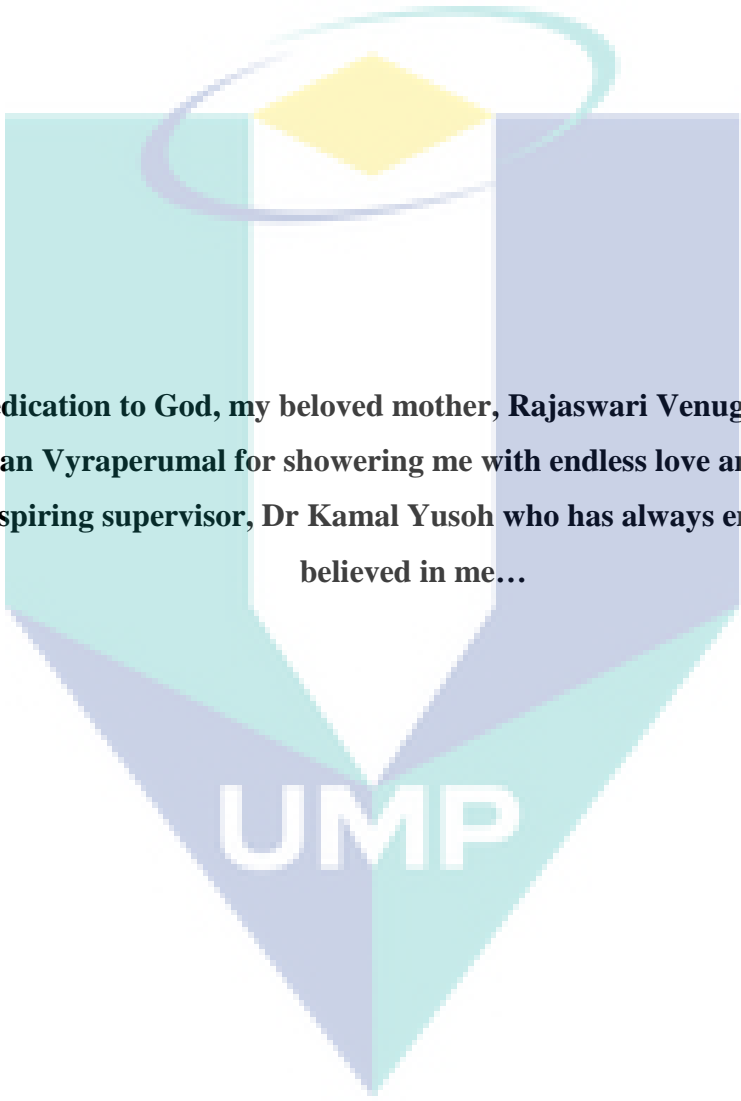
Signature :

Name : SHAMINI A/P GUNASEELAN

ID Number : MKC12018

Date : 02<sup>ND</sup> SEPTEMBER 2014





**Special dedication to God, my beloved mother, Rajaswari Venugopal and father, Gunaseelan Vyraperumal for showering me with endless love and support, and to my inspiring supervisor, Dr Kamal Yusoh who has always encouraged and believed in me...**

## ACKNOWLEDGMENTS

I am grateful and would like to extend my sincerest gratitude to my supervisor, Dr Kamal bin Yusoh for his continuous encouragement and constant support in making this research possible. It was his endless faith and believes in me that motivated me in completing this research. I truly appreciate his consistent support, invaluable guidance and incipient ideas from the first day of my post graduate life to these concluding moments. I am truly grateful and sincerely thank him for all the time spent in correcting my mistakes and mentoring me throughout this path.

My sincere thanks to all my team mates in the research group and the staffs of the Faculty of Chemical and Natural Resources Engineering (FKKSA) lab, Institute of Postgraduate Studies, and to all whom helped me in many ways and making this research a successful one. I would also like to extend my gratitude to Universiti Malaysia Pahang for the research grants, RDU1203109 and RDU130341 that enabled a smooth flow of the experimental works

I acknowledge my sincere indebtedness and gratitude to my parents for their endless love and sacrifice throughout my life. I am truly grateful for their sacrifices, patience and continuous faith in me. It was their devotion that became my source of strength and motivation. Special thanks to my family members and friends whom supported me throughout this work.



UMP

## ABSTRACT

In this thesis, the effect of modification through transition metal ions (TMI) on montmorillonite (MMT) clay that was incorporated into thermoplastic polyurethane (PU) was discussed. The TMI modification was intended to achieve a good dispersion of the clay into PU with fewer agglomerates. The modification of the MMT clay was carried out using Copper (II) Chloride and Iron (III) Chloride. The fabrication of the nanocomposites was done via solution intercalation method by employing chloroform as the solvent. The clay content was varied at three different clay loadings (1 to 3 weight percentage). The existences of the TMIs on the modified clay were confirmed through Inductive Couple Plasma Mass Spectrometry (ICP-MS) whereas its morphological structure was tested through Field Emission Scanning Electron Microscope (FESEM) and X-Ray Diffraction (XRD). The morphology of PU-MMT nanocomposites was determined through Fourier Transform Infrared Spectroscopy (FTIR), Scanning Electron Microscope (SEM), XRD and FESEM. The mechanical properties of the nanocomposites were studied through its tensile stress and elongation at break whereas its thermal properties were analysed using Thermogravimetric Analysis (TGA), Differential Scanning Calorimetry (DSC) and thermal conduction. Gas and water permeation through the nanocomposites was employed to investigate the nanocomposite's barrier properties. The modification process was proved successful as high amount of copper and iron ions were detected in the ICP-MS and even distribution of the clay was obtained in FESEM. XRD data with higher d-spacing values was obtained for PU with modified clay which suggests that a good intercalated structure has been achieved. SEM micrographs illustrated lesser agglomerates in PU with modified clay nanocomposites due to the TMI modification that enables an even distribution of the clay into PU. The homogeneous dispersion of the clay strengthened the structure of PU which led to a remarkable improvement in its mechanical properties. The highest increase in tensile stress was obtained in 2% PU-MMT Cu which showed 148% hike in its 1% and 3% clay loading. The thermal stability was also improved in the modified nanocomposites due to its higher thermal degradation temperature however there were no significant effect of the clay on the melting temperature of the nanocomposites. Thermal conductivity of the PU nanocomposites decreased with increasing clay loading which makes it a suitable thermal insulation material. Both the gas and water permeability decreased in PU with modified clay nanocomposites due to the formation of the tortuous path in its matrix. The highest significant decrease in the gas permeation analysis amounted to 68% in 3% PU-MMT Fe and 40 times decrement in water permeation coefficients were obtained in 1% PU-MMT Fe. The results obtained showed that the incorporation of modified clay into PU has brought significant improvements in its properties.

## ABSTRAK

Dalam tesis ini, kesan pengubahsuaian melalui ion logam peralihan (TMI) pada montmorillonit (MMT) yang telah dimasukkan ke dalam poliuretana termoplastik (PU) telah dibincangkan. Pengubahsuaian TMI bertujuan untuk mencapai penyerakan MMT yang menyeluruh ke dalam PU. Pengubahsuaian MMT telah dijalankan dengan menggunakan kuprum (II) klorida dan ferum (III) klorida. Fabrikasi nanokomposit telah dilakukan melalui kaedah interkalasi dengan menggunakan kloroform sebagai pelarut. Kandungan MMT telah diubah dalam tiga jenis pembebanan yang berbeza (1 hingga 3 peratus). Kewujudan TMIs di struktur MMT yang diubah suai telah disahkan melalui Induktif Plasma Mass Spektrometri (ICP-MS) manakala struktur morfologinya telah diuji melalui Mikroskop Imbasan Elektron (FESEM) dan X-Ray Belauan (XRD). Morfologi nanokomposit PU-MMT telah ditentukan melalui Spektroskopi inframerah transformasi Fourier (FTIR), Mikroskop Imbasan Elektron (SEM), XRD dan FESEM. Sifat-sifat mekanik nanokomposit telah dikaji melalui tekanan tegangan dan pemanjangan pada takat putus manakala sifat haba dianalisis dengan menggunakan analisis Termogravimetri (TGA), Kalorimeter Pengimbasan Perbezaan (DSC) dan pengaliran haba. Resapan gas dan air melalui nanokomposit telah digunakan untuk menyiasat ciri-ciri kebolehtelapan nanokomposit ini. Proses pengubahsuaian telah terbukti berjaya apabila jumlah kuprum dan ferum yang tinggi dikesan di ICP-MS dan juga penyerakan MMT yang homogen telah diperolehi dalam FESEM. Data XRD dengan nilai-nilai d-jarak yang lebih tinggi telah diperolehi bagi PU-MMT yang diubahsuai menunjukkan bahawa struktur interkalasi yang baik yang telah dicapai. Analisis SEM menunjukkan pengelompokan yang kurang di dalam PU-MMT nanokomposit diubahsuai kerana pengubahsuaian TMI telah membolehkan penyerakan MMT yang lebih teratur ke dalam PU. Komposisi MMT yang lebih homogen telah memantapkan struktur PU yang membawa kepada peningkatan luar biasa dalam sifat mekanikalnya. Peningkatan tertinggi sebanyak 148% dapat dilihat dalam tegangan pada 1% dan 3% muatan MMT di dalam 2% PU-MMT Cu. Kestabilan haba juga telah bertambah baik pada nanokomposit yang diubah suai disebabkan oleh suhu degradasi haba yang lebih tinggi berbanding sampel lain, walaubagaimanapun tidak ada kesan yang ketara pada suhu lebur nanokomposit. Kekonduksian terma daripada nanokomposit PU menurun dengan bebanan MMT yang tinggi di mana ini dapat menjadikan ia sebagai bahan penebat haba yang sesuai. Kedua-dua kebolehtelapan gas dan air menurun dalam PU nanokomposit yang diubahsuai kerana pembentukan laluan rumit dalam matriks itu. Penurunan yang tertinggi dalam analisis resapan gas berjumlah 68% didapati dalam 3% PU-MMT Fe. Keputusan yang diperolehi menunjukkan bahawa serakan tanah liat diubahsuai ke dalam PU telah membawa peningkatan besar yang ketara dalam sifat-sifatnya.



## TABLE OF CONTENTS

	<b>Page</b>
<b>SUPERVISOR'S DECLARATION</b>	iii
<b>STUDENT'S DECLARATION</b>	iv
<b>DEDICATIONS</b>	v
<b>ACKNOWLEDGMENTS</b>	vi
<b>ABSTRACT</b>	vii
<b>ABSTRAK</b>	viii
<b>TABLE OF CONTENTS</b>	ix
<b>LIST OF TABLES</b>	xiv
<b>LIST OF FIGURES</b>	xvi
<b>LIST OF SYMBOLS</b>	xx
<b>LIST OF ABBREVIATIONS</b>	xxi
<b>CHAPTER 1                    INTRODUCTION</b>	
1.1    Background of Study	1
1.2    Problem Statement	5
1.3    Research Objectives	6
1.4    Scope of Study	7
1.5    Significance of Research	8
1.6    Summary	10

**CHAPTER 2      LITERATURE REVIEW**

2.1	Introduction	11
2.2	Polyurethane (PU)	13
2.2.1	Synthesis of Polyurethane	14
2.2.2	Properties of Polyurethane	19
2.2.3	Applications of Polyurethane	22
2.3	Nanofillers	23
2.3.1	Layered Silicates	23
2.3.2	Organically Modified Layered Silicates	26
2.3.3	Transition Metal Ions (TMI) Modified Layered Silicates	27
2.4	Polymer Nanocomposites	28
2.4.1	Structure of Polymer Layered Silicates	29
2.4.2	Preparation of Polymer Nanocomposites	32
2.5	Morphological Study of Polymer Nanocomposites	37
2.5.1	Scanning Electron Microscope (SEM)	37
2.5.2	Field Emission Scanning Electron Microscope (FESEM)	39
2.5.3	Transmission Electron Microscope (TEM)	40
2.5.4	Fourier Transform Infrared Spectroscopy (FTIR)	42
2.5.5	X-Ray Diffraction (XRD)	43
2.6	Testing And Analysis of Polymer Layered Silicates Nanocomposites (PLSN)	46
2.6.1	Mechanical Properties of PLSN	46
2.6.2	Thermal Characterization of PLSN	47
2.6.3	Permeability Analysis of PLSN	51

**CHAPTER 3 RESEARCH METHODOLOGY**

3.1	Introduction	53
3.2	Materials	53
3.2.1	Polyurethane (PU)	54
3.2.2	Cloisite Na <sup>+</sup>	55
3.2.3	Copper (II) chloride and Iron (III) chloride	56
3.2.4	Methanol	57
3.2.5	Chloroform	58
3.3	MMT Clay Modification Using Transition Metal Ions	59
3.3.1	Pre-treatment of MMT Clay	59
3.3.2	Preparation of TMI's solution and Modification Phase	59
3.4	Characterization of the Modified MMT Clay	61
3.4.1	Inductively Coupled Plasma Mass Spectrometry	61
3.5	Preparation of PU-MMT Nanocomposites	62
3.6	Characterization of Polyurethane Nanocomposite	63
3.6.1	Fourier Transform Infrared (FTIR)	63
3.6.2	X-Ray Diffraction (XRD)	64
3.6.3	Scanning Electron Microscopy (SEM)	66
3.6.4	Field Emission Scanning Electron Microscopy (FESEM)	68
3.7	Properties of Polymer Nanocomposites	70
3.7.1	Mechanical Testing	70
3.7.2	Thermal Analysis	72
3.8	Permeability Studies	76
3.8.1	Gas Permeability	76
3.8.2	Water Permeability	78

**CHAPTER 4 RESULTS AND DISCUSSION**

4.1	Introduction	79
4.2	Modification of MMT Clay	79
4.2.1	Mechanism of Transition Metal Ion (TMI) Modification	79
4.2.2	Characterization of Modified MMT Clay	82
4.3	Morphologies Studies of PU Nanocomposites	86
4.3.1	Fourier Transform Infrared Spectroscopy (FTIR)	86
4.3.2	Scanning Electron Microscope (SEM)	90
4.3.3	Field Emission Scanning Electron Microscopy (FESEM)	97
4.3.4	X-Ray Diffraction (XRD)	99
4.4	Mechanical Properties	104
4.4.1	Tensile Strength	104
4.4.1	Elongation at Break (EB)	107
4.5	Permeability Properties	109
4.5.1	Permeability	109
4.5.2	Gas Permeability Analysis	109
4.5.3	Water Permeability Analysis	114
4.6	Thermal Properties	117
4.6.1	Thermal Gravimetric Analysis (TGA)	117
4.6.2	Differential Scanning Calorimetry (DSC)	124
4.6.3	Thermal Conductivity	127
4.7	Summary	130

**CHAPTER 5 CONCLUSION AND RECOMMENDATIONS**

5.1	Conclusions	132
5.2	Recommendations for Future Work	134

<b>REFERENCES</b>	135
-------------------	-----

<b>APPENDICES</b>	149
-------------------	-----

A	Modification of MMT Clay And Fabrication of PU Nanocomposites	149
B	Mechanical Properties	163
C	Modification Method and Fabrication of PU Nanocomposites	164
D	List of Publications	168

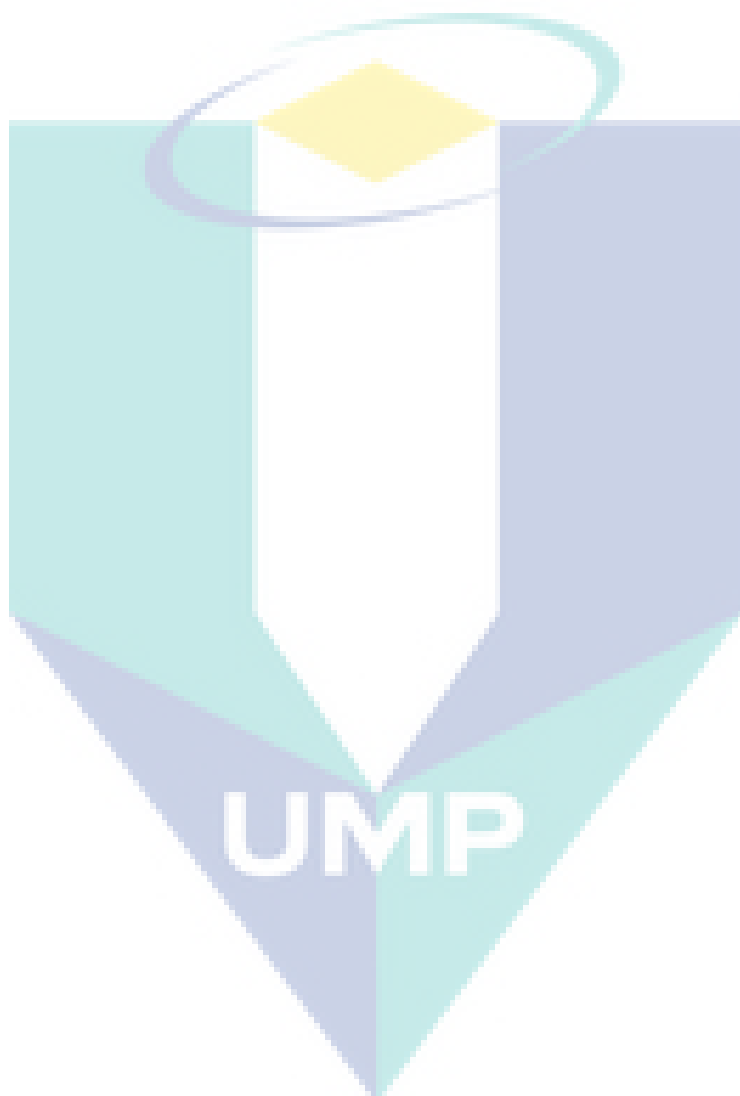


UMP

## LIST OF TABLES

<b>Table No.</b>	<b>Title</b>	<b>Page</b>
2.1	Example of diamine chain extenders	17
2.2	Example of diol chain extenders	18
2.3	Mechanical properties of conventional TPU	20
2.4	Thermal properties of conventional TPU	20
2.5	Chemical formula and characteristic parameter of commonly used 2:1 phyllosilicate	24
3.1	Physical and chemical properties of PU	54
3.2	Properties of Cloisite Na <sup>+</sup>	55
3.3	Physical and chemical properties of Copper (II) Chloride	56
3.4	Physical and chemical properties of Iron (III) Chloride	56
3.5	Physical and chemical properties of Methanol	57
3.6	Properties of Chloroform	58
3.7	TMI Salts used in the modification Process	59
3.8	Weight percentage PU-MMT prepared	62
3.9	Parameters used in SEM analysis	66
4.1	ICP-MS data	82
4.2	Tentative FTIR band assignments of PU nanocomposites	88
4.3	Assignment of the main FT-IR peaks of PU nanocomposites and their comparison with data in literature	89
4.4	The value of angular spacing, $d$ and reflection angle, $2\theta$ of the polyurethane nanocomposites	101
4.5	Effect of clay on tensile stress	104
4.6	Effect of clay on elongation at break	107
4.7	Permeability coefficients of polymer clay nanocomposites	110
4.8	Time recorded for water permeability analysis of PLSN	114
4.9	Flux values of PU nanocomposites	115
4.10	Water permeability coefficients	115
4.11	Thermogravimetric properties of polyurethane and its nanocomposites with different clay loading (0-3wt %)	121

4.12	Characteristic temperatures of PU nanocomposites' melting curve	124
4.13	Thermal conductivity data of polyurethane nanocomposites	128



## LIST OF FIGURES

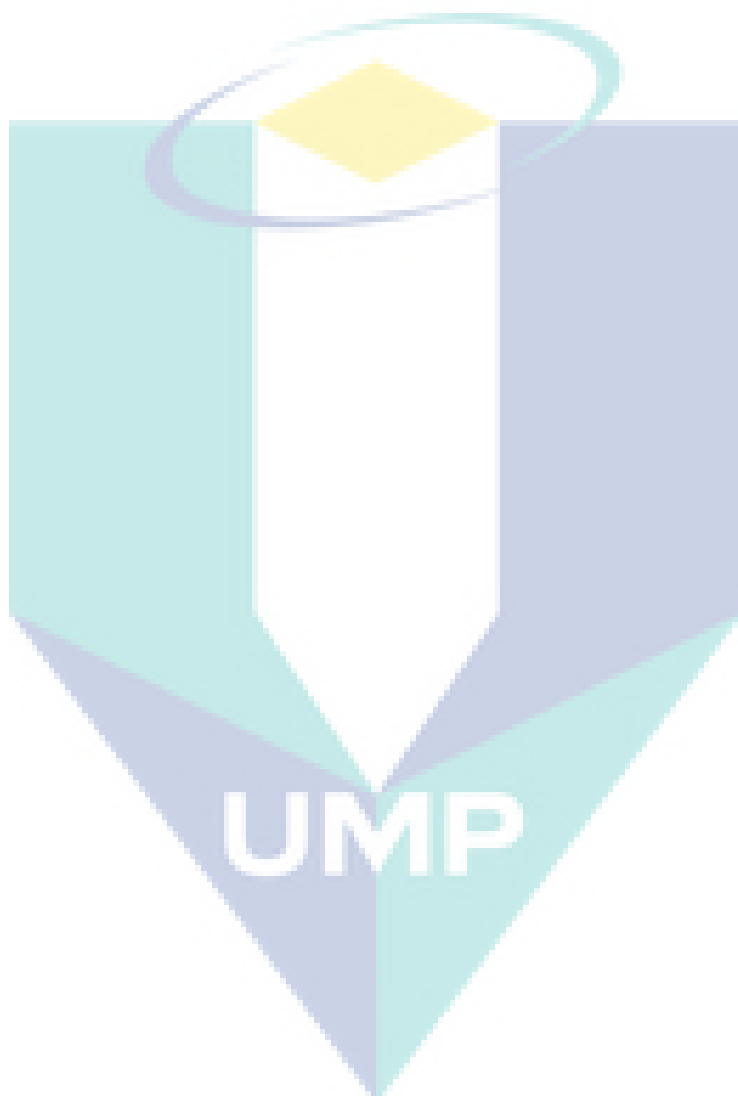
<b>Figure No.</b>	<b>Title</b>	<b>Page</b>
2.1	Structure of PU	13
2.2	Schematic of the PUs two-step polymerization synthesis route based on diol chain extenders	15
2.3	Chemical structure of 2,4-TDI, 2,6-TDI and 4,4'-MDI	15
2.4	Hard and soft segment domains of PU	19
2.5	SEM images of the porous structure of PU	21
2.6	Structure of 2:1 phyllosilicate	24
2.7	Chemical structure of montmorillonite nanoclays	25
2.8	Schematic diagram of an ion exchange reaction	26
2.9	Illustration of different types of polymer layered silicate composites	30
2.10	TEM images of exfoliated and intercalated PU-MMT	31
2.11	Schematic representation of PLS obtained by intercalation from solution	33
2.12	The melt intercalation process	34
2.13	Synthesis route of Pu/Go/Ep nanocomposites	36
2.14	(a) Scanning electron micrograph (b) Elemental mapping of Si for PU-MMT nanocomposites	38
2.15	FESEM micrographs of PU and PU-Ag nanocomposites	39
2.16	TEM of PU clay nanocomposites	40
2.17	Transmission electron micrographs of cross-section views of PU nanocomposites (a) PU/MMT-Oh (b) PU/MMT-Tin	41
2.18	XRD patterns of: (a) Phase separated microcomposite (b) Intercalated nanocomposite and (c) Exfoliated nanocomposite of modified Fluorohectorite in HDPE, PS and silicone rubber	44
2.19	XRD of 5% MMT-Oh/PU nanocomposites prepared by different mixing procedures	45
2.20	DSC experimental arrangement	47
2.21	TGA thermogram of PU, PU-Il-Mt (A) and PU-Qas-Mt (B)	50



2.22	Permeation in polymer composites (a) Conventional composite (b) Formation of tortuous path in layered silicates	51
3.1	Structure of PU	54
3.2	ICP-MS Equipment	61
3.3	FTIR Equipment	64
3.4	XRD Equipment	65
3.5	Zeiss Evo 50 scanning electron microscope	67
3.6	Baltec SCD 005 Sputter Coater	67
3.7	Joel Fesem JSM-7800f Equipment	69
3.8	Dogbone sample	71
3.9	Instron Universal Testing Machine	71
3.10	TGA Q500 Equipment	73
3.11	DSC Q100 Equipment	74
3.12	KD2 Pro Thermal Conductivity Analyzer	75
3.13	Schematic design of permeation apparatus	77
3.14	Membrane separation unit	77
3.15	Water permeability testing system	78
4.1	Stacks of platelet that are tightly held together	80
4.2	TMI modification of MMT clay via (a) $\text{Cu}^{2+}$ (b) $\text{Fe}^{3+}$	80
4.3	Mechanism of the modification process	81
4.4(a)	FESEM micrograph of MMT clay	83
4.4(b)	FESEM micrograph of MMT Cu	84
4.4(c)	FESEM micrograph of MMT Fe	84
4.5	XRD patterns of pristine MMT and modified MMT	85
4.6	FTIR Spectra Of 1% PU, PU-MMT, PU-MMT Cu & PU-MMT Fe	86
4.7	FTIR Spectra Of 2% PU, PU-MMT, PU-MMT Cu & PU-MMT Fe	87
4.8	FTIR Spectra Of 3% PU, PU-MMT, PU-MMT Cu & PU-MMT Fe	87
4.9	SEM micrograph of PU	91
4.10	SEM micrograph of 1% PU-MMT	91
4.11	SEM micrograph of 2% PU-MMT	92

4.12	SEM micrograph of 3% PU-MMT	92
4.13	SEM micrograph of 1% PU-MMT Cu	94
4.14	SEM micrograph of 2% PU-MMT Cu	94
4.15	SEM micrograph of 3% PU-MMT Cu	95
4.16	SEM micrograph of 1% PU-MMT Fe	95
4.17	SEM micrograph of 2% PU-MMT Fe	96
4.18	SEM micrograph of 3% PU-MMT Cu	96
4.19	FESEM micrographs of (a) PU (b) 2% PU-MMT (c) 2% PU-MMT Cu (d) 2% PU-MMT Fe	98
4.20(a)	XRD diffractograms of 1% polyurethane nanocomposites	100
4.20(b)	XRD diffractograms of 2% polyurethane nanocomposites	100
4.20(c)	XRD diffractograms of 3% polyurethane nanocomposites	101
4.21	Tensile stress of polyurethane montmorillonite nanocomposite	105
4.22	Elongation at break of polyurethane montmorillonite nanocomposite	108
4.23	Permeability coefficients of PU-Clay Nanocomposites In nitrogen gas	111
4.24	Permeability coefficients of PU-Clay Nanocomposites In oxygen gas	111
4.25	Tortuous path in layered silicate nanocomposites; $d_1$ is the actual distance travelled in the absence of clay and $d_2$ is the tortuous path length with the presence of clay	112
4.26(a)	Thermogravimetric curves of pure PU and 1% modified PU	118
4.26(b)	Thermogravimetric curves of pure PU and 2% modified PU nanocomposites	118
4.26(c)	Thermogravimetric curves of pure PU and 3% modified PU nanocomposites	119
4.27(a)	Derivative thermal gravimetric (DTG) of pure PU and modified 1% PU nanocomposites	119
4.27(b)	Derivative thermal gravimetric (DTG) of pure PU and modified 2% PU nanocomposites	120

4.27(c)	Derivative thermal gravimetric (DTG) of pure PU and modified 3% PU nanocomposites	120
4.28	Heating curve for 1% clay loading of PU nanocomposites (melting transitions)	125
4.29	Thermal conductivity of polyurethane nanocomposites	126



**LIST OF SYMBOLS**

$\lambda$	Wavelength
$\theta$	Angle
$^{\circ}\text{C}$	Degree Celcius
$\varepsilon$	Elongation
%	Percentage
$J_{st}$	Flux
$a$	Water activity
$T_d$	Degradation temperature
$T_{pm}$	Melting temperature peak
$q$	Heat Flow
$t$	Interface Thickness
$A$	Area
$\Delta$	difference

The logo for UMP (Universidade do Minho) is a large, downward-pointing arrow shape. It is composed of four triangular sections meeting at a central point. The top-left and bottom-right sections are light blue, while the top-right and bottom-left sections are a slightly darker shade of blue. The letters 'UMP' are printed in a bold, white, sans-serif font across the center of the arrow.

UMP

**LIST OF ABBREVIATIONS**

PU	Polyurethane
HS	Hard Segment
SS	Soft Segment
MMT	Montmorillonite
PLSN	Polymer layered silicate nanocomposites
PNC	Polymer nanocomposites
TMI	Transition Metal Ions
Cu	Copper
Fe	Iron
LS	Layered silicates
ICP-MS	Inductively Coupled Plasma Mass Spectrometry
XRD	X-Ray Diffraction
SEM	Scanning Electron Microscope
FESEM	Field Emission Scanning Electron Microscope
TGA	Thermal Gravimetric Analysis
DSC	Differential Scanning Calorimetry
FTIR	Fourier Transform Infrared Spectroscopy

The logo for UMP (Universitas Muhammadiyah Purwokerto) is a large, downward-pointing triangle. It is divided into four quadrants by a vertical and a horizontal line. The top-left and bottom-right quadrants are light blue, while the top-right and bottom-left quadrants are light purple. The letters 'UMP' are written in a bold, white, sans-serif font across the center of the triangle.

UMP

## CHAPTER 1

### INTRODUCTION

#### 1.1 BACKGROUND OF STUDY

The development of polymer clay nanocomposites began as early as 1930s by a MIT professor, E.A. Hauser who worked on latex systems. The evolution of the technology was continued by Jordan and colleagues, who produced highly dispersible organo bentonites in 1940s, however the field only began to gain wide attention with a research progressed by Toyota Motor Co when they reported unusual property improvements in nylon-6/montmorillonite nanocomposites (Kim et al., 2003). Resurgence in interest in polymer nanocomposites has then started to begin due to the property improvements. Polymer nanocomposites consist of a filler reinforcement material, usually found in a nanometer scale size dispersed in a polymer matrix and often this reinforcement creates a new class of polymer composite with improved physical and functional properties (Usuki et al., 2005). The fillers can be one dimensional; nanotubes and fibers, two dimensional; clay and graphite or three dimensional; spherical particles (Ray and Bousmina, 2006). It can be noted in general that polymer nanocomposites exhibit improved polymer properties and their use may invent certain new properties that cannot be derived from its pristine state (Hussain et al., 2006).

The synthesis of polymer nanocomposites is seen as a great scientific and industrial importance due to their improved properties. The synthesis of polymer nanocomposites such as polymer/clay nanocomposites (PCN) is seen as an opportunity to tailor its properties for a wide range of applications and has expanded into most of the engineering polymers such as polycarbonate, polyurethane, polystyrene, polyvinylchloride and polylactide. A review by Reddy (2011) reported that currently the application of polymer nanocomposites in the engineering world has become state of

the art due to the improved mechanical, thermal, conductivity and barrier properties of the polymer composites. The enhancement in properties of the polymer is obtained through the complete exfoliation of the fillers in its polymer matrix and amongst the many types of fillers available, clay minerals are usually the preferred choice as a filler as it is naturally abundant, environmentally friendly, chemically stable and inexpensive (Tjong, 2006).

The improvement in the mechanical properties was first reported by Wang and Pinnavaia (1998) whom reported a more than 100% increase in modulus, strength and extensibility in PCN. Improvements in mechanical properties of nylon 6-clay nanocomposites were also reported by Fornes et al. (2002) whereby they obtained a twofold increase in the Young's modulus with an addition of 3 wt% clay. Hasegawa et al. (2003) also reported a hike of 28% and 14% in tensile and flexural moduli with the incorporation of only 1.6 wt% clay. Polymer nanocomposites have also been reported to portray excellent enhancements in its thermal properties. According to a study conducted by Usuki et al. (1993), a loading of 4.2 wt% clay showed an increase of 80°C in the heat distortion temperature of nylon 6-clay nanocomposite compared to the pristine polymer. According to Saha et al. (2008), the decomposition of nanophased polyurethane foams shifted to a high temperature with the infusion of nanoparticles. This proves that the incorporation of nanoparticles into the foam offers a stabilizing effect against decomposition and creates protection against thermal degradation.

Apart from the improvements in the mechanical and thermal behavior, remarkable advancement was also seen in the barrier properties of polymer nanocomposites. The platelet structure of the layered silicates is seen to improve the barrier properties according to a tortuous path model whereby great significance in reducing the diffusivity of gases through nanocomposites are seen with only small addition of platelet particles. Yano et al. (1997) investigated in their study and found that at 2 wt% of clay, the relative permeability coefficient of polyamide-clay hybrid films decreases. Apart from that, in a study by Osman et al. (2003), the oxygen transmission rate asymptotically decreased with increasing aluminosilicate volume fraction whereby 30% reduction was achieved at 3 vol%.

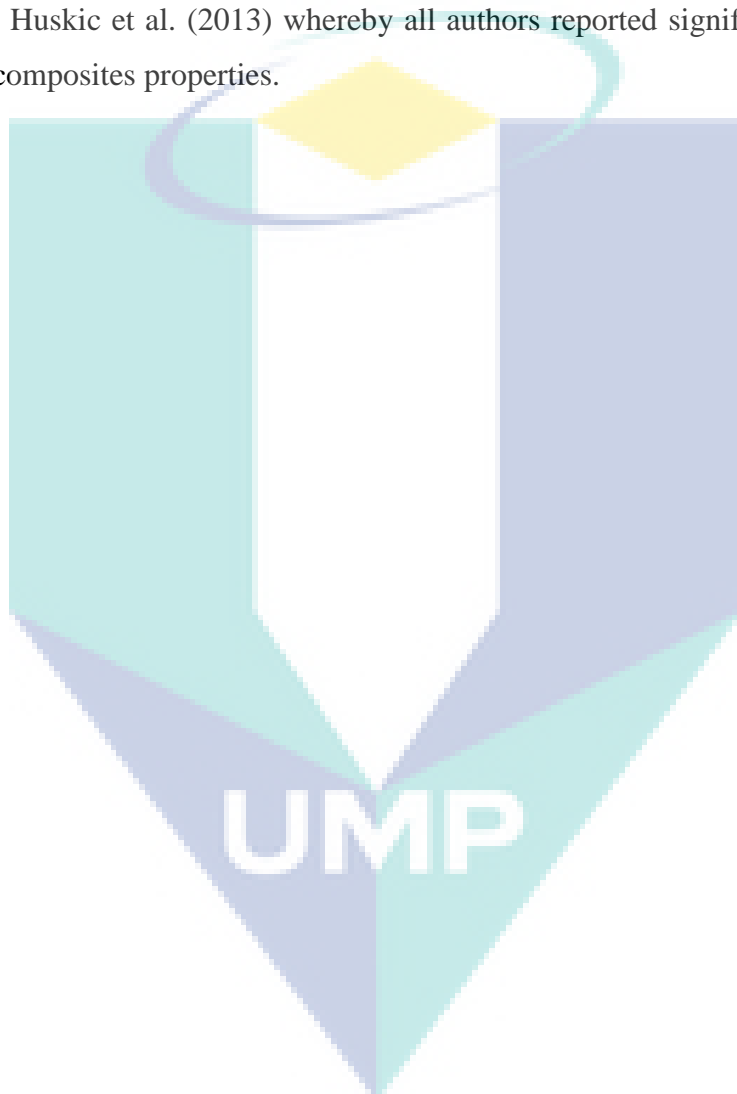
The field of polymer composites has been expanded into almost all types of polymer. One of the most versatile polymers that are being researched is polyurethane (PU) due to its wide usage in many fields such as in coatings, composites, roofing materials and as adhesives, however pristine PU is seen to possess insufficient physical and functional properties to accommodate these applications. The incorporation of clay into a polymer could improve its properties according to the desired applications (Wang et al., 2008 and Liu et al., 2006) and the same is applicable to PU. Recently, the application of PU as a thermal insulator was seen to be in the lime light due to the high demand of energy conservation and the importance of heat management. The heat absorption capacity, chemical stability and the ability to form sandwich structures with various facer materials makes PU as a preferred thermal insulation material choice (Demharter, 1998).

Lately, the use of clay based materials as reinforcement fillers for polymers has attracted much scrutiny. There are various techniques applied in preparing the PCNs such as melt intercalation, *in situ* polymerization, and solution intercalation method. It is important to ensure that the techniques applied are suitable with the polymeric material used. This study describes the synthesis of polyurethane/montmorillonite clay nanocomposites (PU-MMT) using solution intercalation technique. Layered silicates (LS) have attained much attention in the past because they can be dispersed in a polymer matrix at the nanometer scale to yield reinforced PCN (Usuki et al., 1993) however the modification of clay is seen as an essential requirement. Several authors such as Singla et al. (2012) and Nawani et al. (2007) have reported the usage of organic cations to modify clay for the preparation of PCNs. As part of this study, the use of transition metal ions (TMI) as a modifier for the montmorillonite clay was studied.

The TMI modification was carried out to change the nature of the clay which is hydrophilic as this particular nature creates poor mixing and interaction with most polymer matrices that are hydrophobic (Olphen, 1977, Giannelis, 1996). Apart from that, the structure of the layered silicate consists of stacks that are held tightly by electrostatic forces and it is crucial for the clay to undergo modification before the preparation of nanocomposites to exfoliate it into single layers. Clay that is not modified would not be effective as it will not be able to interact with the polymer matrix (Singla, 2012). Naturally occurring LS consists of cations that are not strongly bound to the clay



surface and transition metal ions (TMI) are used to exchange the cations present in the clay. This process helps to separate the clay platelets in order for them to be more easily intercalated or exfoliated, and also enables the clay to be more compatible with a wide range of polymer matrix. The TMIs that were chosen in this work was copper (Cu) and iron (Fe) ions due to their catalytic performance. Previous work on polymer clay nanocomposites using organic modifiers were reported by Xie et al. (2001), Davis et al. (2002), and Huskic et al. (2013) whereby all authors reported significant improvement in the nanocomposites properties.



## 1.2 PROBLEM STATEMENT

The study of polyurethane composites has acquired great importance due to its wide applications. One of the most important applications of PU is as a thermal insulation material, however, there are certain drawbacks that need to be rectified in order for it to be durable and effective. In this work, PU is studied as a thermal insulation material. It is important for an insulation material to have good mechanical protections, barrier protections, and its main requirement is that it possesses low thermal conductivity. Generally, an intrinsic property of a thermal insulation material is that it has a porous structure and this porosity allows conduction through it due to the air contained in the small pores (Roymech, 2013).

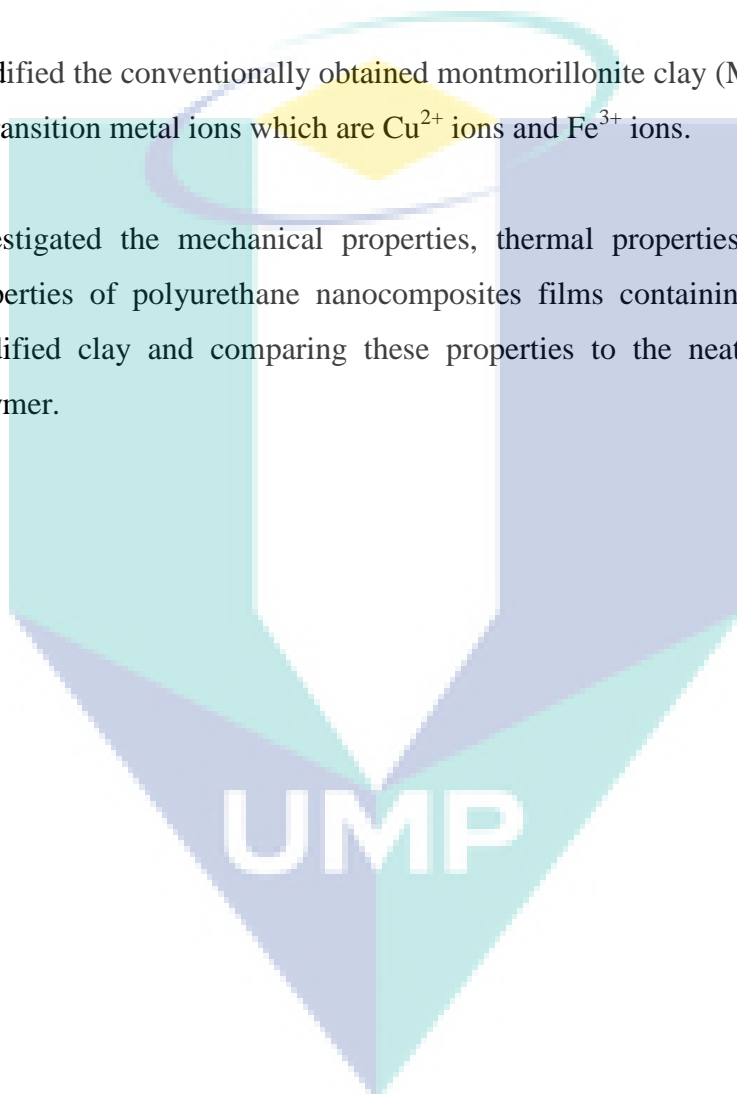
Jiawen et al. (2004) reported in their study that PU has poor thermal stability and poor barrier properties. The barrier properties of PU are meager as compared to other polymers (Osman et al., 2003) due to its porous structure which enables easy transportation of gases and water. They also stated that this may contribute to the poor conduction property of PU. Apart from that, PU has also been reported to possess poor high temperature capabilities due to its a restriction by an upper temperature capability of approximately 175°C and if exposed to higher temperature, it has a tendency to soften and lose its strength (Elder Rubber Company, 2013). Furthermore, PU is also known to have a low sustainability to direct sunlight. It is important for a thermal insulation material to meet certain characteristics such as low thermal conductivity and it also crucial for these materials to be able to maintain it even when they are perforated by external force or objects.

The incorporation of layered silicates into PU often creates a nonhomogeneous dispersion due to the clay's interlayer Van der Waals forces which creates clay agglomerates. The clay agglomerate that appears in the structure of the nanocomposites hinders the property advancement of the polymer thus it is also very important to ensure that the dispersion of the clay platelets into its matrix is achieved successfully.

### 1.3 RESEARCH OBJECTIVES

The objectives of this study were the following:

1. Investigated the use of solution intercalation method for the preparation of polyurethane nanocomposite using pristine and modified  $\text{Na}^+$  montmorillonite clay.
2. Modified the conventionally obtained montmorillonite clay (MMT) by two types of transition metal ions which are  $\text{Cu}^{2+}$  ions and  $\text{Fe}^{3+}$  ions.
3. Investigated the mechanical properties, thermal properties and permeability properties of polyurethane nanocomposites films containing the pristine and modified clay and comparing these properties to the neat properties of the polymer.



## 1.4 SCOPE OF STUDY

A general scope or an experimental framework of this thesis was established by underlining the steps taken to achieve the objectives of the proposed research. Following are the designed scopes that were seen as a guidance and assistance in achieving the research objectives of this work.

1. The preparation of PU-MMT nanocomposites was achieved through solution intercalation method due to the better mixing performance and to avoid the degradation of the PU's structure. The morphology of the obtained nanocomposites lattices and their films will be characterized to investigate whether the synthesis created an intercalated or exfoliated morphology.
2. The modification of the MMT clay was carried out through the transition metal ions which were copper (II) chloride and iron (III) chloride ions. The characterization of the modified clay was executed using inductively coupled plasma mass spectrometry (ICP-MS), x-ray diffraction (XRD) and Field Scanning Electron Microscope (FESEM). During the preparation of PU-MMT nanocomposites, a series of clay content (from 1% to 3%) are varied.
3. The structure of PU-MMT is characterized using (XRD) and visually interpreted through the application of scanning electron microscopy (SEM) and FESEM. The thermal stability of the PU-MMT samples is investigated by using thermo gravimetric analysis (TGA), differential scanning calorimetry (DSC) and thermal conductivity. The mechanical study of the PU-MMT nanocomposites are carried out via Universal Testing Machine whereby the data obtained for its tensile stress and the elongation at break is analyzed. The permeability analyses of the samples were employed through the membrane separation unit for the gases and water permeability unit.

## 1.5 SIGNIFICANCE OF RESEARCH

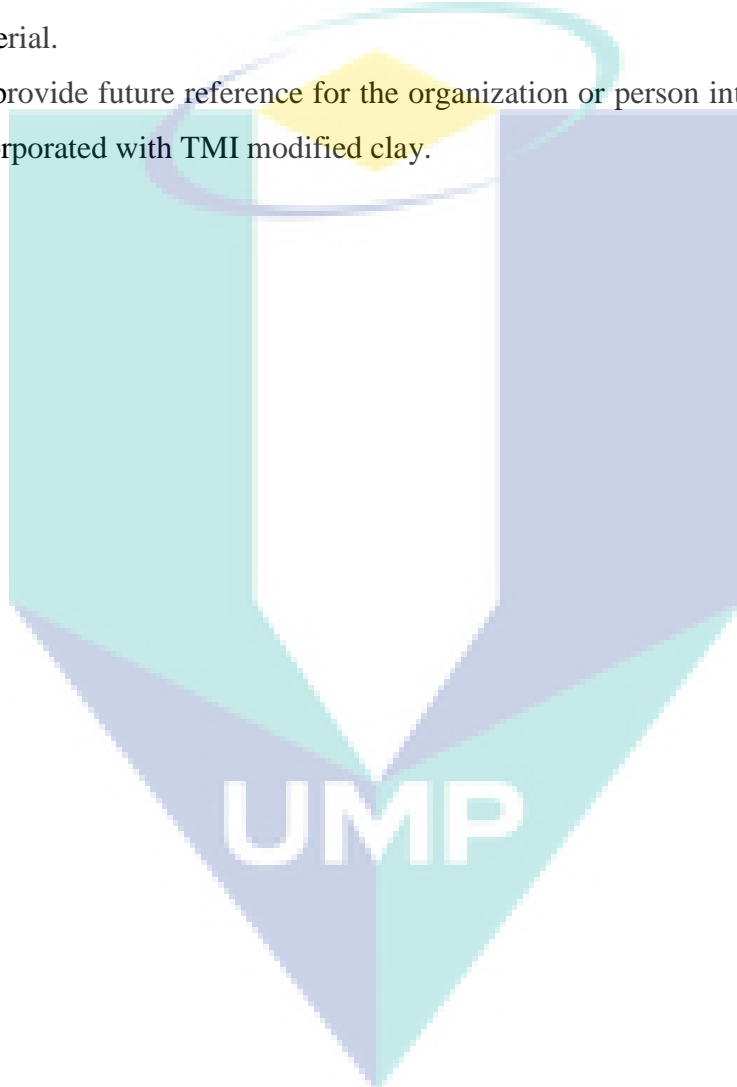
In this research, it was aimed to obtain well dispersed clay into PU to minimize the clay agglomerations and hinder the deterioration of the nanocomposites properties. In order to aid this effort, transition metal ions modification was done on the clay to create a good compatibility with PU and to ensure that a homogeneous dispersion of the clay has been achieved, the preparation of PU-MMT nanocomposite should be executed under certain processing conditions. Solution intercalation was employed in preparing the PU-MMT in order to reduce the risk of thermal degradation as PU is known to have a low melting temperature due to the low glass transition temperature of polyol which is less than 70°C (Rlhudson, 2011).

The study of polymer nanocomposites is an interesting topic which has been studied extensively however to the best of the authors knowledge, there are no reports to date that studied the properties of PU with clay modified with transition metal ions. Although there are reports on the improved properties using MMT clay, the clay used are modified by the supplier and is often classified as Cloisite 10A, 15A, 20A and 30B. In this work, the MMT clay was modified using copper and iron ions before it was incorporated into PU. Properties of the nanocomposites that were studied include mechanical, thermal and barrier. It is to be noted that there are no previous work on the gas and water barrier properties of polyurethane with TMI modified clay nanocomposites. It is presumed that the incorporation of organically modified clay will be able to generate a new class of nanocomposites with improved properties.

This study is to aid industries that are based on insulation materials such as roofing industry. It is anticipated that the PU-MMT will serve as a good insulation material by creating a good heat shield and temperature the environmental temperature variations. According to Stockton (2011), it is also important for the material to withstand the ravages of sun, rain and leakages thus it is expected that the advancement in the thermal, mechanical and barrier properties of this nanocomposites will accommodate to the necessary needs that are required for an insulation material.

Thus, the accumulated result from the research reckoned to be important due to the listed factors below:

1. To establish the effect of transition metal ions (TMI) modification on the clay incorporated into PU.
2. To synthesize PU-MMT nanocomposites with higher mechanical, thermal and permeability stability for industrial's roofing applications as a thermal insulation material.
3. To provide future reference for the organization or person interested in polymer incorporated with TMI modified clay.



## 1.6 SUMMARY

The transition metal ions modification done on the clay is presented as a successful strategy in creating well dispersed and homogeneous polyurethane nanocomposites. The main advantage of this approach is that it could hinder the formation of large clay agglomerates during the solution mixing process. In this research, solution mixing was opted as the intercalation method to avoid the risk of thermal degradation of PU as compared to melt mixing and *in-situ* polymerization. The produced PCN would then be prepared according to the ASTM standards as per required by the respective analysis. The intended morphology studies to be carried out are the x-ray diffraction (XRD), scanning electron microscopy (SEM) and field emission scanning electron microscopy (FESEM). Comparison of the polyurethane clay nanocomposites and the neat polymer are to be carried out in three different testing which are the mechanical testing, thermal testing and permeability analysis. The purpose of this approach is to create a good thermal insulation material for the application in the roofing industry.

The logo for UMP (Universiti Malaysia Perlis) is a large, downward-pointing arrow shape. It is composed of several overlapping geometric shapes in shades of teal, light blue, and yellow. The letters 'UMP' are printed in white, bold, sans-serif font across the bottom of the arrow.

UMP

## CHAPTER 2

### LITERATURE REVIEW

#### 2.1 INTRODUCTION

The recent developments in the nanoscience and nanotechnology field have enabled polymer composites to receive much attention from the scientific research field. The introduction of fillers as additives in polymer systems has resulted in polymer composites exhibiting higher performance in its composites as compared to pristine polymers (Koo et al., 2005). Interests in these materials stem from the fact that there is a unique physical state in the polymer at its silicate-polymer interface. According to Ray et al. (2003), this is due to their demonstrated significant enhancement in physical properties, barrier properties, fire resistance, thermal and environmental stability as well as the rate of biodegradability.

There are three main advantages of nanoscale reinforcement in polymers. The first is the dispersion of the filler particles in the polymer matrix that contributes to the polymer chain's confinement effects whereby this leads to improved mechanical properties of the polymer and the enhancement in the stiffness and strength of the material is attributed to the high aspect ratio and large surface area of the nanofiller particles (Strawhecker and Manias, 2006). The second advantage is the advancement in the thermal stability of the nanocomposites as a result of the intercalation of the polymer chains into the galleries of the nanolayered filler, whereby this is due to the filler particles acting as an insulator between the heat source and the surface area of the polymer (Jianqi and Zhidong, 2006). Finally, the fillers aid in enhancing the barrier properties of the polymers by acting as impermeable obstacles that provides longer and tortuous diffusion paths across the polymer matrix (Okamoto, 2006).



There are various types of nano reinforcement materials such as layered silicates (LS), carbon nanotubes, graphene sheets, and talc however LS carries a particular interest due to the significant changes that they bring in the properties of the polymer at low clay loading which is usually lesser than 5 wt. % (Ray et al., 2003). Moreover, the availability of the clay and the ease of intercalation with a wide range of polymers have brought a great interest in it (Chen and Gong, 2002). The ultimate reason for the improved properties lies in the interfacial interaction between the LS and its matrix. Many types of polymer nanocomposites has been synthesized to date using polymers such as polyurethane (Berta et al., 2006, Barick and Tripathy, 2011), polycarbonate (Suin et al., 2014), polylactic (Fukushima et al., 2012), nylon (Shelly et al., 2001) and fillers such as clay (Yusoh et al., 2010, Pinto et al., 2011, Osman et al., 2004), graphene (Chang and Wu, 2013), and carbon nanotubes (Sahoo et al., 2013). These polymer nanocomposites create much importance in the industrial applications as multi-functional materials due to their unique properties.

PU is a part of a versatile group of materials that has a large scope of domestic and industrial applications due to its wide range of chemical and physical properties that enables it to be tailored accordingly. The development of PU nanocomposites has attracted great attention since its introduction by Wang and Pinnavaia (1998). Its application has broaden in various fields such as coatings and adhesives for textile, leather, paper, wood and glass fibers due to its properties which are non-toxic, non-flammable and does not cause pollution (Kim et al. 2002). One of the applications that have created a particular interest is polyurethane nanocomposites as thermal insulation material (Demharter, 1998).

This chapter gives a brief insight on the relevant scientific achievements in the synthesis of polymer nanocomposites, particularly PCN. An overview of the mechanical, thermal and permeability properties of the polymers is also included.

## 2.2 POLYURETHANE (PU)

Polyurethanes are a broad class of polymers which are produced by the polyaddition reaction of a diisocyanate with a polyol (Prisacariu, 2012). It was found in 1937 by a German scientist, Otto Bayer who discovered that the polyaddition reaction of a diisocyanate to a diol in the presence of a catalyst resulted in polyurethane. PU is a unique material that has the elasticity of rubber combined with the toughness and durability of metal, however, certain limitations of its properties such as mechanical, thermal and barrier were reported in literature (Xiong et al., 2004, Tien and Wei, 2002). The properties of polyurethane can be adjusted by two different approaches whereby the first is by changing the molecule's structure through modification and the second is by introducing inorganic fillers into the PU matrix (Song et al., 2005).

Typically, PU is formed through the chemical reaction of three main constituents which are the diisocyanates (aromatic or aliphatic), a long chain diol and a small molecule chain-extender diol (diamine). The chemical structure of PU is shown in Figure 2.1.

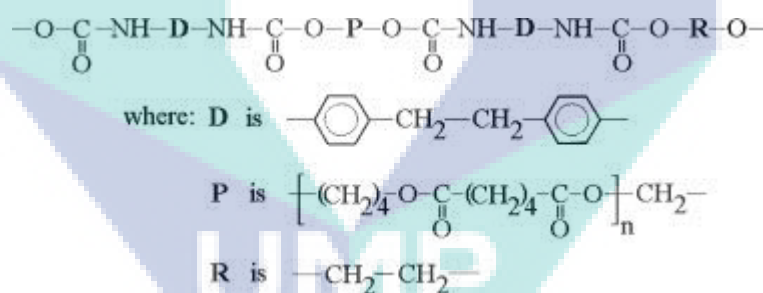


**Figure 2.1:** Structure of PU

Source: Ciobanu et al. (2008)

PU can be considered as a copolymer of the macrodiol and diisocyanate chain extenders sequence termed as the soft segment (SS) and hard segment (HS). HS originates from the diisocyanate and chain extender. It is a rigid aromatic molecule with its glass transition above ambient temperature, whereas the SS comes from the polyol and its glass transition is below ambient temperature.

The difference in the polarity and the chemical structure of HS and SS creates a phase separation in PU. These HS and SS are linked together by means of both the covalent bond and hydrogen bond through the urethane group links (-NH-CO-O-). In general, the properties of PU are highly dependent on their macromolecular structure which is the nature and functionality of their monomers. Two types of PU that are commercially available are the thermoplastic PU; able to be processed thermally and thermoset PU; cannot be thermally processed. Due to its unusual properties, PU has widespread applications as coatings, adhesives, foams, rubbers and thermoplastic elastomers (Asim et al., 2004) and its ability to be fabricated by any conventional technologies enables it to be a leading polymeric material.

### 2.2.1 Synthesis of Polyurethane

In general, PU can be synthesized using the one step synthesis route or the pre-polymer synthesis route. The main differences between the PU prepared through these methods are that the PU obtained through the pre-polymer method is more regular in the chain sequence of polyester-diisocyanate-glycol-diisocyanate-polyester whereas the PU prepared through the one step synthesis route has a more random sequence and higher order of crystallinity (Prisacariu et al., 2011).

In the one step synthesis route, all the reagents involved in the production of PU such as the SS macrodial, diisocyanate and chain extender are added at one during the initial reaction. The drawback in this method is that this procedure is not being able to generate a regular block sequence in the structure of the polyurethane (Hepburn, 1992). The pre-polymer technique consists of two procedures as shown in Figure 2.2. The first step involves the production of pre-polymer through the reaction of a soft segment oligomer with an excess diisocyanate. The second step is the chain extension with a short diol (urethane or ester) or a diamine (urea, urethaneurea, amide or ester-amide) to form the HS. The overall molecular weight of the polymer is increased through this step.

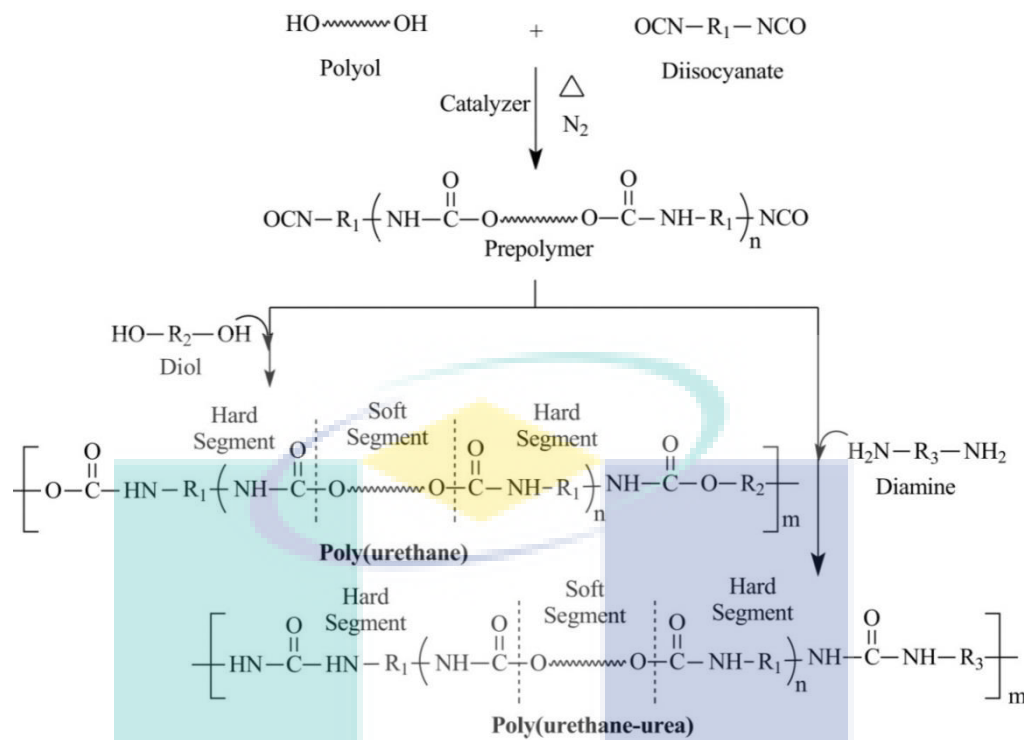


**Figure 2.2:** Schematic of the PUs two-step polymerization synthesis route based on diol chain extenders

Source: Rodriguez et al. (2013)

The first important component in PU is the isocyanate which is produced through the phosgenation of primary amines as shown below.



The three main isocyanates used in industry to produce PU which are toluene diisocyanate (TDI), 4,4' diphenylmethane diisocyanate (MDI) and 1,5-naphthalene diisocyanate (NDI) as shown in Figure 2.3.

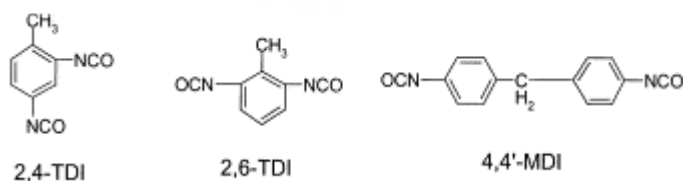


**Figure 2.3:** Chemical Structure of 2,4-TDI, 2,6-TDI and 4,4'-MDI

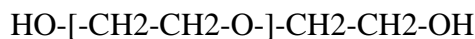
Source: Zhu et al. (2002)

The aromatic diisocyanates are more reactive than the aliphatic diisocyanates and the reactivity of an isocyanate group varies according to its position and the surrounding groups. This reactivity is very important as PU's degree of phase separation is highly dependent on this. According to Seefried et al. (1975), an increased symmetry and bulkiness in the isocyanate MDI leads to better elastomeric properties and phase separation as compared to TDI. Apart from that, Caraculacu et al. (1990) reported in their study that the symmetry of diisocyanate may lead to the crystallization of HS and better mechanical properties such as tensile strength, hardness and modulus.

Saunders et al. (1964) mentioned that the chemistry of PU is based on the functionality of the isocyanate group to react with compounds containing active hydrogen atom and the commonly used active hydrogen compounds in the production of PU are alcohol (polyesters and polyethers) and amines. Polyesters are products from the condensation reaction between glycols and dicarboxylic acid. Polyesters' essential feature that enables them to participate in the urethane reaction is that they are hydroxyl terminated. Example of polyester is poly (ethylene terephthalate) and its chemical formula is shown below.

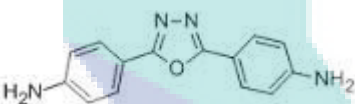
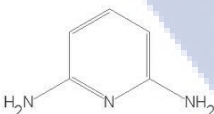
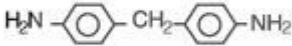


Apart from polyester, there are three types of polyethers used in the production of polyurethane. The first type is polytetramethylene ether glycol (PTMEG) which is a waxy, low crystalline solid that melts near room temperature. It is the most used polyether in the production of PU due to its low crystallinity, low melting point and low viscosity. The second type is polyoxypropylene-glycols (PPG) produced by the polymerization of propylene oxide. This kind of polyether is used in the production of pre-polymers and PU emulsions and the third type of polyether is polyoxyethylene glycols (PEG) which are produced by the polymerization of ethylene oxide. PEG is soluble in water and is mainly used for the production of polyurethanes that requires this characteristic. Example of polyether is poly (ethylene oxide) as shown below.



The third important component in the synthesis of PU is the chain extenders. PU formed by directly reacting diisocyanate and polyols without the addition of chain extenders often has very poor physical properties and does not exhibit microphase separation (Prisacariu et al., 2011). The addition of chain extenders increases the HS length and allows HS segregation which results in good mechanical properties of the PU. There are two types of PU's chain extenders which are the aromatic diols and diamines, and the corresponding aliphatic diols and diamines. Generally, PU's chain extended with an aliphatic diol produces a softer material compared to the aromatic chain extended counterparts (Frisch and Dieter, 1975) and PU prepared with a diamine chain extender are much more reactive due to the HS which has a higher density of hydrogen bonding. Examples of diamine and diol chain extenders are depicted in Tables 2.1 and 2.2 respectively.

**Table 2.1:** Example of diamine chain extenders

Diamine chain extender (Structure)	Name
	2,5-bis-(4-amino-phenylene)-1,3,4-oxadiazole
	2,6-diamino-pyridine
	4,4'-methylene-dianiline

**Table 2.2:** Example of diol chain extenders

Chemical Formula	Name
HO-(CH <sub>2</sub> ) <sub>2</sub> -OH	Ethylene glycol
HO-(CH <sub>2</sub> ) <sub>4</sub> -OH	Butylene glycol
HO-(CH <sub>2</sub> ) <sub>2</sub> -O-(CH <sub>2</sub> ) <sub>2</sub> -O	Diethylene glycol

The reaction between diisocyanate, polyol and a chain extender that synthesizes PU is shown below.



There are several characteristics difference between PU produced from polyester and polyether. Polyether glycol produces PU that is not as strong and tough however they have superior hydrolytic stability due to the hydrolysis reaction of an ester group. The three-centre mechanism hydrolysis is catalyzed by both acid and bases and since a free acid is liberated as a result of the hydrolysis of ester bonds, this reaction becomes autocatalytic. Polytetramethylene glycol (PTMEG) is the standard polyol in this group which gives superior physical and mechanical properties to PU with low abrasion loss (Clemitsen, 2008).

PU produced from polyesters has excellent heat and solvent resistance with high tear and sliding abrasion resistance. However, their disadvantages are that they have poor hydrolytic stability and they are susceptible to fungal attacks. Clemitsen (2008) justified that this is due to the preparation of polyesters through the reaction of a dibasic acid with a diol which needs the perfect condensation process to remove water to a level of 0.03% and this condition is difficult to be attained. Thus, it is important to choose the type of PU according to its applications as its characteristics vary significantly based on their main raw materials and components.

### 2.2.2 Properties of Polyurethane

PU elastomers' segmented structures are made up of long flexible chains (polyols) linked by polyurethane and polyurea aromatic hard segments. The character and properties of PU are determined based on hydrogen bonds between polar groups of the polymeric chain, mainly among the N-H groups (electron acceptors) and carbonyl groups (electron donors) of urea and urethane groups (Chen et al., 2004). The hard and soft segments of PU as shown in Figure 2.4 contribute to the versatility of the polymer.

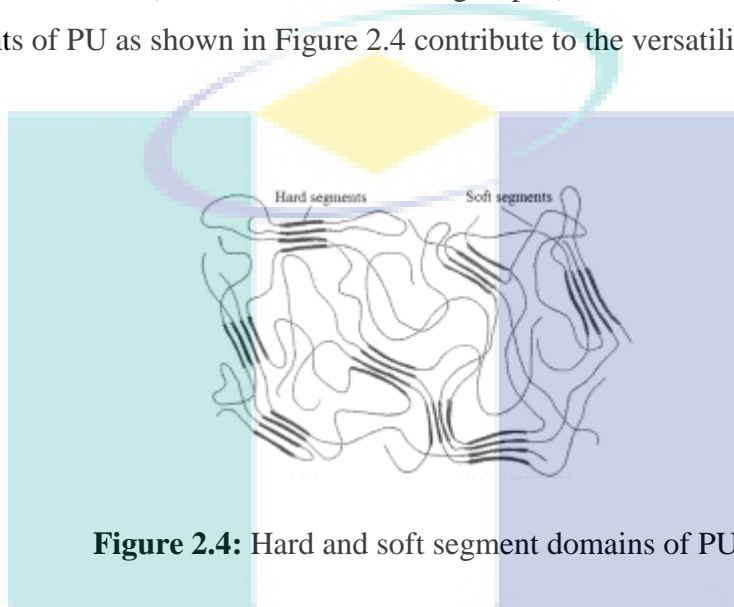


**Figure 2.4:** Hard and soft segment domains of PU

Source: Silva et al. (2012)

The length of the backbone in the structure of PU controls the frequency of the hard segments which influences the modulus, hardness and the tear strength properties whereas the temperature performance and the elastic nature of PU is determined by the soft segment. The micro phase separation of the hard and soft domains results in the mechanical properties of PU in which the tensile strength is dependent on the resistance of the cross linking bonds that are either covalent bonds or hydrogen bonds. Harder materials have denser cross linking which produces a material that is strong with a high modulus value. The conventional mechanical properties of PU are presented in Table 2.3.



**Table 2.3:** Mechanical properties of conventional Thermoplastic Polyurethane

<b>Properties</b>	<b>Units</b>	<b>Values</b>
Hardness, by Shore	Sh A	55-95
Modulus of elasticity 10%	MPa	0.5-6
Modulus of elasticity 100%	MPa	1.6-26
Modulus of elasticity 300%	MPa	2.4-35
Tensile Strength	MPa	13-52
Elongation at break	%	250-600
Tear Strength	kN/m	80-300
Resilience	%	20-65
Abrasion resistance	mm <sup>2</sup>	20-130

Source: Polyurethane Technologies (2009)

The thermal stability of a material can be regarded to the specific temperature or temperature time limit in which the material can be used without excessive loss of properties (Fabris, 1967). Table 2.4 contains the thermal properties of conventional PU. The melting range of the hard segments in linear segmented PU contributes to its thermal stability and the melting range increases as the length of the hard segment increases.

**Table 2.4:** Thermal properties of conventional Thermoplastic Polyurethane

<b>Properties</b>	<b>Units</b>	<b>Values</b> <b>soft - hard</b>
Thermal Conductivity	W/mK	0.19-0.25
Heat of Combustion		
• Heating value	J/g	25000-29000
• Burning value	J/g	26000-31000
Specific Heat		
• Room temperature	J/g K	1.5-1.8
• Melt temperature	J/g K	1.7-2.3

Source: BASF Polyurethane (2011)

Linear PU forms a viscous homogenous liquid that can be processed as a thermoplastic material above the melting range of the hard segments and once the melting range exceeds the PU's decomposition temperature, it will not portray thermoplastic properties (Vilar, 2002) and it forms an easy segmental rotation, which gives the material its rubber-like behavior or elastomeric properties (Chattopandhyay et al., 2007). According to a study by Clemitson (2008), the thermal conductivity of PU is poor compared to other materials and in order to prevent it to undergo thermal degradation, it is important to minimize the heat generated when work is done on PU.

The structure of PU consists of moving chains on the molecular scale and it has molecular size voids that enable the infiltration of small molecules through it. This enables the deduction that PU is permeable to water and gases due to its porous structure as illustrated in Figure 2.5.

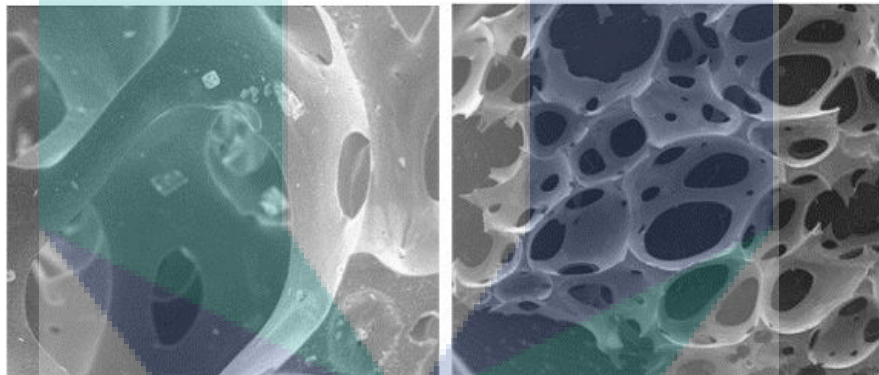


**Figure 2.5:** SEM images of the porous structure of PU

Source: Aviv et al. (2013)

In general, it can be summarized that the strength of the hard segment aggregations, the size and concentration of the hard segment domains and the ability of the segments to orientate in the direction of stress are the main contributors that depict the behavior of PU (Szycher, 1999).

### 2.2.3 Applications of Polyurethane

PU is one of the polymers that are highly ranked in the polymer field. A wide range of properties enables PU to be tailored in order to meet the highly diversified demands of modern technologies such as coatings, adhesives, fiber, and foam (Byung et al., 2002)

Currently, PU is seen as one of the polymers that is dominating the coating material field. Chattopadhyay and Raju (2007) reported in their study that the wide applicability of PU coatings is due to its versatility in selecting monomeric materials from a huge list of macrodiols, diisocyanates and chain extenders. PU coating are found on many materials such as on automobiles to improve the colour retention, in construction and as spray coating for durability against environmental deterioration.

Apart from that, taking into account its properties such as its bio-stability, biodegradability, tailorable backbone structure, toughness and functionality, segmented PU are extensively used in medical applications (Subrata et al., 2012) such as vascular grafts, pacemaker leads, blood bags, bladders and artificial hearts. PU's elastomeric properties also aids in the interaction and mimicking of soft tissue (Theron et al., 2010).

Another important application of PU is as a thermal insulator material. According to Assanpanel (2009), PU is one of the best insulation materials that are able to provide 40% saving in the heating and ventilation expenses. With the increasing demand of polyurethane's usage, the development of polyurethane nanocomposites can be an added value for improving and utilizing the full benefits of this polymer in its applications. In addition, the development of polymer nanocomposites is also an alternative to conventional filled polymer and homopolymer using a range of nanosize fillers.

## 2.3 NANOFILLERS

Nanofillers are nanostructured materials that can be defined as bulk materials made of grains in nanometer size range. The introduction of nanofillers as additives in polymer systems has resulted in polymer nanocomposites exhibiting high performance characteristics compared to pristine polymers.

### 2.3.1 Layered Silicates

LS are the preferred filler materials in nanocomposites due to their lamellar structure as shown in Figure 2.6 that have high in-plane strength, stiffness and a high aspect ratio (Bhattacharya et al., 2009). Dennis et al. (2001) and Wang et al. (2000) stated that the two reasons that makes all groups of lamellar solids the material of choice in designing nanocomposites are their rich intercalation chemistry that permits them to be chemically modified and made compatible with polymer hosts and they can be obtained easily at low costs.

The layered silicates used in fabricating the nanocomposites origins from the structural family known as the 2:1 layered phyllosilicates (Alexandre and Dubois, 2000). Na<sup>+</sup> MMT clay originates from this family. Their crystal lattice consists of two dimensional layers where a central octahedral sheet of alumina of magnesia is fused to two external silica tetrahedron by the tip (Michael et al., 2000) as shown in Figure 2.5. The thickness of each layer is approximately 1 nanometer (nm) and the lateral dimensions vary from 30 nm to several micrometers and sometimes larger depending on the particular layered silicate. The stacking of the layers and the inter-stack ionic force results in interlayer or intergallery spaces (Giannelis et al., 1999). The isomorphic substitution within the layers (Al<sup>3+</sup> replaced by Mg<sup>2+</sup> or Fe<sup>2+</sup> or Mg<sup>2+</sup> replaced by Li<sup>+</sup>) generates negative charges that are counterbalanced by alkali and alkaline earth cations situated inside the galleries (Ray and Okamoto, 2003). The hydration of exchangeable cations and the polar nature of surface silanol groups impart the hydrophilic nature of clay and the number of substituted metals within the layer characterizes these materials. The number of exchangeable alkali or alkali metal ions is expressed by the cation exchange capacity (CEC), and are generally expressed as mequiv/100 gm (Bhattacharya et al., 2008).

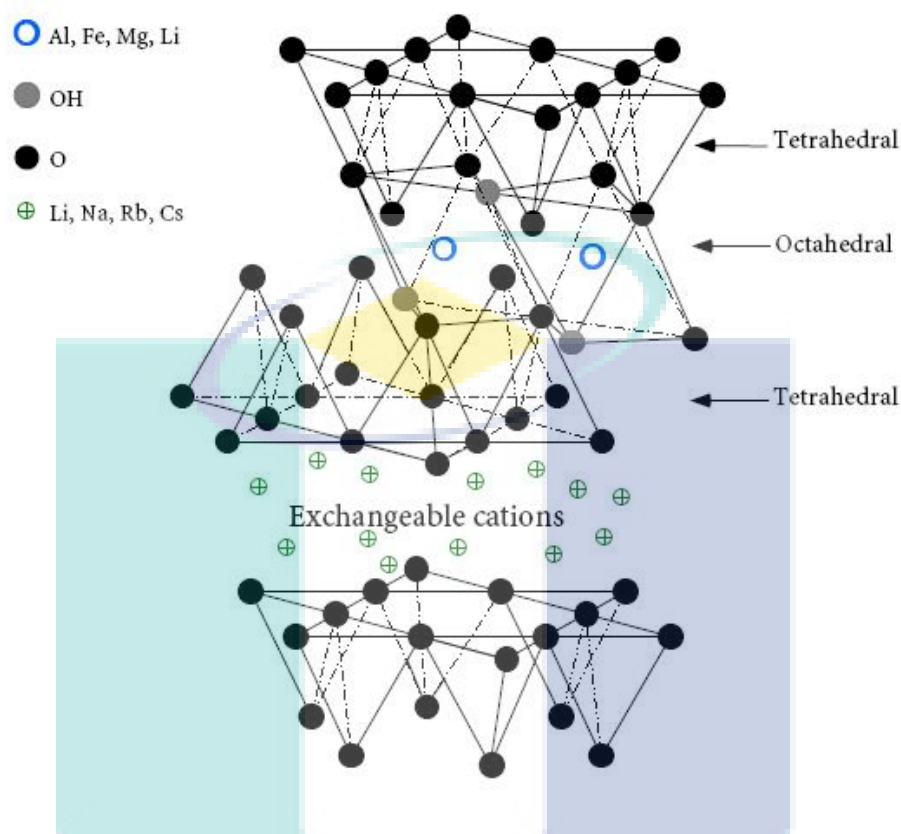


**Figure 2.6:** Structure of 2:1 Phyllosilicate

Source: Ray and Okamoto (2003)

Montmorillonite, saponite and hectorite are the most commonly used LS. The chemical formula and characteristic parameter of these silicates are shown in the Table 2.5.

**Table 2.5:** Chemical formula and characteristic parameter of commonly used 2:1 phyllosilicate

2:1 phyllosilicates	Chemical Formula	CEC (mequiv/100 g)	Particle length (nm)
Montmorillonite	$M_x(\text{Al}_{4-x}\text{Mg}_x)\text{Si}_8\text{O}_{20}(\text{OH})_4$	110	100-150
Hectorite	$M_x(\text{Mg}_{6-x}\text{Li}_x)\text{Si}_8\text{O}_{20}(\text{OH})_4$	120	200-300
Saponite	$M_x\text{Mg}_6(\text{Si}_{8-x}\text{Al}_x)\text{Si}_8\text{O}_{20}(\text{OH})_4$	86.6	50-60

M, monovalent cation; x, degree of isomorphous substitution (between 0.5 and 1.3)

Source: Ray and Okamoto (2003)

MMT is one of the common clay used in creating polymer layered silicates (PLSN). Silica is the dominant constituent of MMT clay with alumina being essential. According to Khoo (2006), MMT clay has sheet structure consisting of layers. The first layer is the tetrahedral silicate layer that consists of  $\text{SiO}_4$  groups linked together to form a hexagonal network of the repeating units of composition  $\text{Si}_4\text{O}_{10}$ . The second layer is the octahedral alumina layer which consists of two sheets of closely packed oxygens or hydroxyls, between which octahedrally coordinated aluminium atoms are imbedded in such a position that they are equidistant from six oxygens or hydroxyls. The two tetrahedral layers sandwich the octahedral layer and these three layers form one clay sheet that has a thickness of 0.96 nm. The chemical formula of MMT clay is  $\text{Na}_{1/3}(\text{Al}_{5/3}\text{Mg}_{1/3})\text{Si}_4\text{O}_{10}(\text{OH})_2$ . The chemical structure of MMT clay is shown in Figure 2.7.

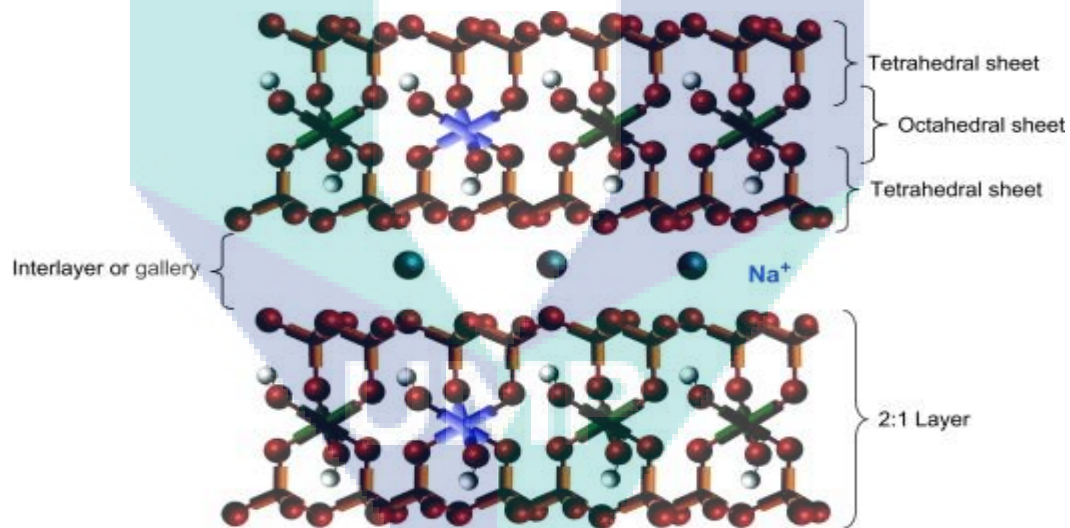


**Figure 2.7:** Chemical structure of montmorillonite nanoclays

Source: Paul and Robeson (2008)

Besides MMT clay, other clays such as bentonite and chlorite are also used in the preparing PLSN. It is important to ensure that the degree of dispersion of the LS in polymer is achieved as LS have high tendency to agglomerate. High degree of dispersion can be obtained through modification of these layered silicates.

### 2.3.2 Organically Modified Layered Silicates

LS are known to be hydrophilic materials and in order for it to be made compatible with hydrophobic polymers, it has to undergo chemical modification as it is only accordant to hydrophilic polymers in its pristine state. This is a great drawback as most of the polymers carry the hydrophobic nature. Without organic treatment, LS will only be able to disperse and phase separate in in the presence of very polar polymers.

The organic treatment is usually carried out through ion exchange between inorganic sodium cations on the clay surface with the desired organic cation that is more reactive such as the primary, secondary, tertiary and quaternary alkylammonium or alkylphosphonium cations. In the ion exchange process, the inorganic (sodium) ions are exchanged with more voluminous organic onium cations and it results in widening the gap between the single sheets. The polymeric movements between them are enabled through this and the surface properties of each single sheet is changed from being hydrophilic to hydrophobic as shown in Figure 2.8 (Fischer, 2003).

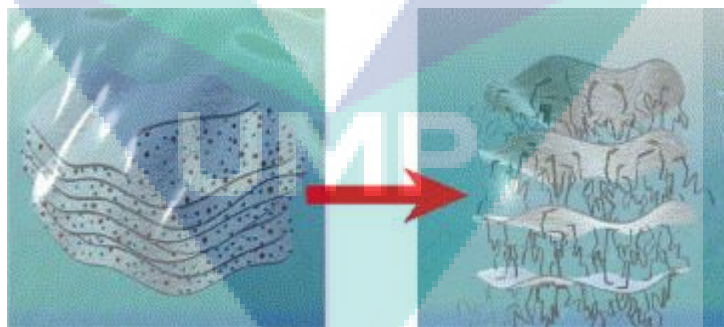


**Figure 2.8:** Schematic diagram of an ion exchange reaction

Source: Fischer, 2003

Alkylammonium or alkylphosphonium cations in organic silicates (OLS) help to lower the surface energy of the inorganic host and improve the wetting characteristics and intercalation with the polymer matrix. This results in larger interlayer spacing. Furthermore, alkylammonium or alkylphosphonium cations provides functional groups that can react with the polymer matrix, or in some cases initiate the polymerization of

monomers to improve the strength of the interface between the inorganic and the polymer matrix (Okamata, 2006). There are several types of modification that can be done such as treating the LS with transition metal ions or clay surface treatments using quaternary ammonium salts.

LS whether organically modified or not possess a hierarchical morphology defined by three general levels of structures which are the crystallite, primary particles and agglomerates. The crystallites are commonly referred as tactoids composed of 100 individual layers stacked together, the primary particles consist of dense face to face stacking of individual tactoids and finally the weak agglomerations. In fabricating PLSN, it is crucial to ensure that there is no disruption of the tactoids and primary particles in order to achieve a homogeneous dispersion. It is crucial to achieve a uniform distribution of the LS in the polymer matrix.

### **2.3.3 Transition Metal Ions (TMI) Modified Layered Silicates**

The modification of LS with transition metal ions (TMI) are not widely explored to date as compared to modifications using organic surfactants. Although organically modified clay are often used, it was reported by Nawani et al. (2007) that these organoclay has insufficient activity due to the degradation of the organic surfactants in their structure whereby the organic components such as the quaternary amine surfactant starts to decompose via the Hoffman elimination process above 170°C. This is seen to hinder the property advancement of the nanocomposites formed especially its thermal and barrier properties. It is presumed that small amount of catalytically active TMI salts in the clay may bring some significance in the charring process of the PCN in which the buildup of carbonaceous-silicate chars during burning can reduce gas permeability and improve thermal stability. The poor compatibility between the polymer host and the clay while casting the nanocomposites is also believed to be overcome through this modification process. It is surmised that the modification process enables penetration of the polymer chains in between the LS with ease due to the separation of the clay platelets that makes the intercalation or exfoliation process to be achieved.



## 2.4 POLYMER NANOCOMPOSITES

The expansion in the current scientific and engineering knowledge has gained polymer nanocomposites a significant attention. The breakthrough of research in this field by Toyota Research Center and Development in the early 90's has even heightened its emphasis (Kojima et al., 1993). Jordan et al. (2005) defined nanocomposites as a composite material which comprises with at least one dimension of component is in the nanometer scale which is lesser than 100nm.

The incorporation of filler as a reinforcement material has been reported in literature for many years. The addition of non-ionic polymers to clay suspensions in the drilling fluid technology was done to reduce its swelling by Olphen (1963). Polymer clay complexes has also been employed by researches in the soil field such as mineral cycling and weathering, profile development and aggregate stabilization (Theng, 1982). Currently, the fabrication of polymer nanocomposites are carried out to improve various properties such as mechanical, thermal and barrier properties of the pristine polymer in order for it to be applied in a wide range of applications. Clay minerals has been one of the preferred choice of filler material as polymer property enhancements were seen to be augmented further when these fillers are dispersed in nanometer scale (Bhattacharya et al., 2008).

The dispersion of clay into its polymer host is quite arduous as the clay layers tend to bond strongly together. This is usually countered via organic modification of the clay in order for it to disperse homogeneously during the fabrication process. The polymer nanocomposites are said to exhibit remarkable advancement in modulus (Biswas and Ray, 2001), increased strength and heat resistance, low gas permeability and flammability (Ray and Okamoto, 2003), increased modulus and strength and improved solvent and heat resistance (Venkataraman, 2005). The hosts used in polymer nanocomposites are often polymeric materials such as thermoplastics, thermosets or elastomers. The establishment of conventional polymer composite may been in a broad spectrum of applications, however, the higher loading of additives required in order to achieve the same characteristic as nanocomposites is a major drawback as higher

contain of the additives leads to increased weight, opacity and brittleness (Alexandre and Dubois, 2000 and Fischer, 2003).

The reliability of polymer nanocomposites to exhibit improved properties with a low percentage of clay loading is due to the large surface area of LS however great care has to be taken during the fabrication process of the PLSN to avoid clay agglomerates as LS has high tendency to agglomerate due to the stacking of the layers in its structure (Ray and Okamoto, 2003).

#### **2.4.1 Structure of Polymer Layered Silicates**

The structure of PLSN can be classified as either nanocomposites or conventional composites depending on the nature and interaction of the components such as the type of silicate material, the nature of the polymer matrix, the organic material used in the ion exchange reaction and the preparation techniques of the nanocomposites (Bhattacharya et al., 2008). PLSN can be categorized into three groups which are the phase separated clay composites, intercalated clay composites and exfoliated clay composites (Alexandre and Dubois, 2000) as below.

1. **Phase Separated Clay Composites:** Phase separated clay composites occur when the polymer chain is unable to penetrate into the clay's gallery as shown in Figure 2.9 (a). The clay particles are seen to flock together within the polymer matrix which results in a phase separated material. In this material, clay exists as agglomerates within the polymer matrix and this type of composites often fails in enhancing the polymer's properties.
2. **Intercalated Clay Composites:** Intercalated morphology is obtained when the polymer chains penetrate deep into the silicate layers while still retaining an ordered structure. The silicate layers expand due to this penetration and due to the mechanical shearing forces between and interactions between the silicates and the polymer, the stack of layered silicates disperse between the matrix (Bhattacharya et al., 2008) as illustrated in Figure 2.9 (b). LeBaron et al. (1999) reported in their study that intercalated structure has regions of both high and low reinforcements.

3. Exfoliated Clay Composites: Exfoliated structure is formed when the individual layers in the clay (~1nm) are randomly distributed and well dispersed in the polymer host and this result in randomly separated clay particles as depicted in Figure 2.9 (c). The large surface area and high aspect ratio of the nanoscale silicates is able to enhance the properties of the nanocomposites to exhibit better properties as compared to their conventional and intercalated counterparts (Etmimi, 2012).

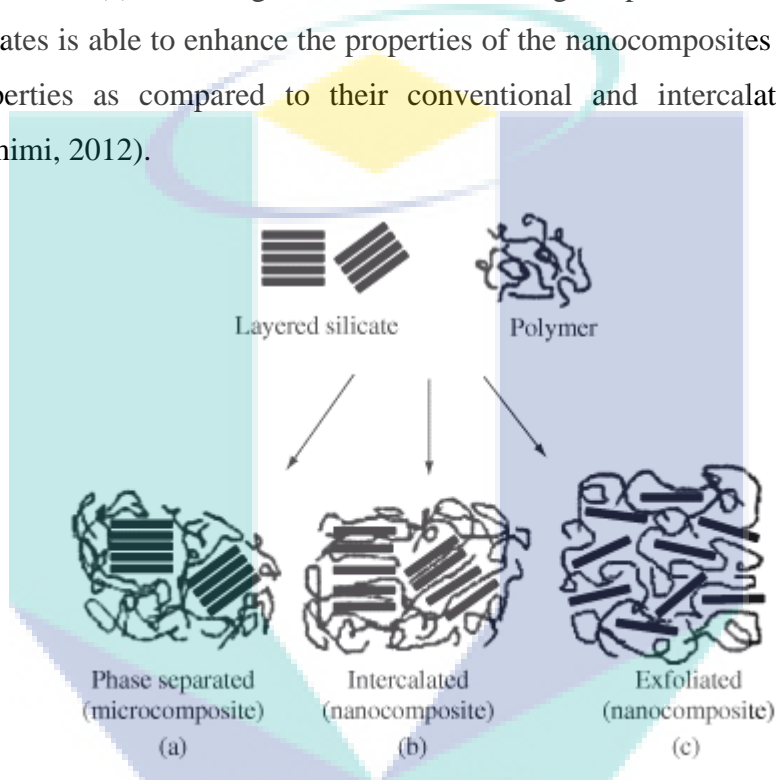


**Figure 2.9:** Illustration of different types of polymer layered silicate composites

Source: Alexandre and Dubois (2000)

Yeh and Gupta (2010) accounted that exfoliated morphology occurs in most cases which use MMT clay as the reinforcement material and due to the high surface area of MMT clay (around  $750 \text{ m}^2/\text{g}$ ), property enhancement of the polymer matrix is significant even at low clay loadings due to the well distributed and strong molecular interaction between the clay surface and its host.

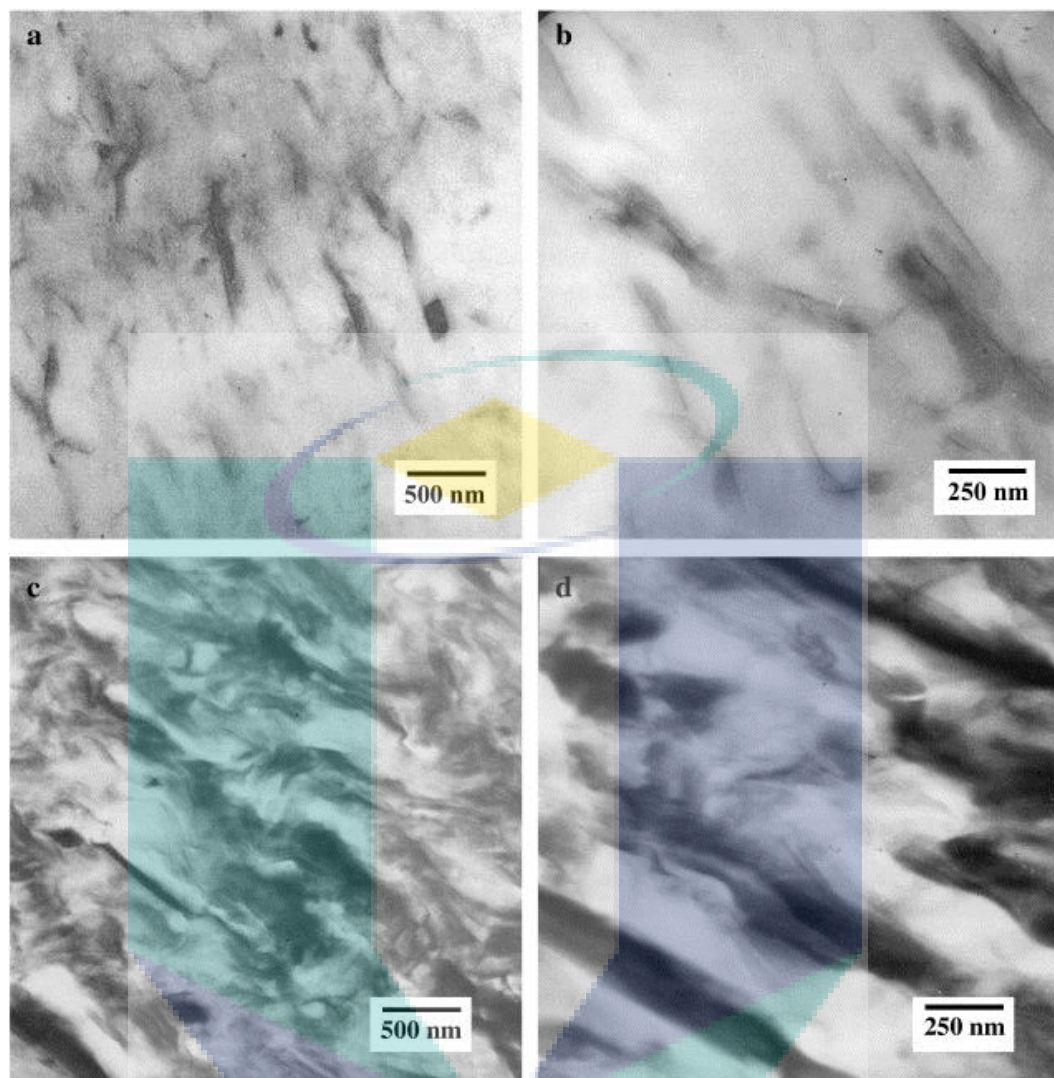


**Figure 2.10:** TEM images of exfoliated and intercalated PU-MMT

Source: Salahuddin et al. (2010)

Salahuddin et al. (2010) synthesized and characterized polyurethane organo montmorillonite (PU-OMMT) nanocomposites and reported both intercalated and exfoliated structures of PU-OMMT in their study. Figure 2.10 (a) and (b) portrays mineral particles that were evenly distributed and showed exfoliation of the silicate layers. The TEM micrographs of the nanocomposites showed aggregation and some areas of the PU matrix with oriented nanodomains in the size ranges of 70–200 nm and 200–500 nm. Domains of the parallel layers were presumed to be the remnants of OMMT particles however with the substantial expansion of the interlayer space, it can be assumed that an intercalated structure was obtained in Figure 2.10 (c) and (d).

## 2.4.2 Preparation of Polymer Nanocomposites

The compatibility between a polymer host and its reinforcement material is important to ensure the formation of an exfoliated nanocomposite. Generally, in the preparation of polymer nanocomposites, the challenge lies in determining the proper synthesis method as failure in the synthesis method will result in a material whose properties are not optimal. There are three approaches that may be used in the fabrication of PCN which are solution dispersion, *in-situ* polymerization and melt intercalation.

### *Solution Intercalation*

In solution intercalation method, the layered silicates are dispersed and exfoliated into single layers in an adequate solvent in which the polymer can be dissolved. The layered silicate is first swollen in a solvent such as water, toluene or chloroform. Following the addition of polymer, the polymer chains intercalate and displace the solvent within the interlayer of the silicate. During the evaporation period, the solvent is removed and the sheet reassembles, sandwiching the polymer to form an ordered, multilayered structure (Koo, 2006) and the intercalated structure remains. The nature of the solvents facilitates the insertion of polymers between the layered silicates in which the polarity of the medium is the determining factor for intercalations (Theng, 2012).

Zheng et al. (2006) prepared polyurethane montmorillonite (PU-MMT) through solution mixing in their study. Polyurethane prepolymer and a diamine curative were dissolved in purified THF to form a 15% solution at 15°C. MMT clay was dispersed in THF with a sonicator to form a 10% solution and both the solutions were combined and sonicated. The solutions were then cast into molds and cured prior to other analysis. Besides Zheng and coworkers, other researches that used this method includes Moniruzzaman and Winey (2006) and Potts et al. (2011). Figure 2.11 shows a schematic representation of the two mechanisms involved in the formation of nanocomposites via solution intercalation method.

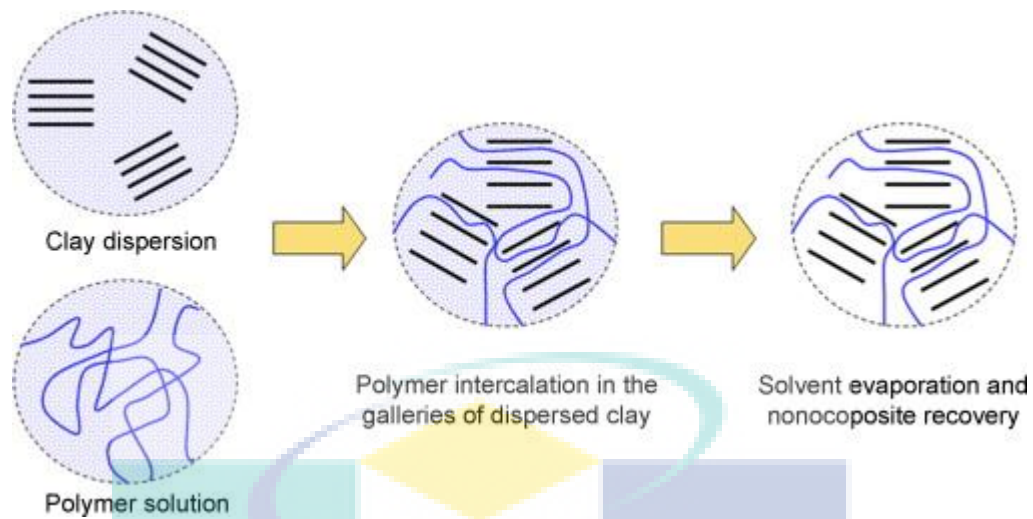


**Figure 2.11:** Schematic representation of PLS obtained by intercalation from solution

Source: Pavlidou and Papaspyrides (2008)

Solution mixing is an attractive route in preparing water or solution soluble PLSN. One of the benefits of solution mixing is that the filler's de-aggregation and dispersion may be facilitated through the rigorous mixing of the filler with the polymer. A study by Toyota Research Group showed that an organic filled polyamic acid film that was prepared through solution mixing showed excellent gas barrier properties which led the researchers to conclude that an exfoliated nanocomposite structure was formed through this method.

There are few disadvantages in this method. One of the disadvantage is that a large amount of solvent is consumed which results in higher costs. Apart from that, the types of polymer that can be used in this method are dependent on the selection of a proper solvent. However, solution method is one of the most common methods in preparing the polymer nanocomposites due to its main advantage which is the reduction of aggregation through the mechanical agitation such as ultrasonication.

### ***Melt Intercalation***

Melt intercalation is one of the standard techniques in preparing polymer nanocomposites and it is a preferred choice due to its low cost and simplicity in facilitating large scale productions. In the melt intercalation process, the layered silicate is mixed with the solid polymer matrix in the molten state.

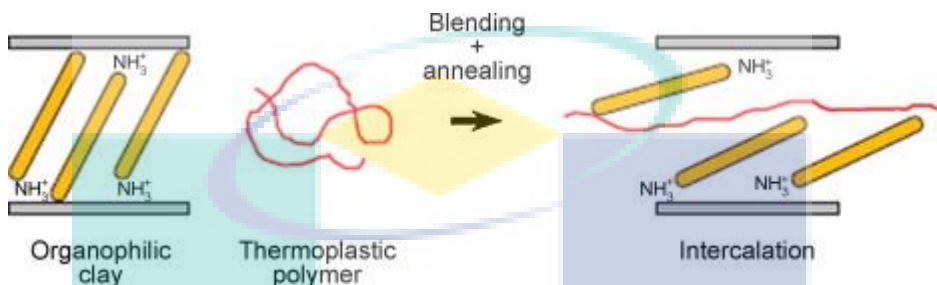


**Figure 2.12:** The melt intercalation process

Source: Pavlidou and Papaspyrides (2008)

In direct melt intercalation as shown in Figure 2.12, a mixture of polymer and LS are annealed, whereby the mixture of polymer and LS are heated and slowly cooled down to remove the internal stress in it and toughen it. During the annealing process, the polymer chain diffuses from the bulk polymer melt into the galleries between the LS. A range of nanocomposites with structures from intercalated to exfoliated are obtained depending on the degree of penetration of the polymer chains into the silicate galleries. Hussain et al. (2006) reviewed that if the layer surfaces are sufficiently compatible with the selected polymer, the polymer is then inserted into the interlayer space to form an intercalated or exfoliated nanocomposite. In melt intercalation, no solvent is required (Koo, 2006).

The study on the direct melt intercalation was first demonstrated by Vaia and Giannelis (1997). Finnigan et al. (2004) reported in his research on the preparation of polyurethane nanocomposites based on organosilicates by melt compounding technique. In their research, a large increase in stiffness and higher hysteresis was observed. Barick and Tripathy (2011) prepared PU and organically modified MMT through melt intercalation and reported significant improvements in the dynamic rheological studies of the nanocomposites.

The advantages in using melt intercalation are that it is environmentally friendly and economical in terms of cost because it does not use any solvent. Moreover, many types of polymer can be processed using this method however the drawbacks in this method are that polymers that undergo thermal degradation easily are not advised to be processed using this method as the temperature profile in an extruder is usually high. In addition, a perfect exfoliation process cannot be obtained. Furthermore, the distribution of the reinforcement materials may not be even as compared to solution intercalation method which might result in nanocomposites having poor morphology.

### ***In-situ Polymerization***

In *in-situ* polymerization, the LS is swollen within the liquid monomer so that the polymer formation can occur between the intercalated sheets. Initiation by different types of polymerization method such as heat or radiation, diffusion of a suitable initiator, or an inorganic initiator or catalyst fixed through cationic exchange inside the inter layer are done before the swelling step of the monomer (Koo, 2006). The characteristic of the low viscosity of the monomer helps to break up particle agglomerates and achieve a more uniform mixing of particles into the interlayer region. One of the main advantages in *in-situ* polymerization is that partially or fully exfoliated nanocomposites can be obtained which results in better dispersion with lesser agglomerations and stronger interaction between the polymer chain and the reinforcement material (Etmimi, 2012).

*In-situ* polymerization was first reported by the Toyota researches. They prepared Nylon-6/MMT through *in-situ* polymerization using  $\epsilon$ -caprolactum as the monomer (Usuki et al., 1993). Great advancement was seen in the thermal and mechanical properties of the fabricated Nylon-6/MM with only a small amount of clay loading. Li et al. (2013) prepared PU/graphene oxide/epoxy nanocomposites via *in-situ* polymerization method. The PU prepolymer was first *in-situ* synthesized on the graphene oxide (GO) nanosheets prior to adding epoxy and the curing agent in preparing the PU nanocomposites. The synthesis route for the preparation of the PU/GO/EP nanocomposites is depicted in Figure 2.13.



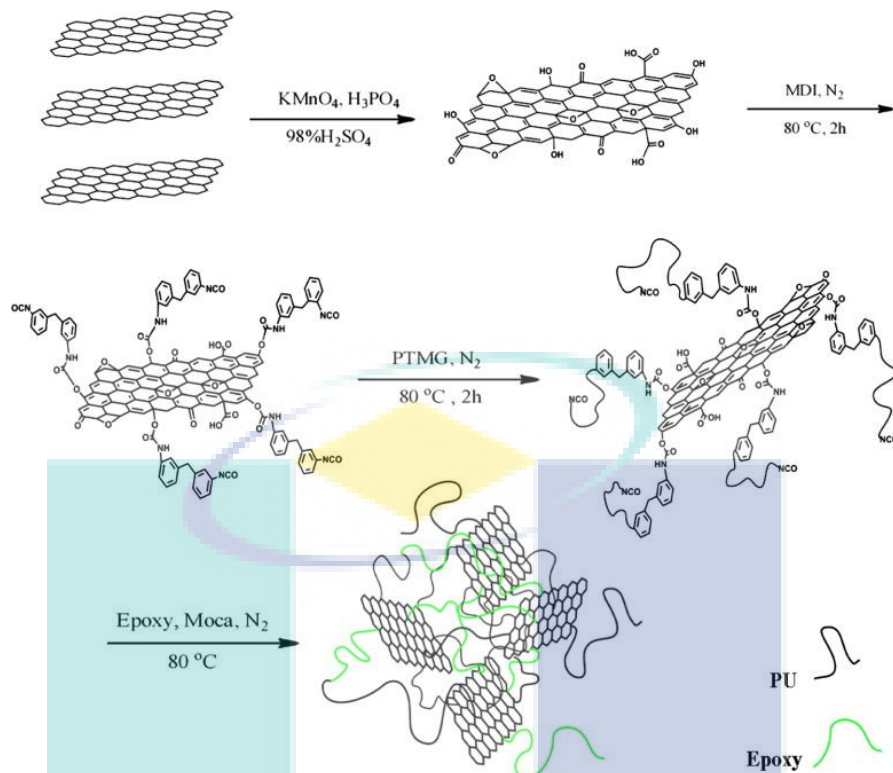


**Figure 2.13:** Synthesis route of PU/GO/EP nanocomposites

Source: Li et al. (2013)

From their morphological study the GONS was dispersed well in the PU/EP matrix and formed a strong interfacial interaction between the GONS and the matrix due to the chemical bonding. The tensile strength and elongation at the break of the PU/GO/EP nanocomposites increased more than 52% and 103% with the incorporation of 0.066 wt% of GONS.

## 2.5 MORPHOLOGICAL STUDY OF POLYMER NANOCOMPOSITES

The improvement in properties of the polymer is most often determined by the dispersion of the layered silicates in the polymer matrix. Enhancements in the chemical and physical properties of PLSN are usually dependent on the exfoliation and the intercalation of the silicates layers. The quality and the morphological structure of the clay dispersion can be investigated and analyzed through the characterization studies such as scanning electron microscope (SEM), field emission scanning electron microscope (FESEM), transmission electron microscope (TEM), fourier transform infrared spectroscopy (FTIR), and x-ray diffraction (XRD).

### 2.5.1 Scanning Electron Microscope (SEM)

In SEM analysis, a very fine electron incident beam is scanned across the surface of the sample through scattered electrons and this electrons produces a signal that is transformed into a two dimensional image of the sample's morphology (Etmimi, 2012). In the general SEM, the electrons are emitted from the electron source and accelerated in a space that comprises of a negative electric potential and an anode electrode at ground electric potential. The material's surface at the ground electric potential is then scanned with electron beam (Todokoro et al., 1999) which results in electrons and x-rays being ejected from the sample whereby this electrons and x-rays are then converted into a signal that produces the final image.

SEM is used to determine the degree of exfoliation of the layered silicates into the polymer matrix however great care must be exercised to identify the dispersed filler within the polymer matrix (Potts et al., 2011). Rehab and Salahuddin (2005) were one of the many researches that used SEM to determine the dispersion of MMT clay into PU. In their study, the SEM examination of the fracture surface of the models did not portray any mineral domains as shown in Figure 2.14 (a) however through element mapping for Si, they found that the uniformity of the white dots were Si's representative as shown in Figure 2.14 (b). This enabled them to deduct that the mineral domain are submicron's which were homogeneously dispersed in the matrix.

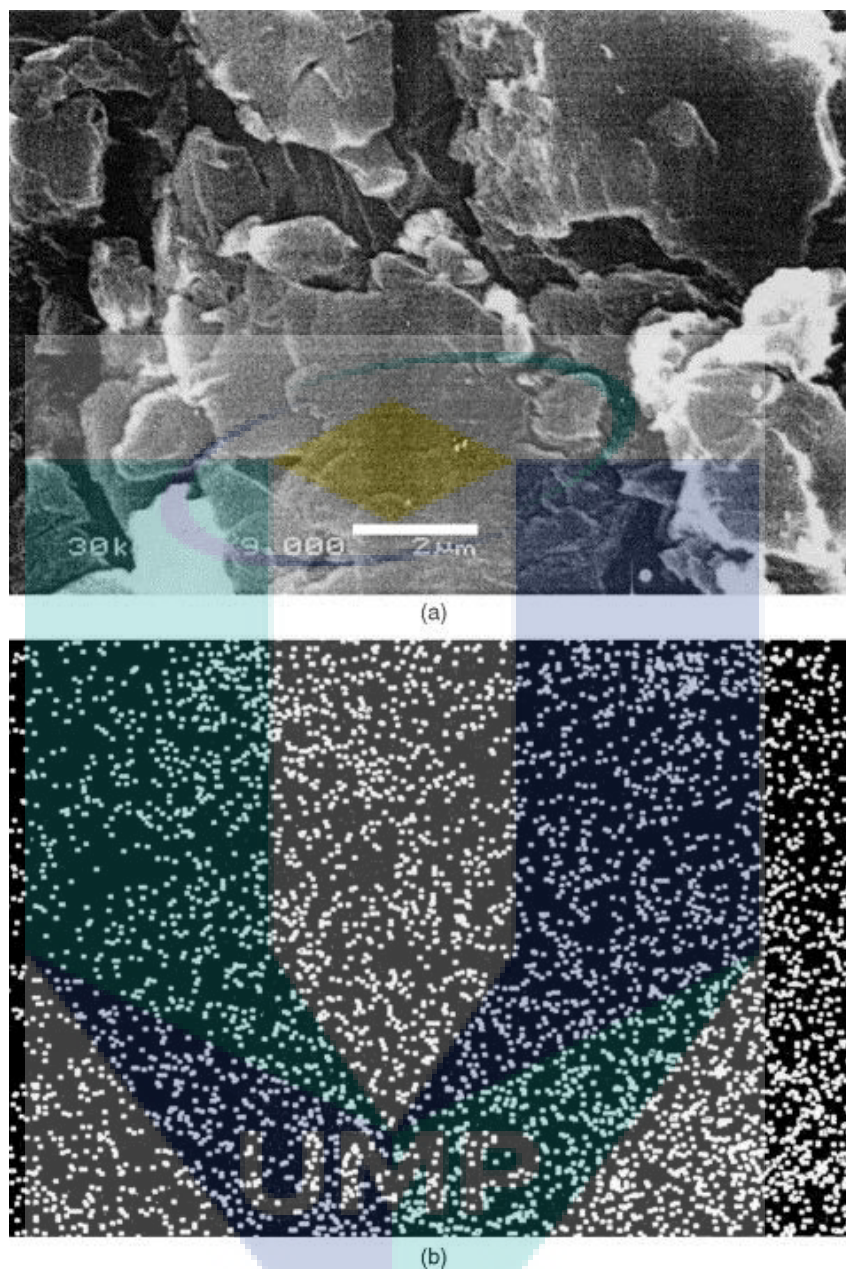


**Figure 2.14:** (a) Scanning electron micrograph (b) Elemental mapping of Si for PU-MMT nanocomposites

Source: Rehab and Salahuddin (2005)

Morphological study by SEM can only verify the presence of agglomerates in the polymer host up to a certain level of view magnifications. In order to investigate whether intercalation or exfoliation of the clay has occurred, morphological characterizations such as TEM and FESEM have to be employed.

### 2.5.2 Field Emission Scanning Electron Microscope (FESEM)

Field Emission Scanning Electron Microscope (FESEM) is an analysis tool that is employed in investigating the morphology structure of PLSN with a domain size of less than 0.8nm to 1.2nm. It consists of an electron gun in the field emission cathode whereby this electron gun provides narrow probing beams towards the sample which results in x-rays being emitted (PhotoMetrics, 2012). These x-ray spectra are collected and analyzed in order to yield the quantitative elemental information about the sample. In characterizing solid materials such as PLSN, FESEM is usually used to visually study the morphological structure such as the surface texture of the nanocomposites at certain magnification range to give a clear understanding on surface structure (Ismail, 2013) and it produces clearer and less electrostatically distorted images with spatial resolution down to 1 ½ nm as compared to SEM (PhotoMetrics, 2012).

Chou et al. (2006) studied the structure of PU and PU nanocomposites filled with silver (Ag) nanoparticles using FESEM micrographs as shown in Figure 2.15. In their micrographs, PU had a rougher surface which was related to the microphase segregation occurring in its pristine state howbeit, the PU-Ag nanocomposite portrayed a smoother surface and they argued that this could be the result of a better phase mixing when Ag was incorporated into the PU matrix due to the hydrogen bonding and phase mixing between the hard and soft segments.

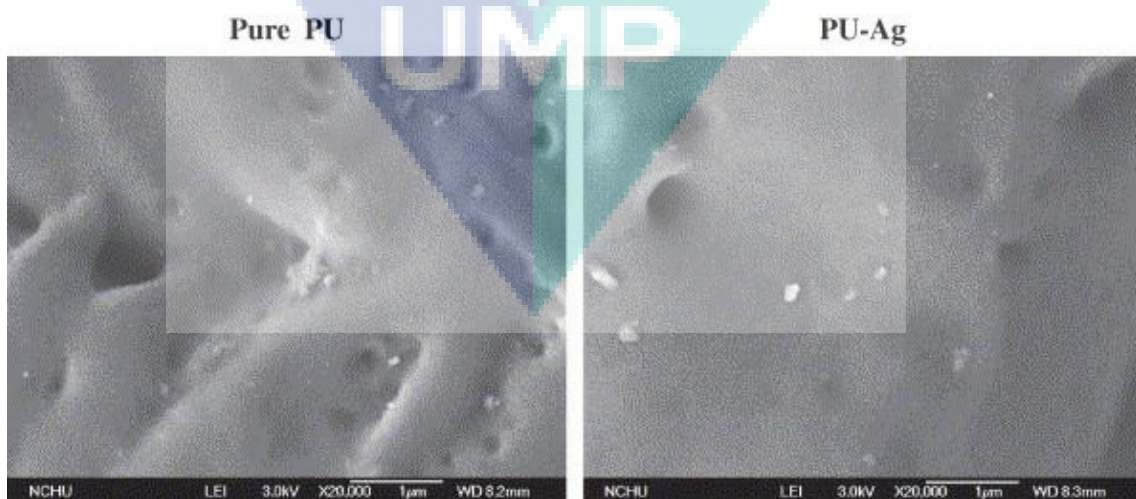


**Figure 2.15:** FESEM micrographs of PU and PU-Ag nanocomposites

Source: Chou et al. (2006)

### 2.5.3 Transmission Electron Microscope (TEM)

TEM is a characterization study that is employed to visually see the morphology of PLSN at the nanometer scale. It uses electromagnetic lenses to focus and direct thermal electron are accelerated by applying high voltage to form an electron beam from the electron gun to penetrate the sample. The electromagnetic lenses are used to form the image that can be observed on a fluorescent screen. TEM analysis is more advantageous as compared to SEM due to its ability to visually determine the pattern of the clay dispersion in the polymer matrix (Ismail, 2013).

Berta et al. (2006) used TEM in order to gain an insight into the latter feature of the organoclays dispersed in the polyurethane lamellar nanocomposites. The superstructure of the organoclay dispersion consisted of separate clay layers. Agglomerates of the tactoids with a variety of size were present in the PU matrix as shown in Figure 2.16.

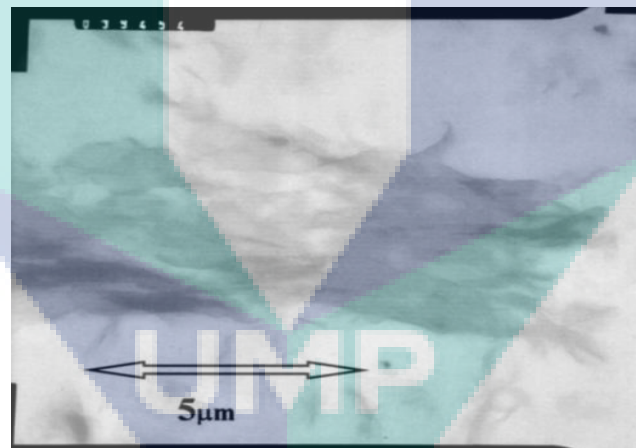


**Figure 2.16:** TEM of PU clay nanocomposites

Source: Berta et al. (2006)

Cao et al. (2004) studied the processing, structure and properties of PU clay nanocomposites to investigate the effect of nanoclay on the cell size, cell density and the mechanical properties and they found that nanocomposites containing MMT modified by methyl tallow bis-2-hydroxyethyl ammonium (MMT-OH) and organophilic montmorillonite with catalytic function (MMT-Tin) revealed good clay dispersion as shown in Figure 2.17.

Exfoliation of the clay can be observed with MMT-Tin and stacking of clay layers with substantial layer separation is visible in part (a) and (b) of the figure.

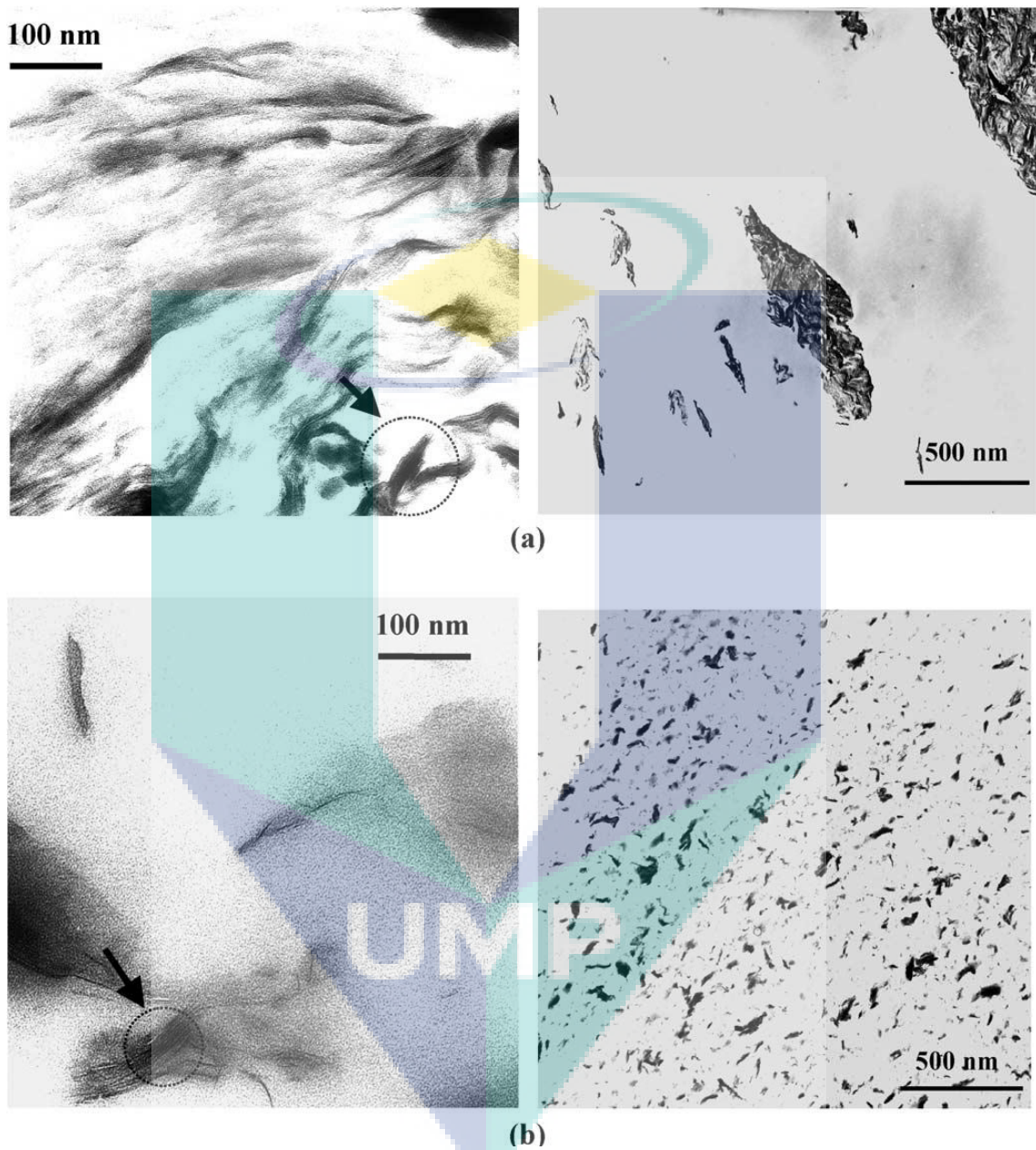


**Figure 2.17:** Transmission electron micrographs of cross-section views of PU nanocomposites (a) PU/MMT-OH (b) PU/MMT-Tin

Source: Cao et al. (2004)

#### 2.5.4 Fourier Transform Infrared Spectroscopy (FTIR)

Fourier Transform Infrared Spectroscopy (FTIR) is a technique that exploits the vibration response of molecules in response to infrared (IR) radiation. Molecules absorb energies that correspond to their frequency and transmit the unabsorbed frequencies when they are exposed to IR and these unabsorbed frequencies are recorded by a detector which enables the identification of the molecules by matching the wavelength of the molecule with the frequency to those already known (Bhattacharya et al., 2008). The typical bonds within their molecules and their corresponding wavelength are listed in Table 2.6.

**Table 2.6:** Example of atomic groups with their IR absorption wavelengths

Molecule	Absorption wavelength ( $\text{cm}^{-1}$ )
C=O	1870-1650
O-H	3640-3250
C-OH	1160-1030
C-H	2980-2850
N-H	3460-3280

Source: Bhattacharya et al. (2008)

Tien and Wei (2001) used FTIR to investigate the chemical structure of PU-MMT. Based on the spectrum obtained from their sample, the IR bands at  $3480 \text{ cm}^{-1}$  and  $3320 \text{ cm}^{-1}$  were related to the free N-H stretching and the hydrogen bonded N-H stretching in the PU respectively. Free of hydrogen bonding carbonyl caused the band at  $1733 \text{ cm}^{-1}$  whereas hydrogen bonded carbonyls resulted in the  $1703 \text{ cm}^{-1}$  band. No band appeared at  $3480 \text{ cm}^{-1}$  which indicated that the N-H groups in the polyurethane nanocomposites were nearly completely hydrogen-bonded. Tien and Wei (2001) presumed that the possible functional groups acting as the acceptors in the hydrogen bonding with N-H are the urethane carbonyl ( $-\text{C}=\text{O}$ ), the ether ( $-\text{C}-\text{O}-\text{C}-$ ) and the oxygen of the hydroxyl groups ( $-\text{OH}$ ) on silicate layers.

### 2.5.5 X-Ray Diffraction (XRD)

X-Ray Diffraction (XRD) is the most commonly used technique to determine the distance between the galleries or interlayer spacing,  $d_{001}$  in the clay structure (Utracki, 2004). The spacing between the ordered crystalline layers of the organoclay is measure using the Bragg's Law.

$$n\lambda = 2d \sin \theta \quad \text{Eq. (2.1)}$$

Where:

- $d$  = Space between layers of the clay
- $\lambda$  = Wavelength of the X-ray
- $\theta$  = Angle at the maximum point of the first peak into a spectrum
- $n$  = Order of diffraction

Intensity of the diffracted x-ray is measured as a function of the diffraction angle  $2\theta$  whereby the pattern is used to identify the specimen's crystalline phases and to measure its structural properties. The change in the spacing can be used to determine the type of polymer nanocomposites formed such as immiscible; no  $d$ -spacing changes, decomposed;  $d$ -spacing decrease, intercalated;  $d$ -spacing increase and exfoliated;  $d$ -spacing outside of angle ray diffraction.

Alexandre and Dubois (2000) summarized the morphological structure between different matrix bases in Figure 2.18. No change in  $d$  spacing were observed for the immiscible curve as it possessed the peak almost similar to  $2\theta$  which may be due to the lesser number of chained monomer between the galleries. On the other hand, intercalated structure showed a shift of its XRD peak towards the smaller angle of  $2\theta$  which might be caused by the incorporation of the organically modified fluorohectorite in the polymer matrix. In contrast to both of these, there were no peaks observed in the assigned diffractograms of silicone rubber which enable the deduction that exfoliation has occurred since it exceeded the limit of the XRD's diffraction peak. According to Alexandre and Dubois (2000), as far as exfoliated structure is concerned, no diffraction peaks are visible in the XRD diffractograms due to very large spacing between the layers which normally exceeds 8 nm.



Cao et al. (2005) employed XRD to determine the d-spacing for the combination of PU and MMT clay with different mixing procedures. They premixed 5% MMT-OH with either polyol (Tone 0305) or isocyanate (MRS-4) before adding the other monomer to study the effect of the clay-monomer mixing sequence on clay dispersion. Figure 2.20 shows that the nanocomposite prepared by the one-step approach shows a clear peak at  $2\theta = 2.6^\circ$ , which confirms that the PU chains have successfully diffused into the gallery of MMT-OH and caused intercalation.

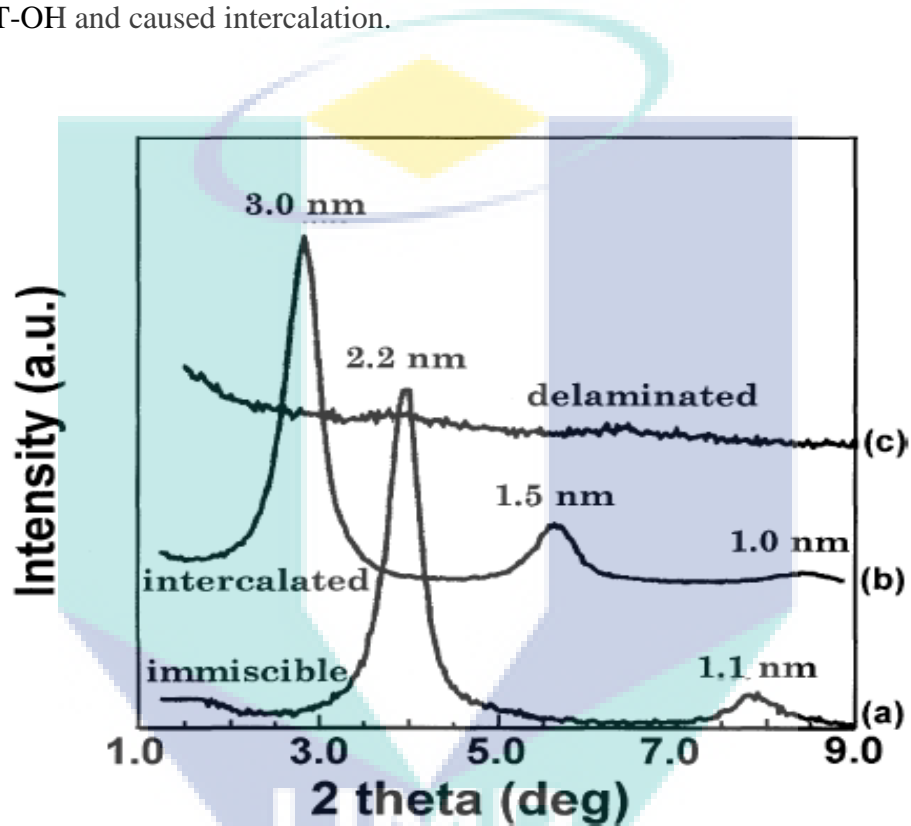


**Figure 2.18:** XRD patterns of: (a) phase separated microcomposite (b) intercalated nanocomposite and (c) exfoliated nanocomposite of modified fluorohectorite in HDPE, PS and silicone rubber

Source: Alexandre and Dubois (2000)

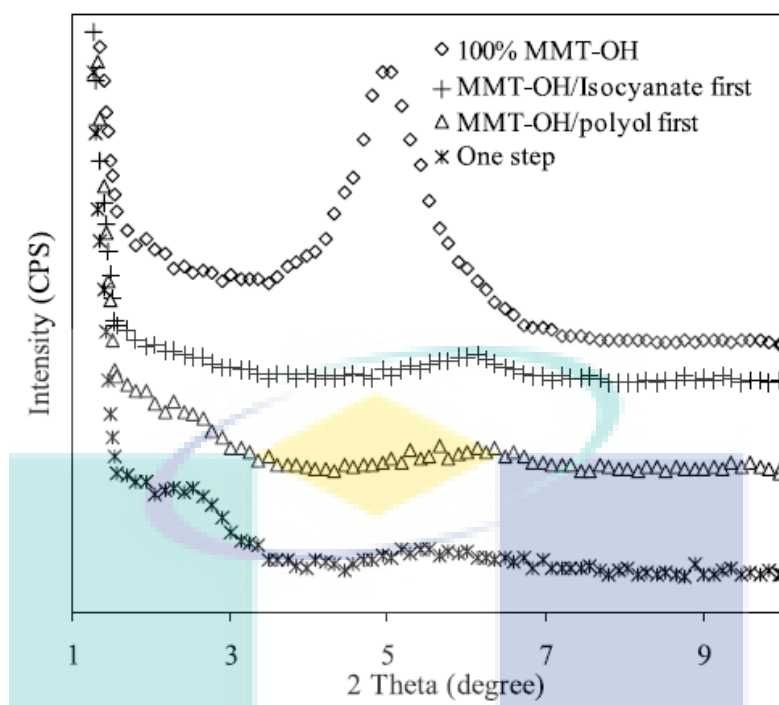


**Figure 2.19:** XRD of 5% MMT-OH/PU nanocomposites prepared by different mixing procedures

Source: Cao et al. (2005)

UMP

## 2.6 TESTING AND ANALYSIS OF POLYMER LAYERED SILICATES NANOCOMPOSITES (PLSN)

Polymer nanocomposites received great attention academically as well as industrially as it exploit a huge reinforcement compared to conventional polymers. Since the demonstration of a very impressive industrial application of nanocomposite by the Toyota Group in 1988, the study of polymer nanocomposite was taken into a higher level as drastic improvements were seen on the properties of the polymer nanocomposite at low clay loading (Khudyakov et al., 2009). The remarkable results stimulated many researches to conduct many testing and analysis of the nanocomposites

### 2.6.1 Mechanical Properties of PLSN

The improvement in the mechanical properties was first reported by Wang and Pinnavaia (1998). They intercalated clay layers with a wide range of polyols prior to reacting it with diisocyanates. The MMT clay exchanged with long chain onium ions had a good compatibility with those polyols. From their study, it was seen that at a loading of only 10 wt% of the clay, the strength, modulus and strain at break increases by more than 100% and all these mechanical properties increased with increasing clay loading. The advancement in the strength and modulus may be attributed to the reinforcement of the dispersed silicate layers whereas the improved elasticity may be related to the plasticizing effect of gallery onium ions.

Yusoh et al. (2010) reported in their study that the incorporation of organoclay into PU showed significant improvement on the hardness and the elastic modulus of the nanocomposites. Both these properties were seen to increase steadily with increasing organoclay content. The addition of 3% organoclay resulted in an increase of approximately 55% and 70%, for the hardness and the elastic modulus respectively. They justified that the two factors which were the main reason for the enhancement of the properties were the dispersion or high aspect ratio of nanoclay platelets and the exfoliation of organoclay as demonstrated by the wide-angle X-ray diffraction (WAXD) in their work.

In a study conducted by Xu et al. (2003) on biomedical polyurethane system, it was found that with 20% clay loading, the nanocomposites showed 300% increase in

initial modulus, 30% increase in strength, 50% in extensibility and 5 fold reductions in water vapour permeability. Apart from them, other researches that conducted the mechanical studies on polyurethane nanocomposites include Zilg et al. (1999). According to their study, polyurethane nanocomposites containing synthetic fluoromica exhibited enhanced tensile strength and elongation at break.

### 2.6.2 Thermal Characterization of PLSN

Thermal characterizations of PLSN are generally techniques in which a property of a specimen is continuously measured through pre-determined temperature profile. It is based on changes in the heat content (enthalpy) or the specific heat of a sample with temperature. The most common thermal analysis done on PLSN includes Differential Scanning Calorimetry (DSC) and Thermal Gravimetric Analysis (TGA).

#### *Differential Scanning Calorimetry (DSC)*

Differential Scanning Calorimetry (DSC) is employed to study the thermal characteristics of a material such as the melting temperature, crystallinity, and glass transition temperature. In the DSC analysis, thermal energy is supplied to the sample resulting in a rise in its enthalpy and its temperature which is determined by the specific heat of the sample. The specific heat of the material alters sharply or discontinuously when a change of state takes place. Physical and chemical changes in the sample accompanied by a change in enthalpy in the form of latent heat of fusion, latent heat of reaction or others can also be detected in this analysis.

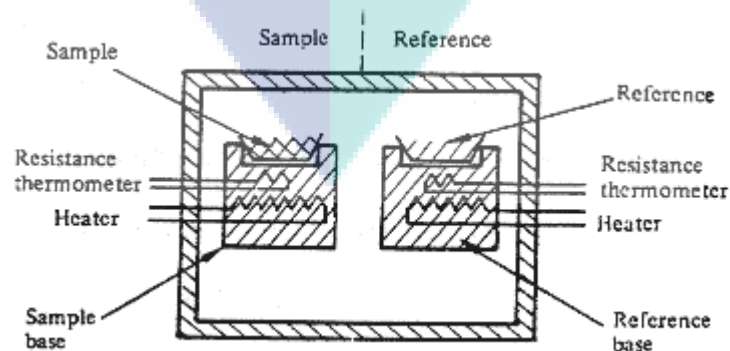


**Figure 2.20:** DSC experimental arrangement

Source: Bhattacharya et al. (2008)

In the experimental setup, both the sample and reference are maintained at the same set temperature and placed in identical environments, in metal pans on individual bases whereby each contains a platinum resistance thermometer and a heater as shown in Figure 2.21.

The thermal properties of polyurethane nanocomposites were seen to improve in many researches with the intercalation of organoclay (Chang and An, 2002, Lee and Lin 2006, Sreedar et al., 2006). The DSC analysis by Naguib et al. (2013) reported that the incorporation of the C30B had no significant effect on the melting temperatures and melting enthalpies of both the segments and nanocomposites, indicating that the organoclay is predominantly confined to the amorphous phase, without significantly affecting the development of crystals in the copolymer matrix. However, the DSC curves after rapid cooling of PUs and their nanocomposites depicted higher  $T_g$  value as compared to neat PU which were caused by the confinement effect of the segmental motions of intermolecular chains of the polymer within the clay galleries. They concluded their study by stating that the crystallization of PCL-PEG-PCL and PHB segments was enhanced by the presence of organoclay fillers.

Pavlicevic et al. (2013) reported in their work that the thermal properties of aliphatic polycarbonate based polyurethanes (PC-PU) were influenced by the dispersion of nanofillers. The addition of 1 wt. % bentonite and MMT increased the melting temperature values ( $T_m$ ) of 5651 based polyurethanes by 9°C and 11°C compared to  $T_m$  of unfilled sample based on the same polycarbonate diol. The positive influence of nanoclay addition on thermal properties of segmented thermoplastic polyurethanes is an evident of the reaction between nanoparticles and hard phase. The cooling DSC curves showed a retarded solidification above 65°C assigned to the crystallization of hard segments and with the addition of organically modified bentonite and montmorillonite, the crystallization temperature ( $T_c$ ) of samples based on diol 5651 is increased from 68 °C to 72 °C and 77 °C.

### ***Thermal Gravimetric Analysis (TGA)***

Thermal Gravimetric Analysis (TGA) is employed to study the thermal degradation of polymeric materials. This analysis involves continuous weighing of a small sample in a controlled atmosphere such as air or nitrogen as the temperature is increased at a programmed linear rate. Xiong et al. (2004) reported in their study that the degradation rates of the PU nanocomposites became slightly slower compared to that of PU, indicating an improvement of thermal stability. The authors attributed this to the incorporation of inorganic material that acts as a preventive measurement to heat expenditure that limits the degradation of the material.

Cervantes et al. (2009) reported in their study that the decomposition temperature for nanocomposites containing 4, 6 and 10 wt. % were 6, 25 and 40 °C higher than that obtained for pure polyurethane. This behavior obtained for nanocomposites was related to strong interactions between the organic clay and PU matrix. Apart from that, Baysal et al. (2013) showed in their study that the introduction of organoclays into polymer backbones increased thermal stability. The two steps of degradation can be seen in Figure 2.22 in which the first degradation is around 260–285°C and the other is upper than 553–593 °C. The first stage is major and sharp, which involves the thermal decomposition of the intercalated polymers whereby the decomposition temperature in this stage started at 260°C and took place to 285°C. The second stage is in the temperature range of  $\approx 553\text{--}593$  °C and in this stage, the nanocomposites displayed higher thermal resistance than its counterpart. They also reported that the high thermal stability of the nanocomposites prepared may be due to the presence of the higher amount of organoclay.

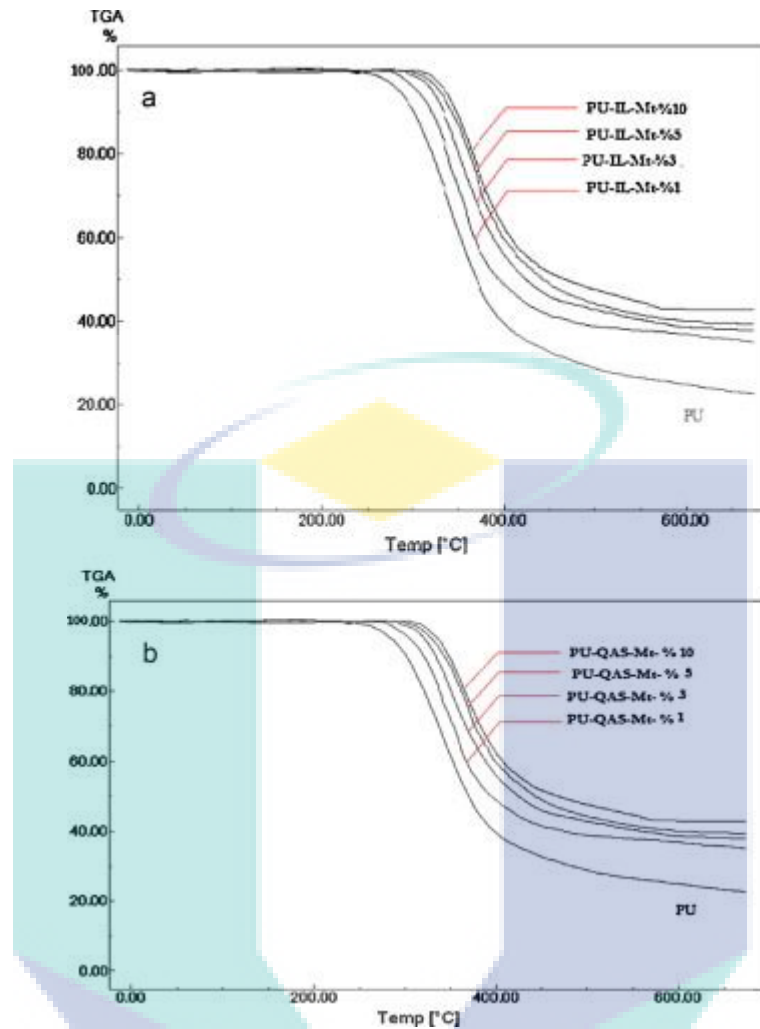


**Figure 2.21:** TGA thermogram of PU, PU-IL-Mt (a) and PU-QAS-Mt (b)

Source: Baysal et al. (2013)

### *Thermal Conductivity*

Thermal conductivity is defined as the quantity of heat transmitted through a unit thickness in a direction normal to surface unit area at a steady state condition. It is an intrinsic property of a material to transfer heat within a material without any motion of the material as whole (Alam et al., 2012). In an insulation material, thermal conductivity is the most important property considered especially in new building constructions due to the energy conservation and thermal performance. A good insulation material has lower coefficient of thermal conductivity which indicates slow movement of heat through the material. Yao et al. (2002) reported a decrease in the thermal conductivity of polyurethane- montmorillonite nanocomposites as a function of

increasing clay concentration. This phenomenon is explained by the increase in thermal resistance at the interface between the polymer and nanoparticles (Nan et al., 1997). This is further supported by a research from Luo and Lloyd (2012). From their study, three methods to enhance the interfacial thermal conductance were the optimization of filler size, increase in polymer density and chemical modification of the filler to promote strong covalent bonds between the polymer and its filler in which the strong interfacial interactions at the atomic level enhances the heat transfer at the interface. Other researches who obtained similar decreasing trend in thermal conductivity were Kim et al. (2007) and Zink et al. (2006).

### 2.6.3 Permeability Analysis of PLSN

In general, the term permeability describes the penetration of low molecular weight substances through a barrier. Permeability can be defined as the transmission of permeate through a resisting material and for a polymer film, its permeability to gases and vapor is very important. The permeability analysis of PLSN was researched by many authors in an attempt to study the effects of the silicate layers as an impermeable material. These layers provides longer diffusion path across the polymer which results in improved barrier properties as shown in Figure 2.23.

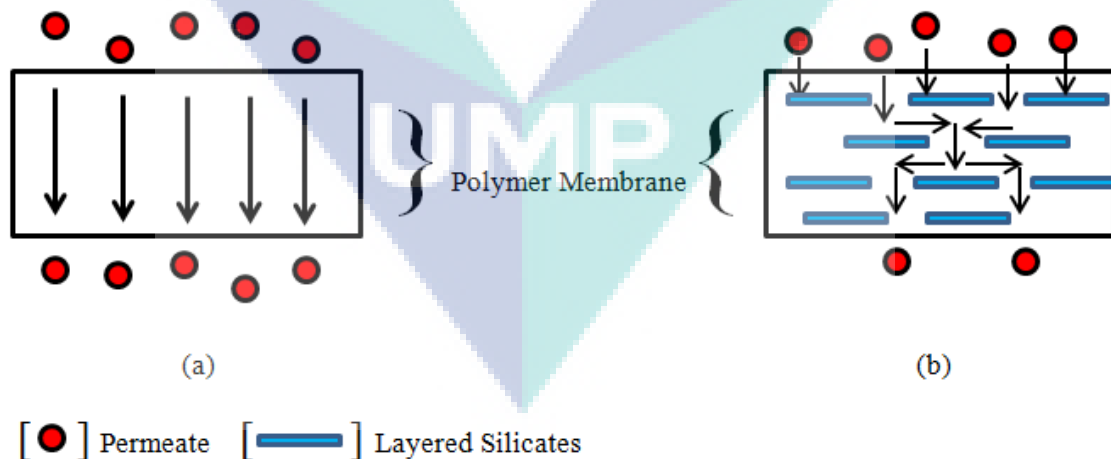


**Figure 2.22:** Permeation in polymer composites (a) conventional composite (b) formation of tortuous path in layered silicates



Osman et al. (2003) prepared adhesive nanocomposites of organically modified montmorillonite and polyurethane and measured their permeability to oxygen and water vapor. From their study, the oxygen transmission rate decayed asymptotically with increasing aluminosilicate volume fraction. They achieved a 30% reduction at 3 vol %. Alonso et al. (2009) studied the transport properties in polyurethane clay nanocomposites as barrier materials. They compared the oxygen (O<sub>2</sub>) and methane (CH<sub>4</sub>) permeabilities in sonicated and stirred nanocomposites with 28 wt% of clay and found that the addition of clay particles decreased the O<sub>2</sub> and CH<sub>4</sub> permeation when compared to pristine polyurethane. The permeation results obtained implied that the clay particles create a more tortuous path for the penetrating gas molecules.

Tortora et al. (2002) prepared nanocomposites of polyurethane and organically modified montmorillonite and found that the permeability of water vapour and dichloromethane showed a remarkable decrease up to 20%. It can be deduced that in general, polymers filled with impermeable nanoparticle have lower permeability as compared to virgin polymers.

The logo for UMP (Universiti Malaysia Perlis) is a large, downward-pointing arrow shape. It is composed of four triangular sections meeting at a central point. The top-left and bottom-right sections are light blue, while the top-right and bottom-left sections are a slightly darker shade of blue. The letters 'UMP' are printed in a bold, white, sans-serif font across the center of the arrow.

UMP

## CHAPTER 3

### RESEARCH METHODOLOGY

#### 3.1 INTRODUCTION

The grade of polymer and the type of organoclay used during this research would be described in this chapter. In addition, the experimental work carried out in order to understand the effect of incorporation of nanofiller on the mechanical properties, thermal and permeability behavior of polyurethane would also be included to outline the designed experimental work.

#### 3.2 MATERIALS

During the preparation of PLSN, an industrial grade of thermoplastic polyurethane was used as the polymer matrix while marketed montmorillonite clay (MMT) under the registered name Cloisite<sup>®</sup>Na<sup>+</sup> was incorporated as nano scaled filler. The modification processes were carried out using copper (II) chloride hexahydrate and iron (III) chloride hexahydrate. Analytical grade methanol was used in the TMI modification process whereas chloroform was used as the solvent in casting the nanocomposites film. The characteristics and the properties of the material used would be further explained in this section.

### 3.2.1 Polyurethane (PU)

In this research, a commercial grade of PU under the trademark of Estane<sup>®</sup> GP 75AE NAT 021 which was manufactured by Lubrizol Advanced Materials Inc. (Belgium) was employed as the polymer base. The structure of PU is shown in Figure 3.1 whereas the physical and chemical features of PU are listed in Table 3.1.

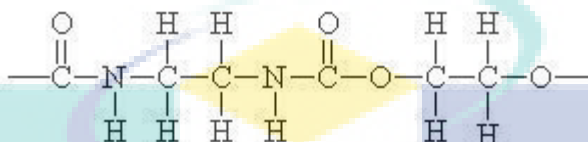


**Figure 3.1:** Structure of PU

**Table 3.1:** Physical and chemical properties of PU

Physical State	solid
Appearance	granules
Colour	colourless
Odour	slight
Specific gravity (g/cc)	>1.00
Density (g/cm <sup>3</sup> )	1.22
Ignition temperature (°C)	407
Melting point (°C)	177-232
Solubility in water	Insoluble
Flash Point	400

### 3.2.2 Cloisite Na<sup>+</sup>

In this work, Cloisite Na<sup>+</sup> was selected as the nano filler. It is a natural montmorillonite used as an additive for plastics to improve various physical properties such as reinforcement and barrier. The MMT was supplied by Southern Clay Products (Rockwood additives, Ltd). The modifier concentration for this clay was determined to be 95 mequiv/ 100g of clay. The physical and the chemical traits of the MMT clay would be listed in Table 3.2.

**Table 3.2:** Properties of Cloisite Na<sup>+</sup>

Physical State	solid
Form	powder
Colour	tan
Odour	mild
Solubility in water	insoluble
Dry particles size	2-13 $\mu$ m
Density (g/cc)	2.86
% Moisture	4-9
% Weight Loss on Ignition	7
X Ray Results	$d_{001} = 11.7\text{\AA}$

UMP

### 3.2.3 Copper (II) chloride and Iron (III) chloride

In this research, Copper (II) Chloride and Iron (III) chloride were the materials used in the modification process of the pristine MMT clay via ion exchange method and they were purchased from Fisher Scientific (M) Sdn. Bhd. The physical and chemical properties of Copper (II) Chloride and Iron (III) chloride are laid out in Tables 3.3 and 3.4 respectively.

**Table 3.3:** Physical and chemical properties of Copper (II) Chloride

Physical State	solid
Form	crystalline powder
Colour	brown
Relative Density (g/cm <sup>3</sup> at 20°C)	3,386
Freezing / Melting Point (°C)	620
Boiling Point (°C)	993
Molecular Formula	CuCl <sub>2</sub>
Molecular Weight	134.45

**Table 3.4:** Physical and chemical properties of Iron (III) Chloride

Physical State	solid
Form	crystals
Colour	yellow
Relative Density (g/cm <sup>3</sup> )	1.82
Freezing / Melting Point (°C)	37
Boiling Point (°C)	280-295
Molecular Formula	FeCl <sub>3</sub> .6H <sub>2</sub> O
Molecular Weight	270.29

### 3.2.4 Methanol

In the modification process of the montmorillonite clay, methanol was used as the solvent and it was purchased from Fisher Scientific (M) Sdn. Bhd. The chemical and the physical properties of methanol are contained in Table 3.5.

**Table 3.5:** Physical and chemical properties of Methanol

Physical State	Liquid
Colour	Clear
Odour	Mild
Vapour Pressure (mmHg at 20°C)	128
Vapour Density	1.11
Viscosity at 20°C	0.55 cP
Boiling Point at 101.3 kPa (°C)	64.7
Freezing/Melting Point (°C)	-97.8
Solubility	Completely soluble
Specific Gravity/Density (g/cm <sup>3</sup> )	7910
Molecular Formula	CH <sub>4</sub> O
Molecular Weight	32.04

### 3.2.5 Chloroform

In the preparation of polyurethane organoclay nanocomposite, Chloroform was used as the main solvent in the film casting procedure and it was purchased from Fisher Scientific (M) Sdn. Bhd. The chemical and physical properties of chloroform are displayed in Table 3.6.

**Table 3.6: Properties of Chloroform**

Physical State	Liquid
Colour	colourless, clear
Odour	Etheric
Boiling Point (°C)	61
Melting Point (°C)	-63.5
Vapour Pressure (kPa at 20°C)	21.1
Vapour Density	4.36
Solubility	mildly soluble in cold water
Molecular Formula	CHCl <sub>3</sub>
Molecular Weight	119.38

UMP

### 3.3 MMT CLAY MODIFICATION USING TRANSITION METAL IONS

In this research work, one of the main objective that were given much emphasis was the modification of the MMT clay through ion exchange process using two types of transition metal ions. This step was taken to ensure the homogeneous dispersion of the clay into the polymer matrix. The experimental works of the modification process are explained in a two steps process as following.

#### 3.3.1 Pre-treatment of MMT Clay

Prior to the modification stages, the clay sample was thoroughly washed in order to remove the excess surfactants and the impurities in it. Initially, the clay sample was added into methanol which was the solvent in this process at a ratio of 2g of clay to 40ml of methanol and the clay suspension was stirred vigorously for 24 hours under room temperature (Nawani et al., 2007). It was observed that the clay started swelling during the stirring process resulting in a viscous slurry solution later on. The slurry was filtered after 24 hours and dried in vacuum oven for 12 hours at 80°C.

#### 3.3.2 Preparation of TMI's solution and Modification Phase

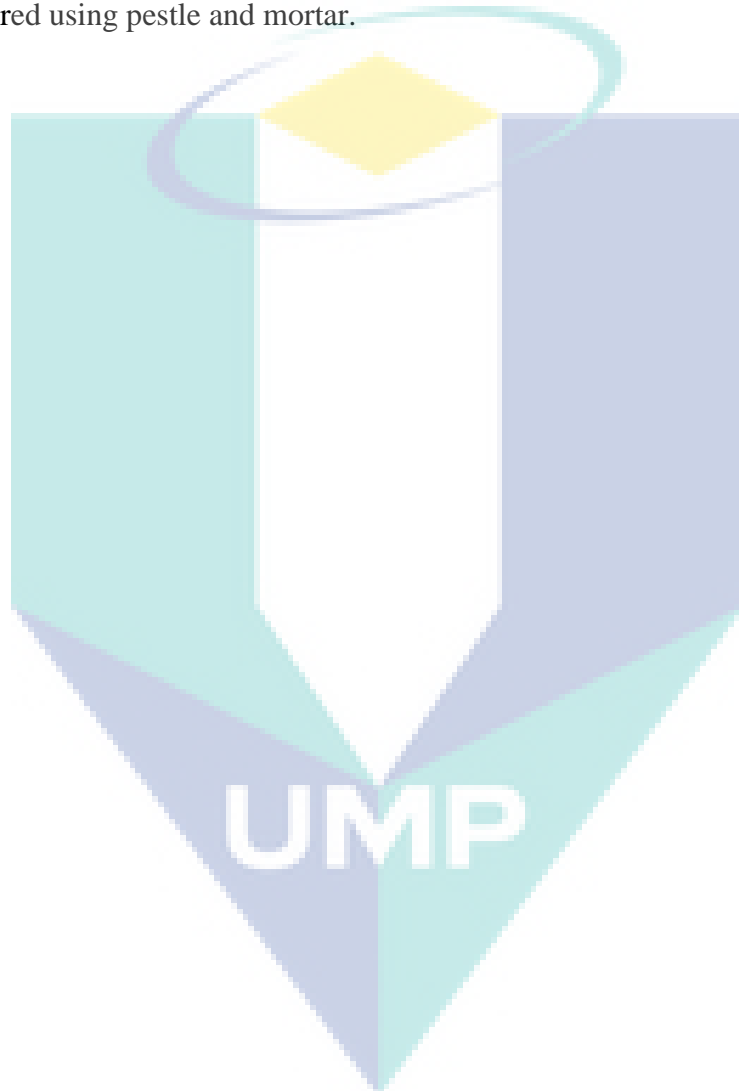
Subsequent to the pre-treatment process, the washed and dried samples were placed in 0.30M of the desired metal ion salts using the same solvent in the washing process for the ion exchange to occur. Two types of metal ions that were employed in this study was copper ( $\text{Cu}^{2+}$ ) and iron ( $\text{Fe}^{3+}$ ). The required weight of the material to produce 200ml of the TMI solution with 0.3M is laid in Table 3.7.

**Table 3.7:** TMI Salts used in the Modification Process

<b>TMI salt used</b>	<b>Concentration [M]</b>	<b>Molecular Weight (g/Mol)</b>	<b>Weight Required (g)</b>
Copper (II) Chloride, $\text{CuCl}_2$	0.30	134.50	8.07
Iron (III) Chloride, $\text{FeCl}_3$	0.30	270.29	16.21



In the modification process, 10g of pre-treated clay was used for every 200ml of the metal ion solution. Firstly, the required amount of the salt and the pre-treated clay was inserted into methanol and the solution was stirred exuberantly for 36 hours (Nawani et al., 2007). The clay suspension was kept in a closed container as a preventive measurement to solvent evaporation. After the TMI treatment, the clay samples were filtered, washed again and dried in a vacuum for 12 hours at 80°C. The dried clay was then powdered using pestle and mortar.



### 3.4 CHARACTERIZATION OF THE MODIFIED MMT CLAY

#### 3.4.1 Inductively Coupled Plasma Mass Spectrometry

Inductively Coupled Plasma Mass Spectrometry (ICP-MS Agilent 7500X) was employed in this study to analyze trace metals in the modified clay to ensure that the ion exchange has occurred successfully during the modification process. The mechanism in this instrument is that ionized or excited atoms produced by the application of plasma to the clay sample are separated and identified according to their mass and charge ratio (Baroi, 2006). Plasma is partially ionized gas with sufficiently high temperature to atomize, ionize and excite most of the elements in the periodic table (Ebdon et al., 1998). Generally, gases such as argon, helium or air are usually used to produce plasma and in this study, argon gas is used as it produces relatively pure form of ions or excited atoms. ICP-MS is very sensitive equipment and it acquires certain special precautions prior to sample analysis.



**Figure 3.2:** ICP-MS Equipment

### 3.5 PREPARATION OF PU-MMT NANOCOMPOSITES

Succeeding the TMI modification process, the polymer nanocomposite is prepared through a solvent casting method. In this work, four compositions of the nanocomposites were varied and it is contained in Table 3.8.

**Table 3.8:** Weight percentage PU-MMT prepared

No	PU		MMT / MMT Cu <sup>2+</sup> / MMT Fe <sup>3+</sup>	
	%	Weight (g)	%	Weight (g)
1	100	4	0	0
2	99	3.96	1	0.04
3	98	3.92	2	0.08
4	97	3.88	3	0.12

This step is begun by measuring the PU and MMT clay according to the weight percentage shown in Table 3.8. PU and MMT clay were poured into 80mL and 20 mL of chloroform respectively. The PU solution was stirred at a temperature of 80°C for five hours whereas the clay solution was stirred separately for one and half hours at the same temperature and after that, it was poured into the PU solution. Both these solutions were mixed and stirred at medium stirring effects. Great importance was given to ensure that the mixture was sealed fully during the stirring process to hinder solvent evaporation. After the stirring time was completed, the solution was then placed in an ultrasonic water bath 30HT for 15 minutes to prevent bubble formation. The resultant solution was then poured into a glass petri dish with a diameter of 11cm and depth of 2cm. The chloroform was allowed to evaporate and dried at room temperature and after two days, a thin layer of the nanocomposite membrane is formed. The same steps are repeated for 1 wt%, 2 wt% and 3 wt% of the pristine MMT clay, modified Cu<sup>2+</sup> and Fe<sup>3+</sup>. Although there have been previous work on higher clay loading percentages on polyurethane such as 10wt% (Wang and Pinnavaia, 1999) and 5wt% (Yusoh et al., 2010), the small clay loading was used in this study as there were no previous work done on polyurethane and clay modified with transition metal ions and the level of aggregations could not be anticipated. In addition, in order to obtain a good dispersion

with lesser aggregates from the modified clay, lower percentage of clay loading was seen to be essential.

### **3.6 CHARACTERIZATION OF POLYURETHANE NANOCOMPOSITE**

This section would be dedicated for disclosing the characterization techniques used in order to understand the morphological structure of the nanocomposites. The characterization of the polyurethane nanocomposites was engaged using Fourier Transform Infrared (FTIR), X-Ray Diffraction (XRD), Scanning Electron Microscope (SEM) and Field Emission Scanning Electron Microscope (FESEM).

#### **3.6.1 Fourier Transform Infrared (FTIR)**

Fourier Transform Infrared (FTIR) is an analytical technique of infrared spectroscopy. It is operated by passing through an IR radiation through the sample to obtain spectrum that represents the molecular adsorption and transmission of the sample. Due to the fact that each material has its own unique combination of atoms, no two compounds is able to produce the same spectrum thus this enables the positive identification of every different kind of material and amount of material present in the sample can be indicated from the size of the peaks in the spectrum.

In this study, FTIR was employed to determine the components present in the sample and to study the effects that were brought by the modified clay during the preparation of the polyurethane nanocomposites in a Nicolet Avatar 370 DTGS infrared spectrophotometer. Attenuated total reflectance (ATR) technique was used in carrying out the measurements and the Golden Gate single reflection Germanium was used as prism. Prior to the analysis, the solid demountable cell was dismantled, cleaned using Kimwipes and solvent and reassembled back. Once the cell is placed into the FTIR spectrometer, the polyurethane nanocomposite film obtained from the preparation stage which was already cut into a small size (~0.25mm diameter) was placed on the compartment. After the infrared sample compartment was sealed, a background spectrum was taken and assigned for subsequent spectra acquisitions. The sample spectrums for all the samples were obtained and compared using Nicolet OMNIC software for further analysis.



**Figure 3.3:** FTIR Equipment

### 3.6.2 X-Ray Diffraction (XRD)

X-Ray Diffraction (XRD) is one of the most established analytical tools to study the state of dispersion and exfoliation of the nanoparticles due to its easiness and availability (Sinha et al., 2003, Biswas and Sinha, 2001 and Alexander et al. 2000). In the XRD analysis, the structure of the nanocomposites whether it is intercalated or exfoliated can be identified by monitoring the intensity of the basal reflections from the distributed silicate layers, its shape and position (Kusmono et al., 2013). The mechanism of XRD is that the X-rays are diffracted when it interacts with the electrons of the analyzed substance as the pattern of diffraction is depended on the wavelength of the employed x-rays. The obtained results are exemplified by  $2\theta$  scans which will characterize the factors that determine the intensity of the x-ray reflections. The determination of the crystal structure can be completed by analyzing the positions and the intensities of diffraction peaks in the range of diffraction angle from  $3-20^\circ$ .

In this study, Rigaku Miniflex II X-Ray Diffractometer is used to analyze the structure of the polyurethane clay nanocomposites. The extent of intercalation or

exfoliation that has occurred in the nanocomposites would be determined by measuring the inter-gallery spacing,  $d_{001}$  that existed between the monomer chain and the layered silicates.

The d-spacing ( $d$ ) of the interlayer gallery of the  $\text{Na}^+$  and the PU based nanocomposites was calculated using Bragg's Law equation.

$$n\lambda = 2d \sin \theta \quad \text{Eq. (3.1)}$$

Where:

- $d$  = Space between layers of the clay
- $\lambda$  = Wavelength of the X-ray which is
- $\theta$  = Angle at the maximum point of the first peak into a spectrum
- $n$  = Order of diffraction



**Figure 3.4:** XRD Equipment

### 3.6.3 Scanning Electron Microscopy (SEM)

Scanning Electron Microscopy (SEM) is a morphological study that is usually employed to study the crystalline structure and orientation of materials making up the sample. The mechanism of SEM is that a largely magnified image is produced by using electrons instead of light. The beam of electrons is produced at the top of the microscope using an electron gun and these electron beams is designated to follow a vertical path through the microscope. The beam travels through electromagnetic field and lensed and once the sample has been hit by the beam, x-rays and electrons are ejected from the sample and it is converted by the detectors into a signal that is sent to the screen displaying the final image.

In this work, SEM was used to determine the size and distribution of particles in the polymer nanocomposites. The samples were prepared by cutting a small piece from the prepared polyurethane nanocomposites film and these small pieces of film were placed on a specimen holder and it was coated with platinum particles using BALTEC SCD 005 Sputter Coater. The coating was done to provide conductivity, protecting the samples from the beam damage and to eliminate charging issues. Once the sample had been coated successfully, it was attached to stub and transferred to the SEM chamber for the analysis. SEM was performed in a ZEISS EVO 50 Scanning Electron Microscope. Once the analysis has been completed, the SEM image that was taken using backscattering detector is obtained. The setup parameters that were used in this analysis are shown in Table 3.9.

**Table 3.9:** Parameters used in SEM analysis

EHT	7 – 10 kV
I probe	100 pA
WD	8.5 mm
Mag	15x – 2kx

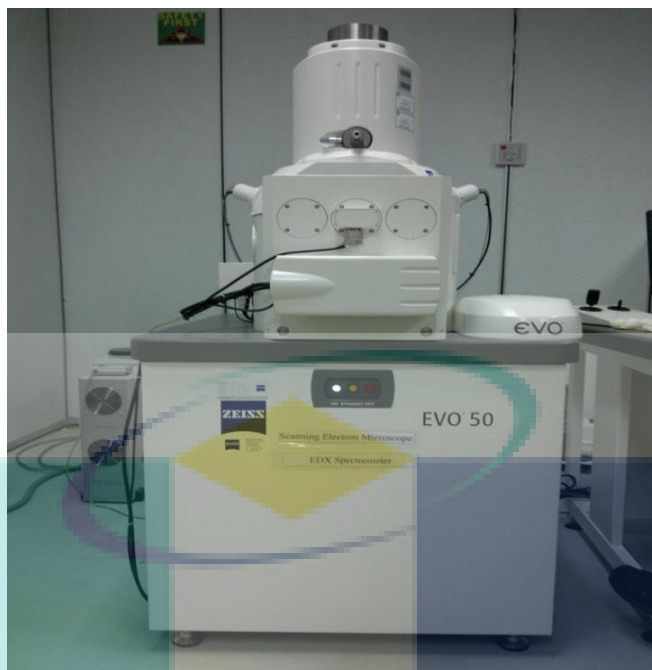


**Figure 3.5:** ZEISS EVO 50 Scanning Electron Microscope



**Figure 3.6:** BALTEC SCD 005 Sputter Coater



### 3.6.4 Field Emission Scanning Electron Microscopy (FESEM)

Field Emission Scanning Electron Microscopy (FESEM) is an analysis that provides topographical and elemental information of the sample at a magnification of 10x to 300 000x. The FESEM analysis is common in fields that require characterization of solid materials such as polymer nanocomposites as it is known to produce clear and high quality images with negligible electrical charging of samples. The FESEM is operated by shooting high energy electron beams onto the sample and the x-ray being emitted as a resultant of this is collected and analyzed where these x-ray spectra yields quantitative elemental information about the sample.

In this research, the FESEM analysis was done to study the morphological structure of the obtained polyurethane clay nanocomposites. The signal derived from the electron-sample interactions would result on the information of the surface structure of the nanocomposites at a certain magnification range to give a better and clearer understanding on the surface structure. The dispersion and the distribution quality of the nanocomposites were characterized using the JOEL FESEM JSM-7800F. The samples were prepared by cutting a small amount of film from the prepared polyurethane nanocomposites and it was coated with platinum particles prior to analysis. The coated samples were mounted on a universal sample holder with stub forceps and the analysis was begun after the samples were transferred into the FESEM chamber. Once the analysis has been completed, the FESEM images are obtained and analyzed accordingly.

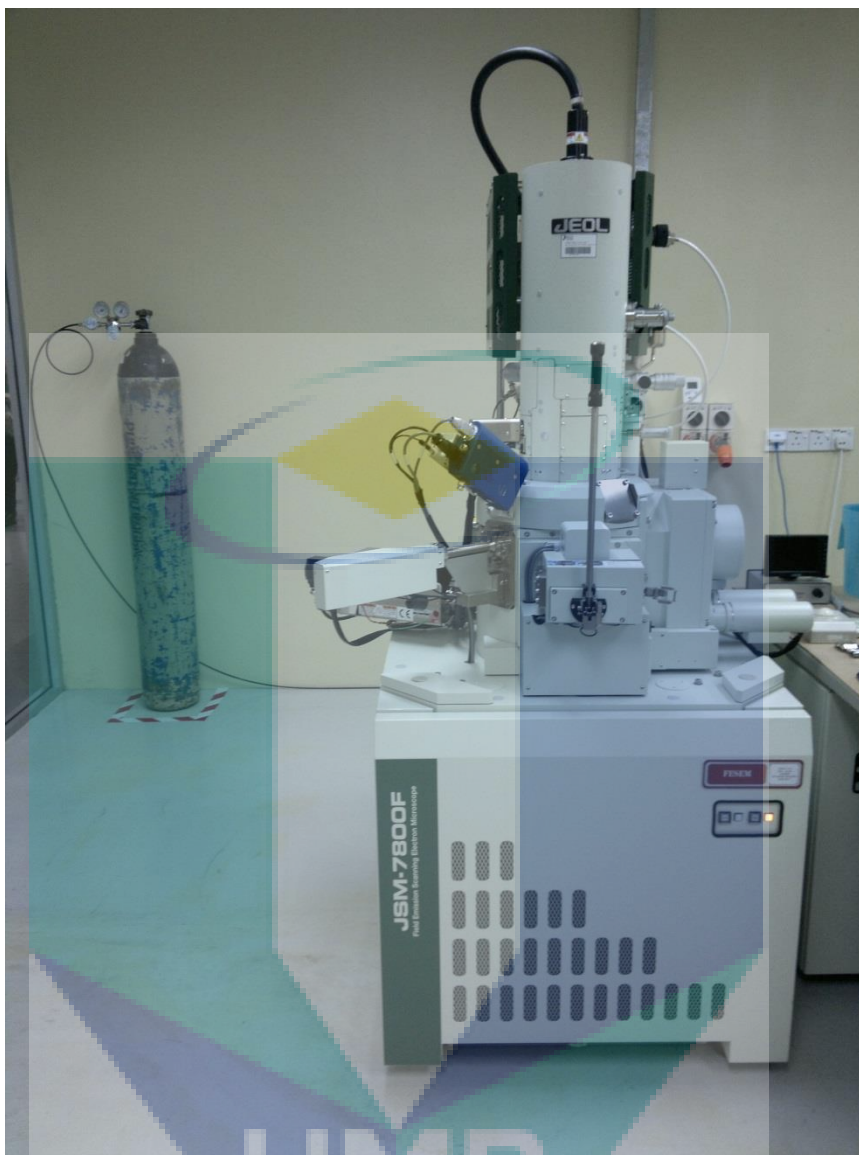


**Figure 3.7:** JOEL FESEM JSM-7800F Equipment

### 3.7 PROPERTIES OF POLYMER NANOCOMPOSITES

Sub sequential to the morphological studies and the characterization study, the polyurethane nanocomposites are then tested in order to analyze and understand the advancement in their properties as compared to pristine polyurethane. In this section of the thesis, the testing methods that assisted in studying the mechanical, thermal and permeability studies of the polymer nanocomposites is disclosed.

#### 3.7.1 Mechanical Testing

In this work, the mechanical testing that were done on the polyurethane nanocomposites was tensile testing whereby two mechanical properties were obtained from this analysis which were the tensile stress and elongation at break ( $el$ ). Prior to testing, the samples had to be prepared in a ‘dogbone’ shaped samples. The polyurethane nanocomposites films were cut into the prescribed shape following the guidelines provided in ASTM document D882. The dimensions of the sample were 0.3 mm in thickness, 4 mm in width and 9.6 mm in length. Great care was taken to ensure no notches existed in the middle region of the sample to avoid necking during the testing process. Figure 3.8 illustrates the prepared sample for the tensile analysis. The tensile testing was performed in an Instron Universal Testing Machine. The edges of the samples were wrapped with two layers of paper to prevent it slipping from the extensometer. The load cell was calibrated preceding the usage. The load applied was 1mm/min and six samples were tested for each batch. The tensile stress and the extension at break were obtained from the test. The data for tensile stress were obtained directly from the analysis however, in order to calculate  $el$ , the following formula was used.

$$\varepsilon = \frac{\Delta l}{l_o} \quad \text{Eq. (3.2)}$$

Where:

- $\Delta l$  = Change in length of the sample  
 $l_o$  = Initial length of the sample

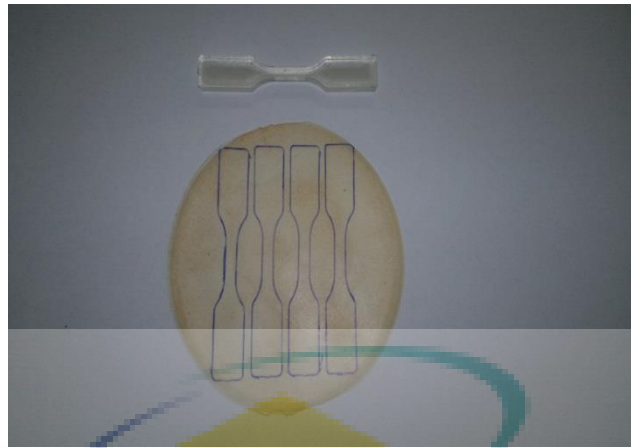


**Figure 3.8:** Dogbone sample



**Figure 3.9:** Instron Universal Testing Machine

### 3.7.2 Thermal Analysis

There were three types of thermal analysis done in this work to study the thermal effects of the incorporation of clay into the polyurethane matrix. The types of thermal testing done were the Thermal Gravimetric Analysis (TGA), Differential Scanning Calorimetry (DSC) and thermal conductivity. The methods employed on these analyses are outlined in this section.

#### *Thermal Gravimetric Analysis (TGA)*

Thermal Gravimetric Analysis (TGA) is a thermal analysis method to determine the physical and chemical changes in the materials properties in terms of temperature accession or in terms of time. Degradation resistance of the materials to heat can also be analyzed using this analysis (Becker and Simon, 2006). In a TGA analysis, the samples were placed in a pan which was held in a microbalance in which the pan and the sample are heated in a controlled manner. The weight change at a specific temperature is said to correspond to reaction or changes in the sample (Materials Evaluation and Engineering, 2009). The weight change observed can be related to decomposition, electrochemical reactions or other changes in the sample.

In this work, TGA was employed to study the thermal behavior of the polyurethane nanocomposites using TGA/DSC-1 Mettler Toledo. The equipment was calibrated prior to analysis and for each set of experiment, the pan was cleaned to remove any impurities or residues. Capped particle samples of approximately 5mg was prepared from the polyurethane nanocomposites film and the TGA analysis was performed at a ramp rate of 20°C/min at a temperature range from 30°C to 800°C under the influence of nitrogen gas. The evaluation of the TGA curve was completed by using “STAR Excellence Software” of Mettler Toledo.



**Figure 3.10:** TGA Q500 Equipment

### *Differential Scanning Calorimetry (DSC) Analysis*

Differential Scanning Calorimetry (DSC) is a thermo analytical equipment that is used to characterize the thermophysical properties of polymers such as melting temperature, heat of melting, percentage of crystallinity and crystallization. DSC can be defined as the measurement of the change of the difference in the heat flow rate to the sample and to a reference sample while they are subjected to a controlled temperature program (Hohne et al., 2003).

In this research work, the melting and crystallization behavior of polyurethane nanocomposites were analyzed using the differential scanning calorimetry model, TA-Instrument DSC/Q 100. The sample amount that was needed for the analysis which was approximately 2mg was weighed accurately prior to placing it in closed platinum pans. The pan was continuously heated under the influence of nitrogen gas from  $-70^{\circ}\text{C}$  to  $80^{\circ}\text{C}$  (Xiong et al., 2004) in the first heating rate. This procedure was completed after the second heating state in the DSC cycle which was followed by a cooling step from  $-70^{\circ}\text{C}$  to  $80^{\circ}\text{C}$ .



**Figure 3.11:** DSC Q100 Equipment

### ***Thermal Conductivity***

Thermal conductivity analysis was employed to study the ability of the nanocomposites to conduct heat and it is measured in watts per meter Kelvin (W/(m.K)). In this study, thermal conductivity was measured using KD2 Pro Thermal Properties Analyser (Decagon Devices, USA) which is based on the transient hot wire method. The dual-needle sensor with 1.3mm diameter, 30mm long and 6mm spacing was used (SH-1). The sensor is built in with a heating element and a thermo-resistor and is connected to a microprocessor for the controlling and conducting measurements. The dual needle was inserted into the polyurethane nanocomposite samples and samples were kept at the same temperature condition for 30 minutes to ensure temperature equilibrium before each measurement. An average of three measurements was taken for each type of the samples. Figure 3.12 shows the thermal conductivity analyzer used.



**Figure 3.12: KD2 Pro Thermal Conductivity Analyzer**

UMP



### 3.8 Permeability Studies

There were two types of permeability studies conducted in this study which were the gas permeability and the water permeability. The permeation tests were done to study the characteristics of the LS on the barrier properties of the polyurethane nanocomposites and the methodologies are described below.

#### 3.8.1 Gas Permeability

The gas permeation test on the polyurethane nanocomposites was done using two types of gases which were the oxygen and nitrogen gas. This study was conducted to analyze the improvements in the barrier properties by the introduction of fillers in the polyurethane matrix. The permeation process consists of three main processes which are the dissolution of the gases into the polymer matrix, molecular diffusion of the gases in and through the polymer matrix and finally the diffusion out (Oguzlu, 2011).

In this work, a Membrane Separation Unit was used to study the permeability of the nitrogen and oxygen gas and it was determined using the constant pressure method at room temperature. The prepared polyurethane nanocomposites membrane was prepared in a circular shape with a diameter of 5.5 cm and placed in the membrane cell of the separation unit as shown in Figure 3.12. The feed side of the membrane was maintained at 1.5 bar whereas the permeate side was maintained at atmospheric pressure. The experiment was repeated three times and the average time taken for each permeation test was recorded. Gas permeability was then calculated from the following equation (Semsarzadech et al., 2007).

$$P = \frac{ql}{(p_1 - p_2)A} \quad \text{Eq. (3.3)}$$

Where:

- |                                   |   |
|-----------------------------------|---|
| P                                 | gas permeability                          |
| q                                 | = flow rate of the permeated gas;         |
| l                                 | = membrane thickness                      |
| p <sub>1</sub> and p <sub>2</sub> | = pressures at both sides of the membrane |
| A                                 | = effective membrane area                 |

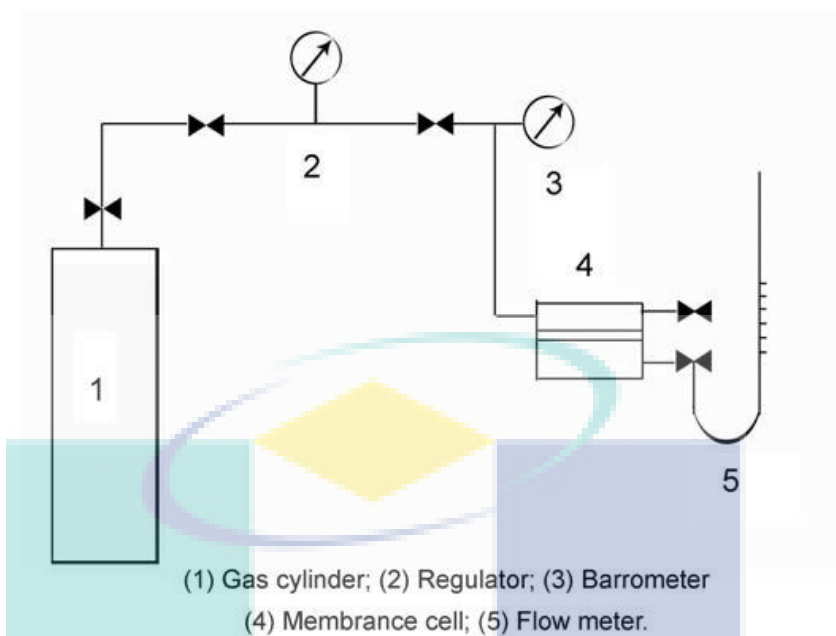


**Figure 3.13:** Schematic design of permeation apparatus

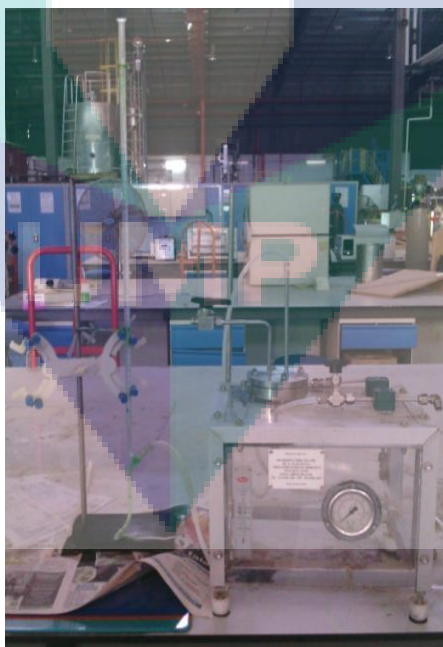


**Figure 3.14:** Membrane Separation Unit

### 3.8.2 Water Permeability

Generally, the water permeability analysis is done to see the permeation of water molecules through the polymer membrane. This is crucial to ensure the durability of the polymer material as absorption of water or water vapour may lead to microbial growth, undesirable changes and deteriorative chemical reactions (Oguzlu, 2011). In this study, the water permeation through the membranes was measured using a Water Permeability Testing System as shown in Figure 3.14. Prior to the analysis, the polyurethane nanocomposites membranes were prepared in a circular shape with a diameter of 5.0cm and placed in the test cell. Nitrogen gas was supplied to the system and the rate of discharge of water under laminar flow conditions was made constant to 10mL. The pressure was varied from 2 bars to 4 bars and time was recorded when 10mL of water were discharged from the system at each different pressure. The permeability rate was obtained from the graph of pressure versus time (Kapteijn et al., 1995).



**Figure 3.15:** Water Permeability Testing System

## CHAPTER 4

### RESULTS AND DISCUSSION

#### 4.1 INTRODUCTION

This chapter discusses the results obtained from analysis and tests made based on Chapter 3. The effectiveness of the modification process on the properties of the nanocomposites is to be discussed and reviewed in this section. The morphological studies through ICP-MS, FTIR, SEM and FESEM are discussed. This chapter is further expanded to the effects of the pristine and modified montmorillonite on the mechanical, permeability and thermal properties of polyurethane.

#### 4.2 MODIFICATION OF MMT CLAY

##### 4.2.1 Mechanism of Transition Metal Ion (TMI) Modification

Transition metal ions (TMI) modification was employed on the clay prior to the fabrication of the nanocomposites using copper ions from copper (II) chloride ( $\text{CuCl}_2$ ) and iron ions from iron (III) chloride ( $\text{FeCl}_3$ ). The modification process was intended to change the nature of the clay which is hydrophilic in order for it to be compatible with the polymer host which is polyurethane (PU). The hydrophilic nature of the clay is caused by the isomorphous substitution of the  $\text{SiO}_4$  tetrahedral with  $[\text{AlO}_6]^{3-}$  tetrahedral and  $[\text{AlO}_6]^{3-}$  octahedral which causes an excess of negative charges within the layers in the sheet and these negative charges are balanced with additional cations such as  $\text{Ca}^{2+}$  and  $\text{Na}^+$  which are located within the layers. The counterions are shared by two neighboring platelets which results in this stacks to be held tightly together as shown in Figure 4.1.

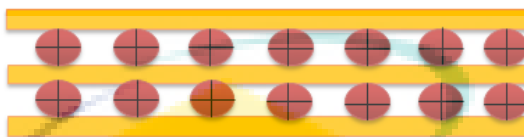
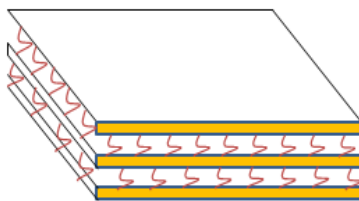
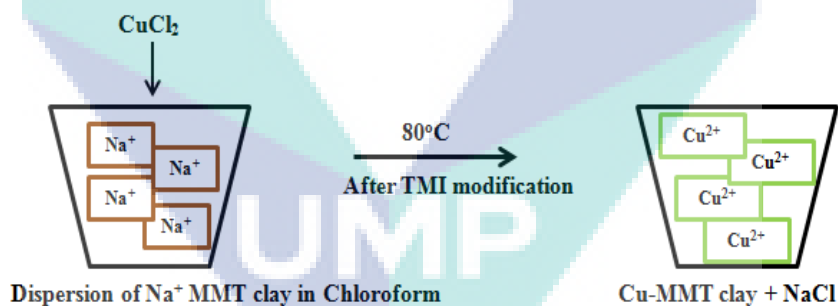


**Figure 4.1: Stacks of platelet that are tightly held together**

Modification of clay using transition metal ion is seen as a prerequisite for a successful formation of polymer and clay nanocomposites. Figure 4.2 shows the cation exchange that took place from the modification whereas Figure 4.3 shows the mechanism of the clay modification.

(a)



(b)

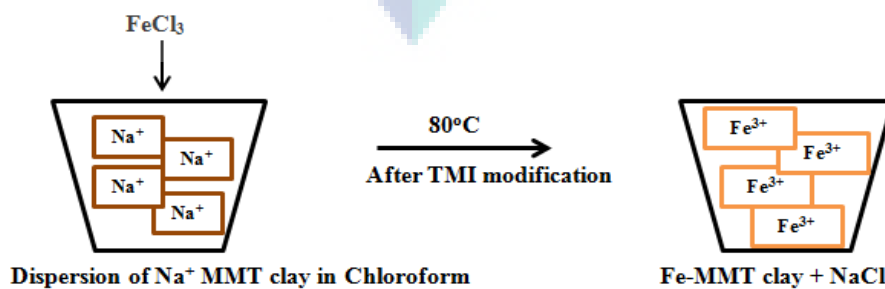


**Figure 4.2: TMI Modification of MMT clay via (a)  $\text{Cu}^{2+}$  (b)  $\text{Fe}^{3+}$**

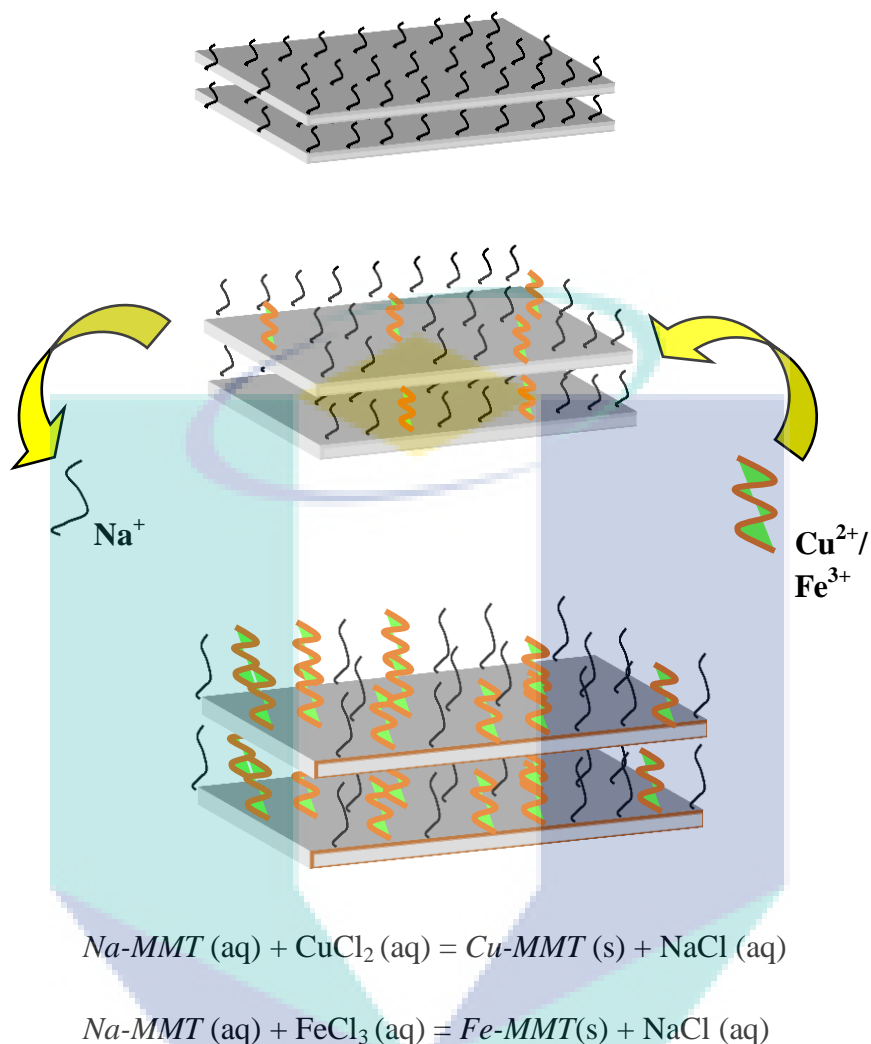


**Figure 4.3: Mechanism of the modification process**

When the cations in the MMT clay are exchanged with metal ions, the surface energy of the silicate surface is lowered and wetting with the polymer is improved. The positively charged cations are tethered to the surface of the negatively charged silicate layers and results in an increase of the gallery height. The diffusion of the  $Cu^{2+}$  and  $Fe^{3+}$  ions between the layers alters the surface properties of each single sheet from being hydrophilic to hydrophobic (Pavlidou and Papaspyrides, 2008). A larger interlayer spacing which facilitates better intercalation process is obtained as shown in Figure 4.3.

## 4.2.2 Characterization of Modified MMT Clay

### *Inductively Coupled Plasma Mass Spectrometry*

The confirmation of the presence of the copper and iron ions and the surface change through the ion exchange modification were carried out using inductively coupled plasma mass spectrometry (ICP-MS). It is one of the most notable methods in atomic spectrometry due to its high detection power and true multi element capabilities (Montaser and Golightly, 1992). In addition, ICP-MS detection allows measurement at extremely low concentrations and it has an excellent sensitivity which enables it to become a good detector for many trace elements (Sakai et al., 2005). Table 4.1 provides the results that were obtained from the analysis.

**Table 4.1:** ICP-MS data

<b>Sample</b>	<b>Parameter</b>	<b>Results</b>	<b>Unit</b>
Pristine MMT	Cu	0.0371	ppm
	Fe	1801.68	ppm
MMT modified with Cu <sup>2+</sup>	Cu	56012.0	ppm
	Fe	1801.68	ppm
MMT modified with Fe <sup>3+</sup>	Cu	0.0371	ppm
	Fe	114005.9	ppm

From the data displayed in the table, the amount of copper (Cu) and iron (Fe) ions were seen to increase tremendously in the modified MMT clay which enables the deduction that the modification of the clay was indeed successful in aiding the TMIs to be able to displace themselves in the lamellar plane of the layered silicates.

### *Field Emission Scanning Electron Microscope (FESEM)*

Field emission scanning electron microscopy (FESEM) was engaged in this study to understand the distribution of the clay particles. Figure 4.4 depicts the micrographs obtained for pristine clay (MMT), modified clay with copper (MMT-Cu) and modified clay with iron (MMT-Fe). It can be seen that pristine MMT clay in Figure 4.4(a) from the FESEM micrographs exists in stacked platelet and forms overlapped layers. These layers could be attributed to the structure of the clay which exists in stacked platelet forms. After the TMI modification process, the clay layers are covered by the metal ions and appears to have a homogeneous distribution. Furthermore, the size of the clay agglomerates in MMT are reduced and numerous separated tactoids are seen in MMT Cu and MMT Fe as shown in Figure 4.4(b) and 4.4(c) with very few smaller agglomerates. The sizes of the pristine MMT tactoids obtained were around 22.6nm whereas MMT Cu and MMT Fe ranged from 9.46nm to 18.4 nm. The reduction in the size may be related to the ion exchange between the  $\text{Na}^+$  ions from the MMT gallery with the  $\text{Cu}^{2+}$  and  $\text{Fe}^{3+}$  from the transition metal ions. The comparison between the pristine MMT clay and modified MMT clay demonstrates a notable impact of the modification done.

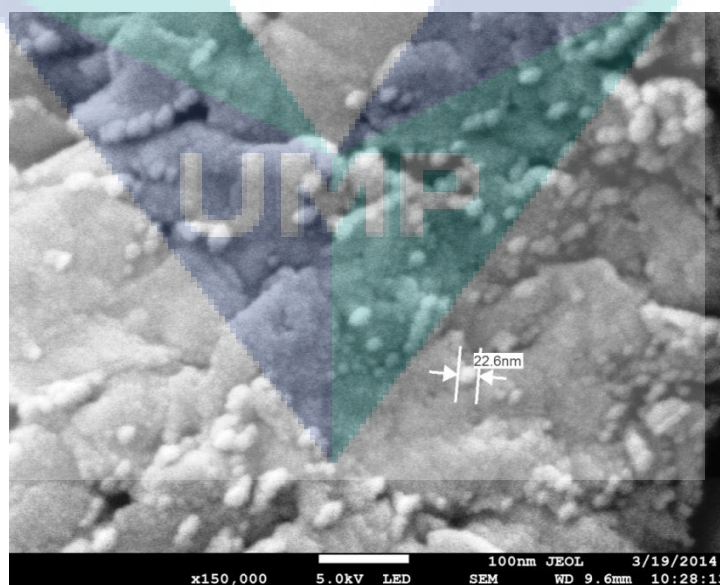


**Figure 4.4 (a) FESEM micrograph of MMT clay**



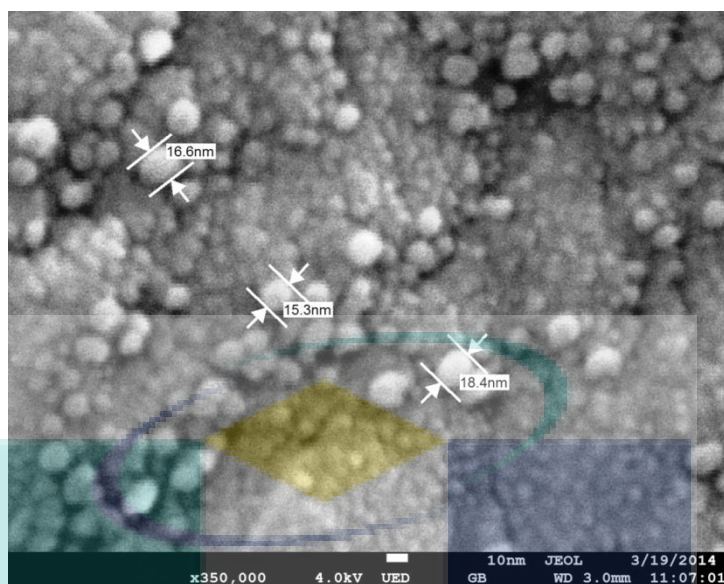


Figure 4.4 (b) FESEM micrograph of MMT Cu

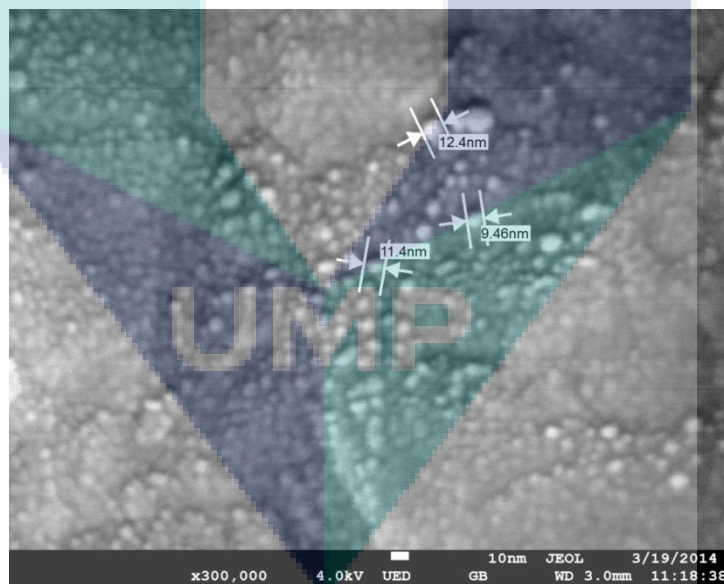
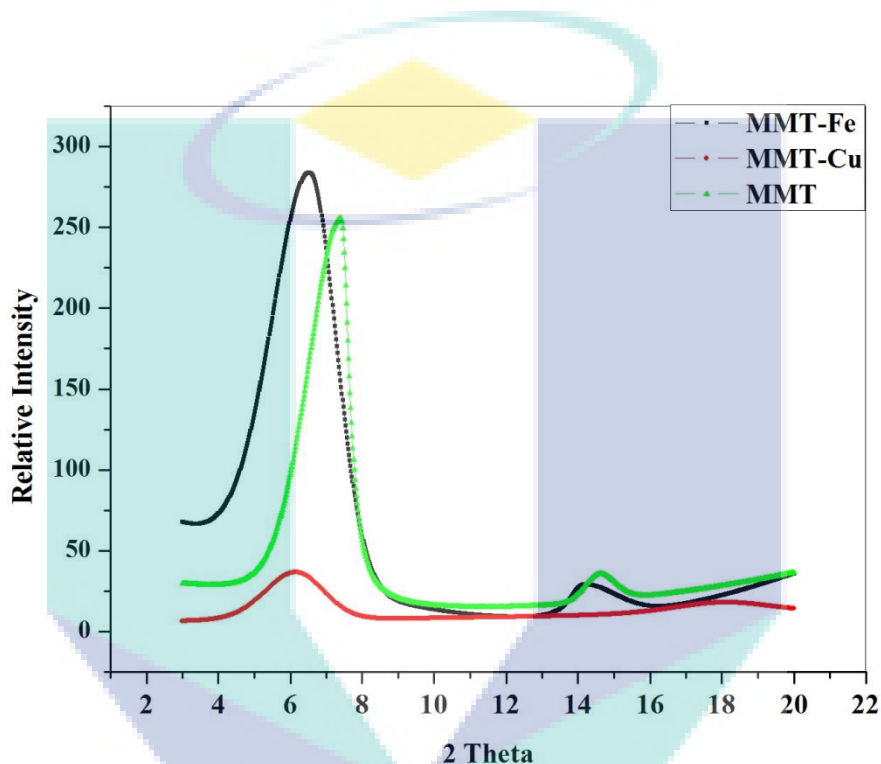


Figure 4.4 (c) FESEM micrographs of MMT-Fe

### *X-Ray Diffraction (XRD)*

XRD analysis was employed to differentiate the structure of the pristine clay and the modified clay. The samples were scanned in fixed step size 0.020 with a step time of 0.1s in the range of 3-20°. Figure 4.5 shows a comparison of pristine MMT clay and MMT clay modified with  $\text{Cu}^{2+}$  (MMT-Cu) and MMT clay modified with  $\text{Fe}^{3+}$  (MMT-Fe).



**Figure 4.5: XRD Patterns of pristine MMT and modified MMT**

Based on Figure 4.5, the characteristic peak of pristine MMT appeared at  $2\theta = 7.5^\circ$  and corresponded to the inter layer space of 11.80 Å. The X-ray data obtained for modified MMT clay is seen to shift to a smaller angle towards the left. The characteristic peak of MMT-Cu and MMT-Fe were seen at  $2\theta = 6^\circ$  and  $6.5^\circ$  respectively with an interlayer spacing of 14.73 Å and 13.60 Å respectively. Increase in the d-spacing of the modified clay indicates that the modified ions were able to intercalate themselves into the gallery of MMT and there is a higher tendency for the formation of an exfoliated or intercalated structure during the fabrication with PU. Similar observations were reported by Nakas and Kaynak (2008) whom stated that modifications on clay improve the interlayer spacing.

### 4.3 MORPHOLOGICAL STUDIES OF PU NANOCOMPOSITES

#### 4.3.1 Fourier Transform Infrared Spectroscopy (FTIR)

In this study, FTIR spectroscopy was employed to identify whether the MMT has been embedded in the polyurethane matrix and chemically bonded to the polymer chains. PU, PU-MMT, PU-MMT Cu and PU-MMT Fe films were investigated and the chemical changes that occurred upon the incorporation of clay are presented in Figures 4.6, 4.7 and 4.8. Infrared absorptions bands that are commonly seen in PU were observed in all four samples in all the three different percentages of the clay loading. The characteristic infrared bands that were observed at  $3325\text{-}3338\text{ cm}^{-1}$  are attributed to the hydrogen bonded primary amines which are a resultant from the chemistry of urethanes that are created from the reaction of organic isocyanates and amines (Szycher, 1999). The peaks that arise at  $2918\text{ cm}^{-1}$  can be related to the stretching vibrations of  $\text{CH}_2$  whereas the stretching vibrations due to the carbonyl present in urethane, urea and ester groups are seen at  $1732\text{ cm}^{-1}$  bandwidth. Similar results recorded for the FTIR spectra were reported by Wang and Sung (2002).

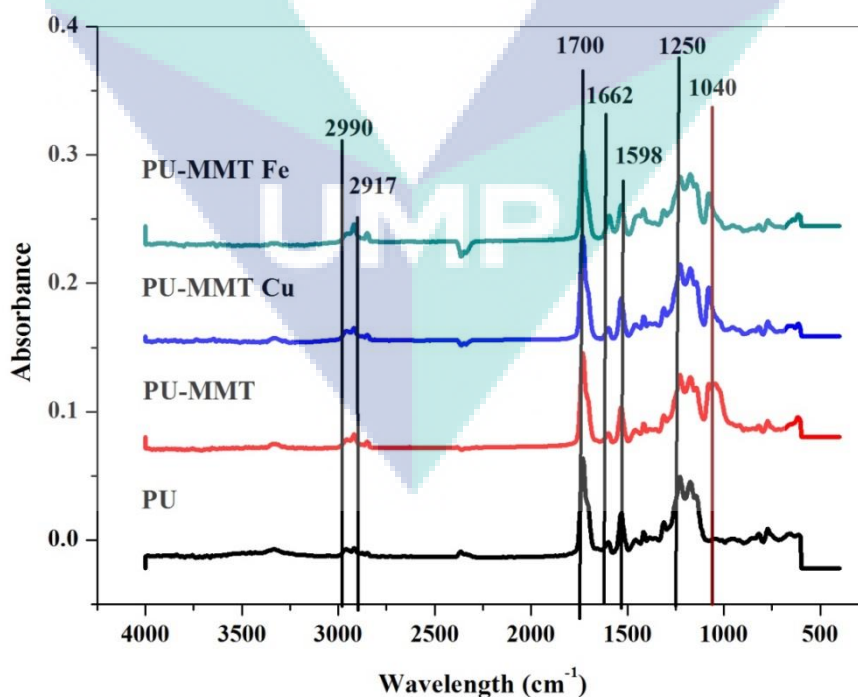


Figure 4.6: FTIR spectra of 1% PU, PU-MMT, PU-MMT Cu & PU-MMT Fe

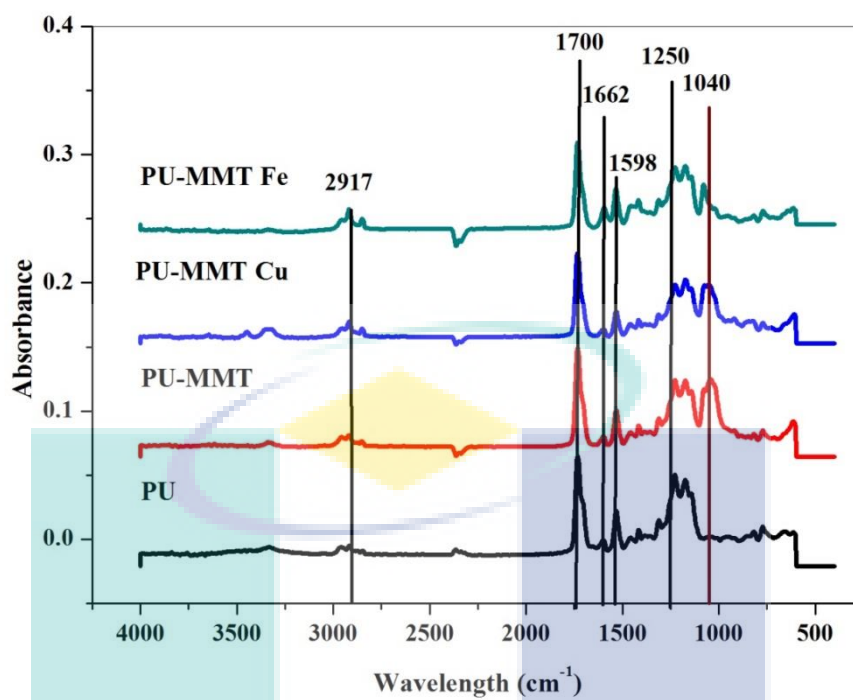


Figure 4.7: FTIR spectra of 2% PU, PU-MMT, PU-MMT Cu & PU-MMT Fe

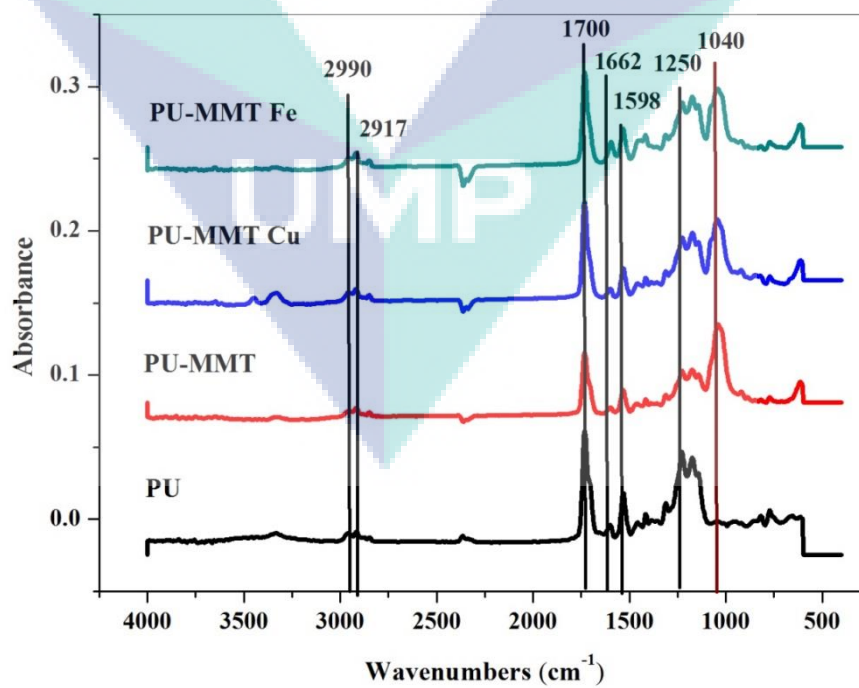


Figure 4.8: FTIR spectra of 3% PU, PU-MMT, PU-MMT Cu & PU-MMT Fe

It can be seen in PU-MMT, PU-MMT Cu and PU-MMT Fe as shown in Figures 4.6 to 4.8 that there is an occurrence of an absorption band at  $1040\text{ cm}^{-1}$ . This occurrence is an indication of the presence of silica oxide (Si-O) bonds due to the incorporation of the clay silicates in the PU matrix and this finding is in line with Tien and Wei (2002). It is known that silica is the dominant constituent of MMT whereby it is present in the tetrahedral layer of the clay. The tentative assignments of the main absorption bands of the FTIR analysis are illustrated in Table 4.2.

**Table 4.2:** Tentative FTIR Band Assignments of PU Nanocomposites

Wavenumber ( $\text{cm}^{-1}$ )	Assignment	Domain origin
3338	Hydrogen bonded NH	Hard Segment
2917	Asymmetric stretching $\text{CH}_2$	Soft Segment
1731	Free C=O	Hard Segment
1598	Hydrogen bonded C=O	Hard Segment
1040	Bending Si-O	Clay

The effects of silica nanoparticles on the phase separation of hard and soft segments of membranes are observed through the peaks that are related to the carbonyl group. The peaks appeared in lower frequency (around  $1530\text{ cm}^{-1}$ ) can be referred to the bonded and the one appeared in higher frequency (around  $1730\text{ cm}^{-1}$ ) can be referred to the free carbonyl. From the peaks shown in PU-MMT, PU-MMT Cu and PU-MMT Fe, it can be seen that the free carbonyl peaks shifts towards the hydrogen bonded carbonyl bond and similar observations were reported by Osman et al. (2004). This observation enables the deduction that the silica nanoparticles are able to distribute themselves in the polymer.

It can be concluded from the above visual observation and spectral analyses that the layered silicates (Si-O) were able to disperse in PU. The chemical bonding between the PU grafted onto the nanoparticles would certainly enhance the filler/matrix adhesion in the composites and contribute to its property enhancement. The comparison of the data obtained and from the literature is revealed in Table 4.3.

**Table 4.3:** Assignment of the main FT-IR peaks of PU nanocomposites and their with data in literature

Functional Group	Salahuddin et al. (2010) (cm <sup>-1</sup> )	Chen et al. (2002) (cm <sup>-1</sup> )	Pinto et al. (2011) (cm <sup>-1</sup> )	This study (cm <sup>-1</sup> )
Stretching vibration of NH group	3284	3328	3333	3324-3338
Asymmetric C-H vibration	2925	2940	2945	2916-2918
Symmetric C-H vibration	2859	2856	2866	2850
Stretching vibration of C=O	1701	1731	1700-1730	1732
Stretching vibration of Si-O <sub>2</sub>	1047	515	1040	1042-1052

### 4.3.2 Scanning Electron Microscope (SEM)

Scanning Electron Microscope (SEM) was used to examine the samples in order to apprehend the MMT clay's dispersion and to determine the particle size for the interphase analysis. Figure 4.9 reveals the SEM micrograph obtained from pure PU film. There were no visible particles appearing on the surface as no clay was incorporated during the sample preparation however the image did not portray a smooth image. This may be caused by poor drying during preparation of the sample, in which complete evaporation of the solvent was not able to be achieved. The effect of incorporation of pristine clay can be seen in Figures 4.10, 4.11 and 4.12. Each sample demonstrated the presence of large aggregates with distinct sphere like grains and this surface morphology may be associated to the layered structure of the MMT clay. Analogous findings were reported by Yapar (2009). The presence of these aggregates may be related to poor distribution of the clay in the matrix as MMT clay is known to have a very high tendency to agglomerate during the fabrication process due to its lamellae structure. Furthermore, MMT clay possesses a hydrophilic nature in its pristine state. It is known that PU is a hydrophobic polymer and a homogeneous dispersion of the clay into its matrix can never be achieved due to the intrinsic incompatibility of hydrophilic layered silicates and hydrophobic polymers (Vaia et al., 1999).

The logo for UMP (Universiti Malaysia Perlis) is a large, stylized letter 'V' shape. The top part of the 'V' is a light blue triangle pointing upwards. The bottom part of the 'V' is a light green triangle pointing downwards. The letters 'UMP' are written in white, bold, sans-serif font across the center of the 'V'.

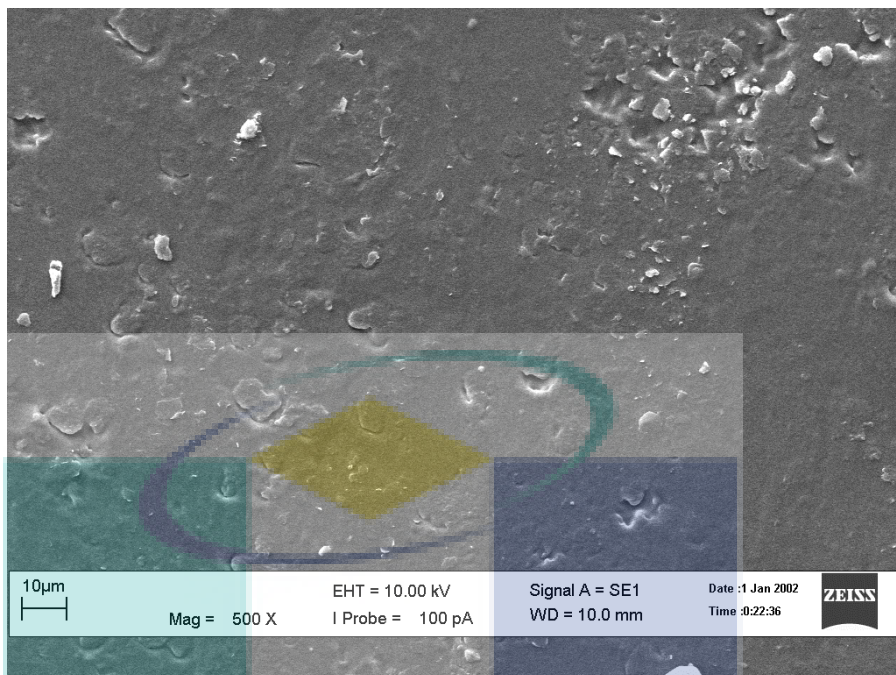


**Figure 4.9: SEM micrograph of PU**

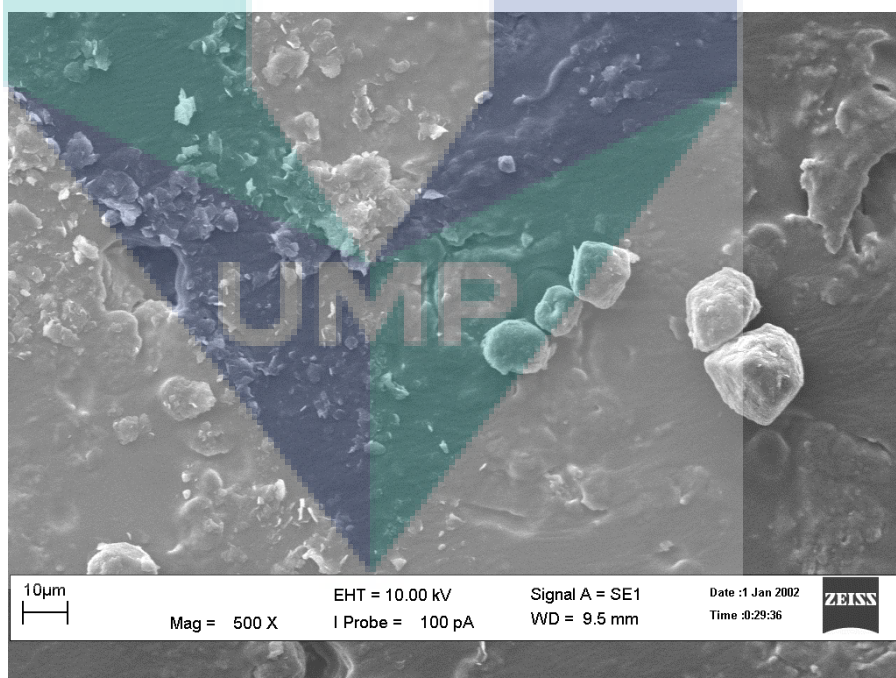


**Figure 4.10: SEM micrograph of 1% PU-MMT**



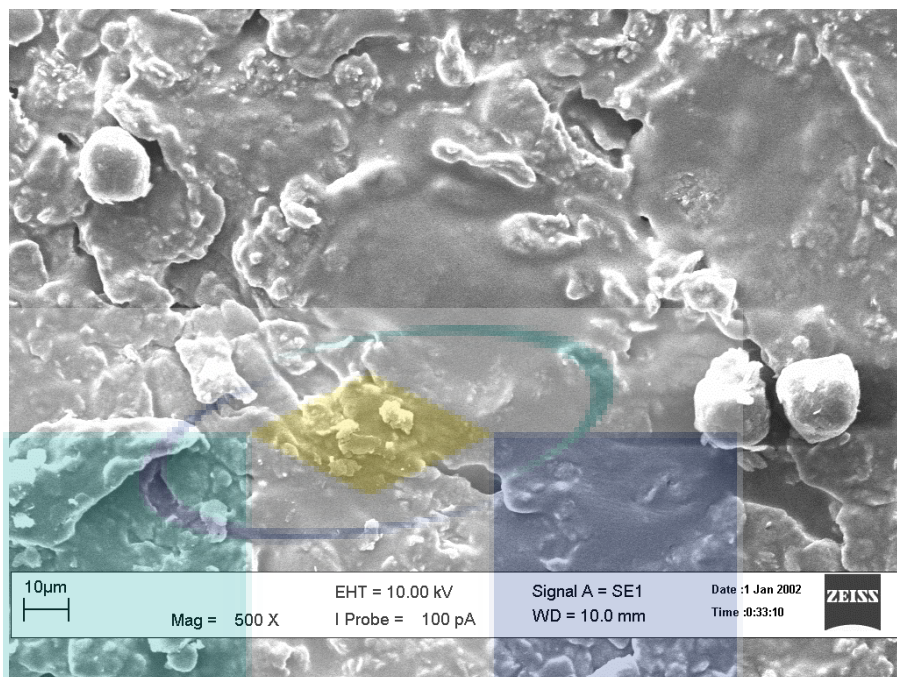


**Figure 4.11: SEM micrograph of 2% PU-MMT**

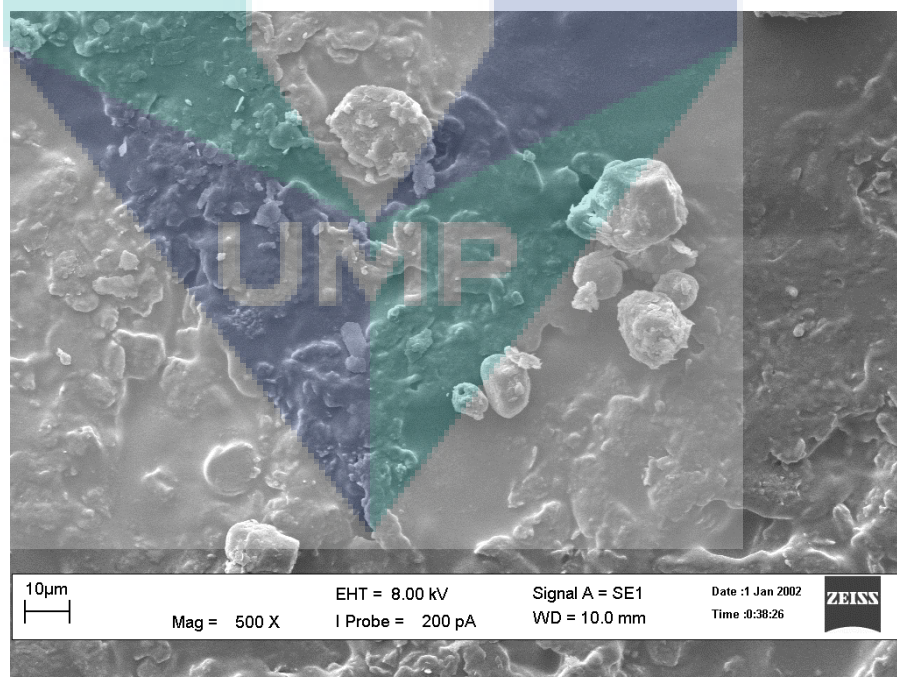


**Figure 4.12: SEM micrograph of 3% PU-MMT**

The TMI modification was done on the clay in order to develop a better dispersion of the clay in the polymer matrix. The replacement of interlayer cations through ion exchange reactions enables natural clay to be compatible with the polymer matrix (Krishnamoorti et al., 1996). The ion exchange reactions with cationic surfactants is able to modify the interlayer interactions by lowering the surface energy of the inorganic component and improve the clay's wetting characteristics with the polymer (Bulmstein, 1965 and Theng, 1979). This can indeed be seen in Figures 4.13, 4.14 and 4.15 of PU-MMT Cu and Figures 4.16, 4.17 and 4.18 of PU-MMT Fe whereby the sizes of the clay agglomerates were seen to reduce. A relatively uniform and smooth surface is formed in the close up view in contrast to the SEM images of PU-MMT. The appearance of tiny agglomerates can be seen in the micrographs of the modified clay nanocomposites however they are well embedded within the polymer and also well dispersed within the PU-MMT Cu and PU-MMT Fe as compared to the agglomerate form of PU-MMT. Findings of a report by Onsy et al. (2010) accounted that the tendency of the clay to distribute itself evenly at high clay loading is seen to be difficult, as with more clay particles, the clays are more prone to settling and this unable a uniform dispersion and distribution of the clay in the polymer matrix. Flake like images of the clay were detected in Figures 4.15 and 4.16. Wang et al. (2008) found identical results in their analysis and they justified that the ion exchange reactions that occurred during the TMI modification might have increased the interlayer distance and enabled the assumption that the particles are intercalated with larger distances. The same assumption can be presumed in this work as these nanocomposites did portray an intercalated form which was confirmed in the XRD data from Figure 4.20. Wang et al. (2008) found similar result in their work where the MMT rolled up and indirectly presented the flake like disordered morphology.

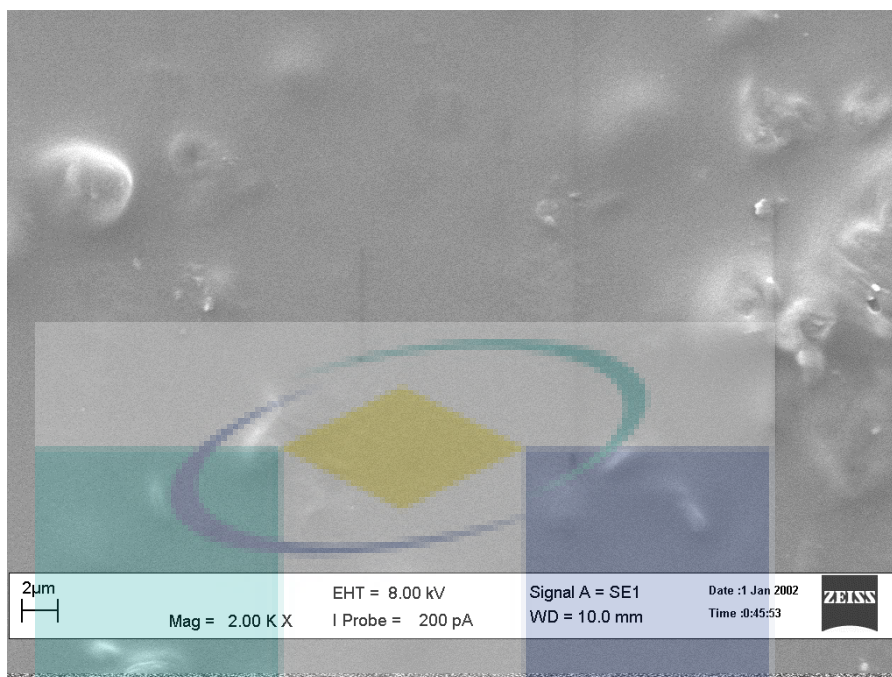


**Figure 4.13: SEM micrograph of 1% PU-MMT Cu**

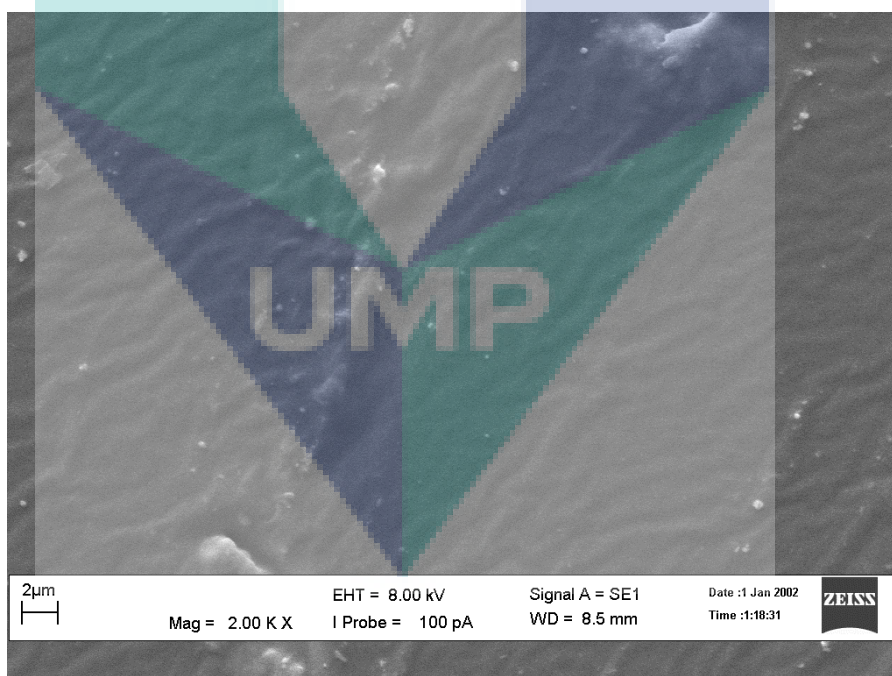


**Figure 4.14: SEM micrograph of 2% PU-MMT Cu**

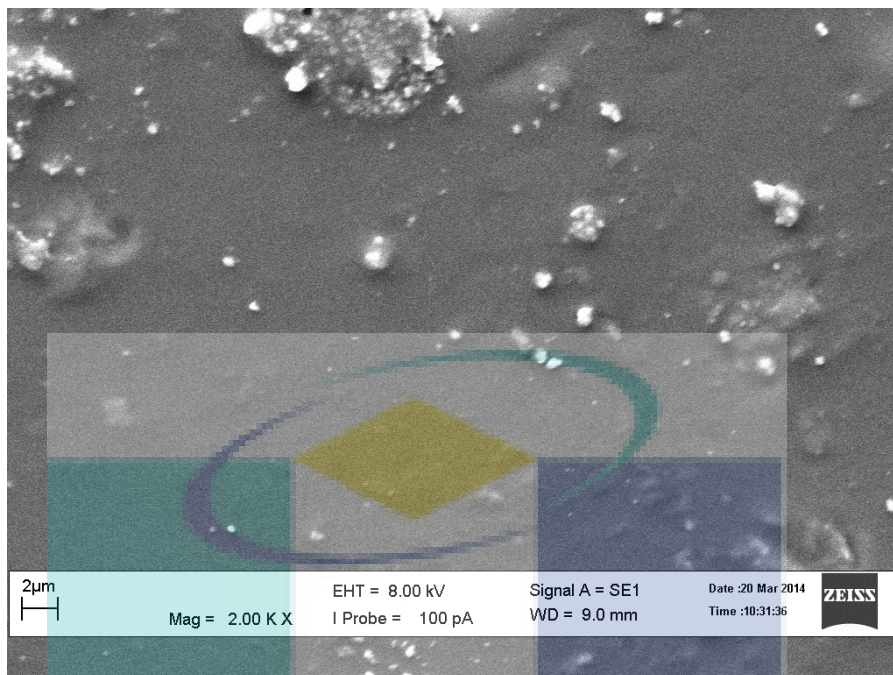


**Figure 4.15: SEM micrograph of 3% PU-MMT Cu**

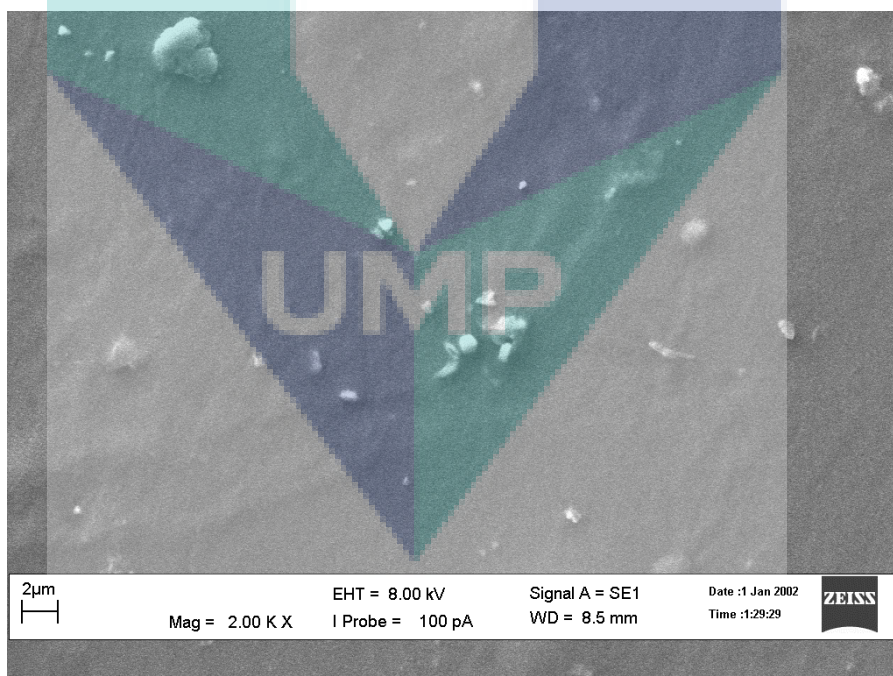


**Figure 4.16: SEM micrograph of 1% PU-MMT Fe**

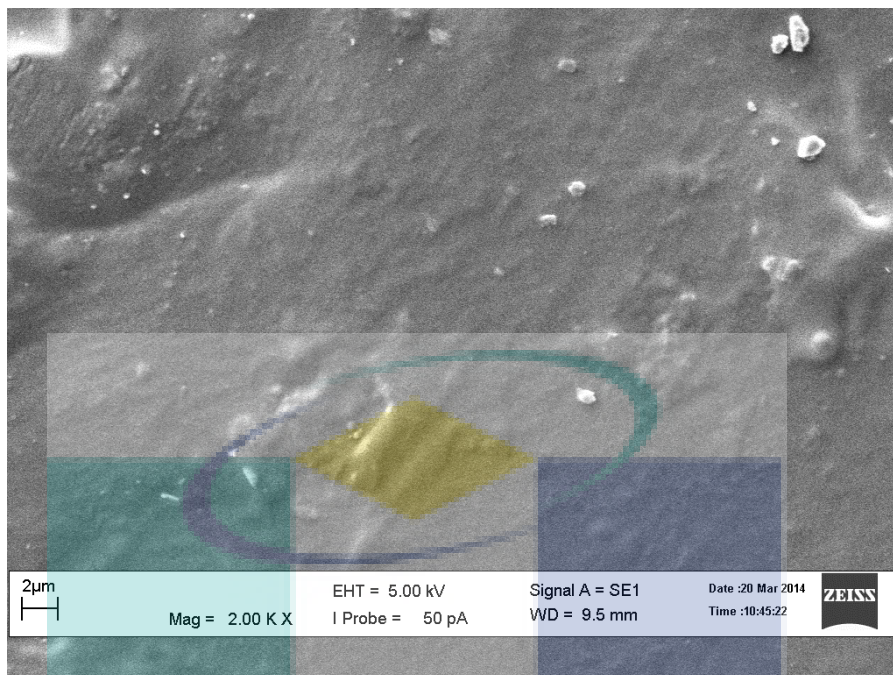


**Figure 4.17: SEM micrograph of 2% PU-MMT Fe**

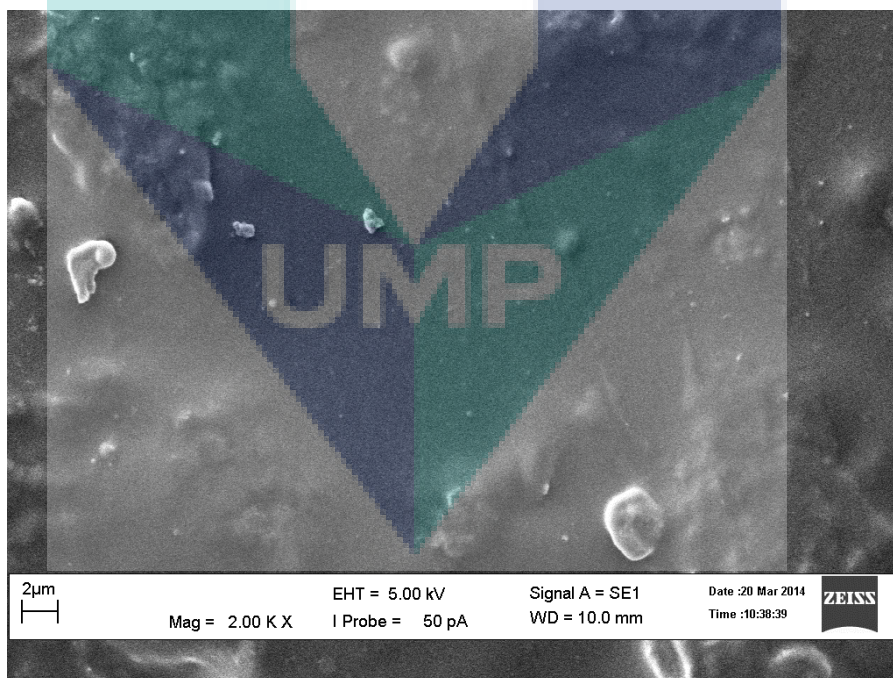


**Figure 4.18: SEM micrograph of 3% PU-MMT Fe**

### 4.3.3 Field Emission Scanning Electron Microscopy (FESEM)

SEM analysis was employed to understand the distribution of clay particles in the polymer matrix; however it may only give a brief suggestion on the degree of intercalation of the clay layers due to the relatively low-resolution capacity of SEM. Field emission scanning electron microscopy (FESEM) has a more intensive and monochromatic electron beam that create a lesser cross over diameter. This smaller cross over in FESEM which is the point at which the electrons are focused when leaving the electron gun gives smaller final electron spot thus creating higher resolution. In this study, FESEM was conducted to investigate the molecular surface structures of the PLSN.

In this work, it can be seen that the quality of dispersion and distribution of the layered silicates were correlated to the amount of clay loading and the TMI modification done on the clay particles as shown in Figure 4.19. The samples analyzed were pristine PU, 2% PU-MMT, 2% PU-MMT Cu and 2% PU-MMT Fe and the nanocomposites were magnified to 10kx in order to obtain a clearer and in depth picture of the clay particles and aggregates. It can be observed that structure of PU incorporated with 2% MMT as depicted in Figure 4.19(b) as compared to pristine PU shows clear agglomerations of the layered silicates. The agglomerations of the particles are expected since the polyurethane nanocomposites were prepared via solution mixing method and when they are suspended in the solvent, the clay particles tend to flock together in order to lower their surface energy (Ciprari, 2004). This explains the cracked and aggregated morphology found in Figure 4.19(b).

However, in Figures 4.19(c) and (d), the agglomerates shrunk tremendously in size and the particles did not flocculate in the sample. It can be observed that the modification done on the clay particles has enhanced its dispersibility on the polyurethane matrix and helped to lower the surface energy of the host, improved the wetting characteristics and intercalation with the polymer matrix which resulted in larger interlayer spacing as supported by the XRD analysis done. This enables the deduction that the TMI modification on the clay particles has indeed aided in better dispersion and the ability to create an exfoliated clay structure.

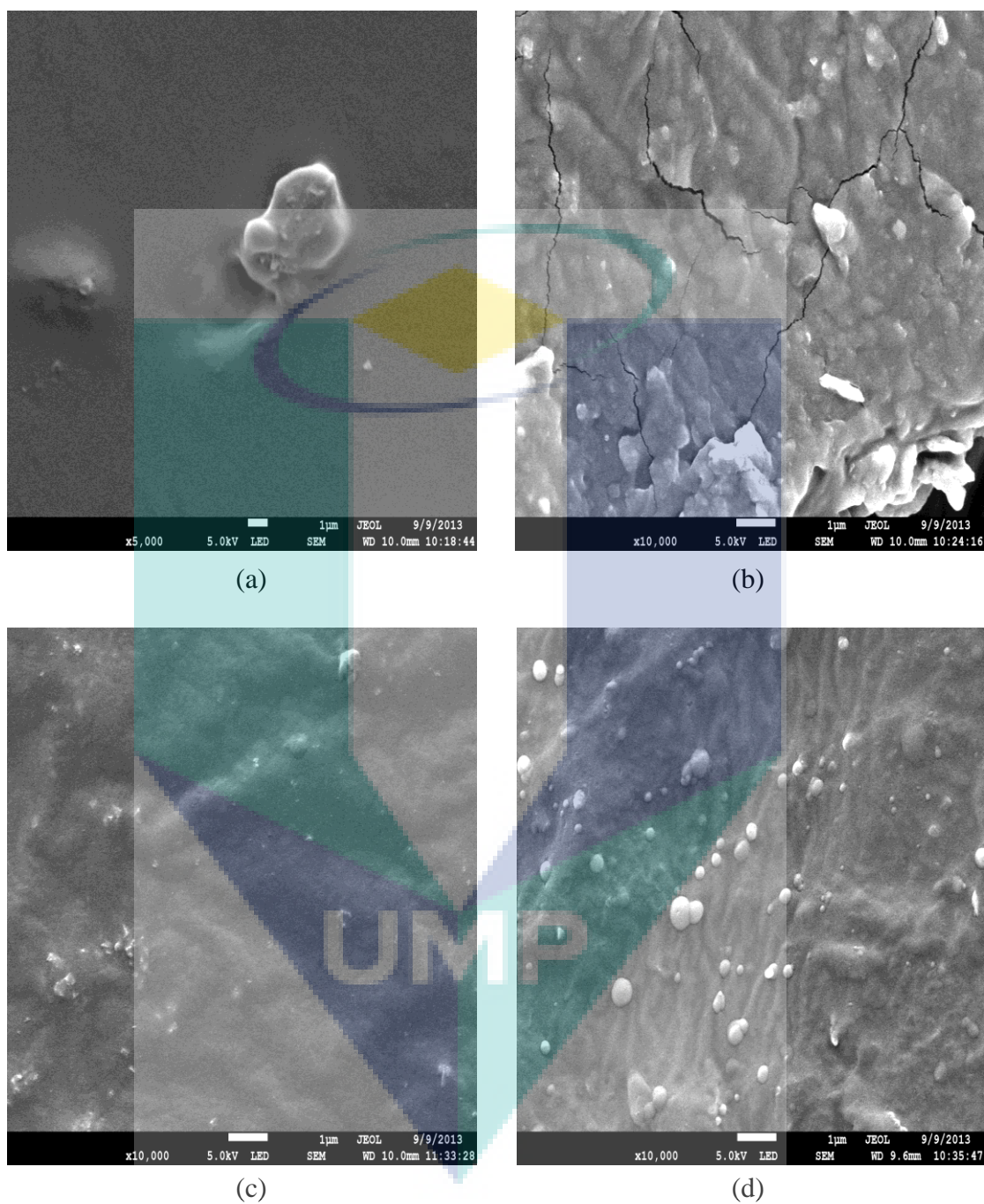


**Figure 4.19:** FESEM micrographs of (a) PU (b) 2% PU-MMT (c) 2% PU-MMT Cu

(d) 2% PU-MMT Fe

#### 4.3.4 X-Ray Diffraction (XRD)

The XRD analysis was employed in this study to characterize the structure of the sample by determining the interlayer spacing of the sample. The samples were scanned in fixed step size, 0.020 with a step-time of 0.1s in the range of 3-20° however the XRD graphs were plotted based from 0-30° due to the significance found at this point from the analysis. An XRD diffractogram with an intensity of 2θ was obtained from the scans. Further calculations of the d-spacing of the interlayer gallery of the polyurethane nanocomposites were calculated using the Bragg's Law equation as stated below.

$$d = \frac{n \lambda}{2 \sin \theta} \quad \text{Equation (4.1)}$$

Where:

- d = Space between layers of the clay
- λ = Wavelength of the X-ray which is 0.154nm
- θ = Angle at the maximum point of the first peak into a spectrum
- n = Order of diffraction

From the analysis done, it could be observed that the nanocomposites analyzed exhibited different characteristic peak which can be related to their regular layered structure whereby the peak is indicative of the platelet separation in the clay structure. According to Bragg's Law, a decrease in the crystallite size cause an increase in the width of the diffraction and in very small crystallites, there are not enough planes to produce complete destructive interference which results in a broadened peak. Increasing d-spacing results in broadening and shifting the XRD peak towards the lower diffraction angle 2θ and vice versa. Figure 4.20 displays the data obtained from the XRD analysis for each type of samples with a diffraction angle from 3-20° whereas Table 4.4 summarizes the interlayer spaces of the nanocomposites.



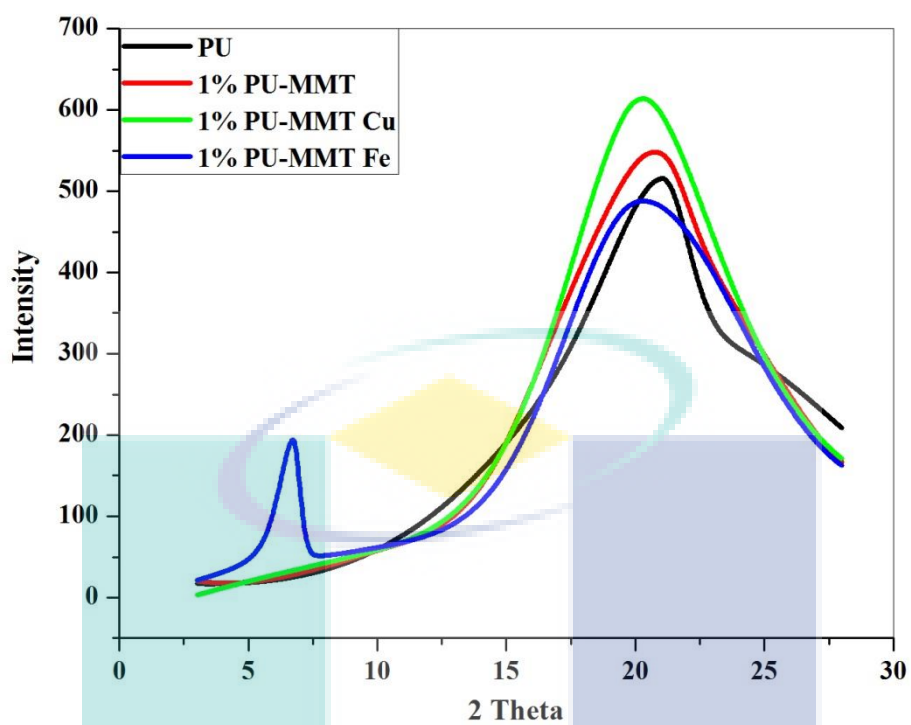


Figure 4.20 (a) XRD diffractograms of 1% polyurethane nanocomposites

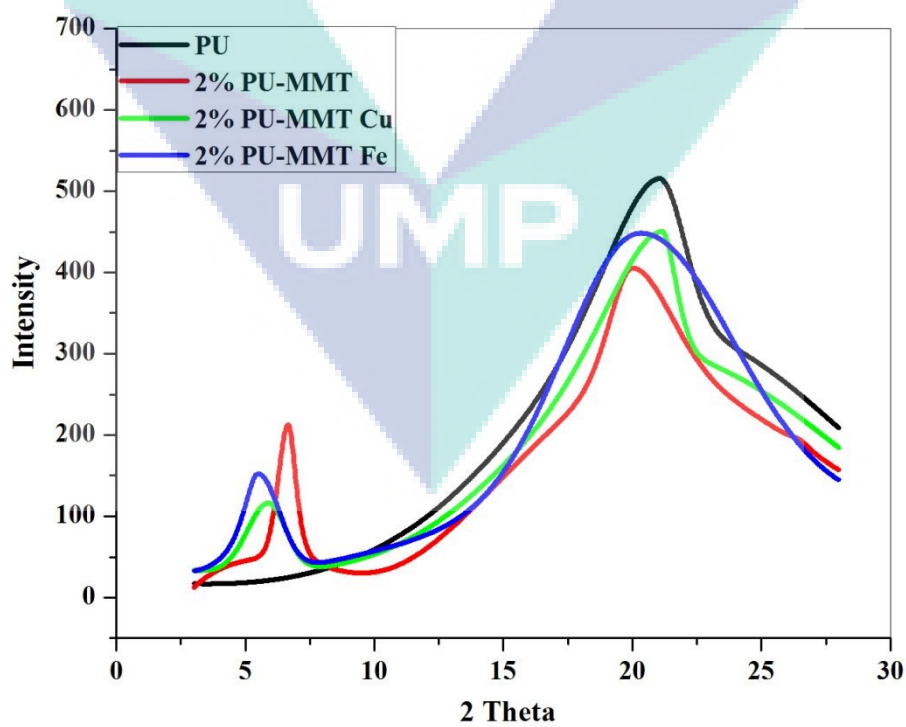


Figure 4.20 (b) XRD diffractograms of 2% polyurethane nanocomposites

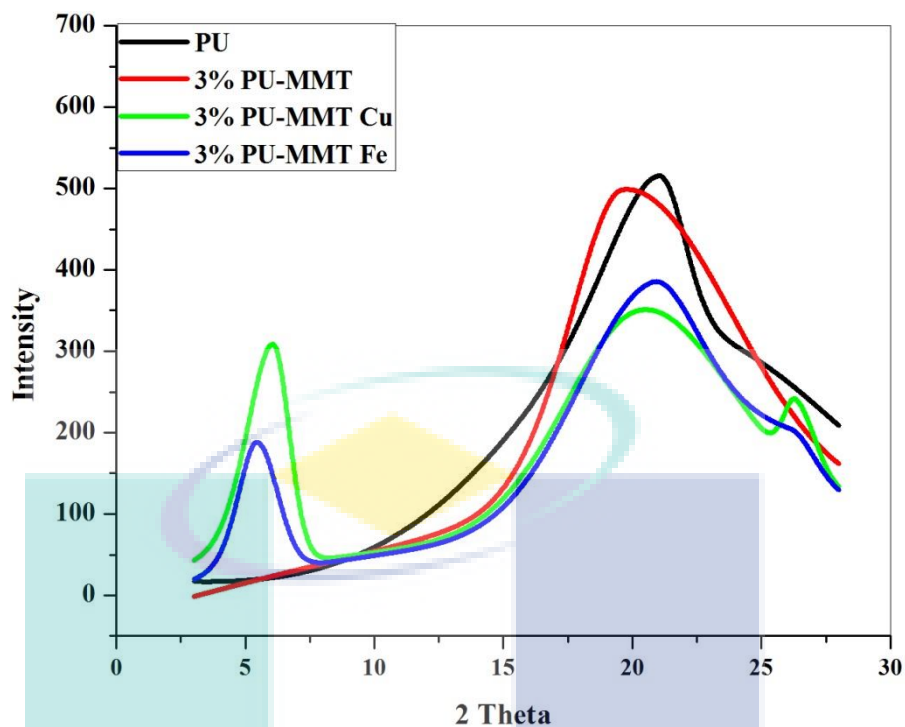


Figure 4.20 (c) XRD diffractograms of 3% polyurethane nanocomposites

Table 4.4: The value of angular spacing,  $d$  and reflection angle,  $2\theta$  of the polyurethane nanocomposites

Sample	Clay Percentage (wt. %)	$2\theta$ ( $^{\circ}$ )	$d$ (nm)
Pure PU	0	20.99	4.23
PU-MMT	1	21.03	4.22
	2	19.96	4.44
	3	19.63	4.52
PU-MMT Cu	1	19.50	4.57
	2	5.89	<b>14.99</b>
	3	6.05	14.59
PU-MMT Fe	1	6.73	13.13
	2	5.48	16.10
	3	5.43	<b>16.20</b>

From Figure 4.20, it can be observed that the final structures of the polyurethane nanocomposites were greatly influenced by the modified and pristine MMT filler content. The structures of the polyurethane incorporated with different types of filler and weight percentage showed a variety of changes in its angular spacing and reflection angle. The XRD pattern obtained were highly dependent on the quantity and the quality of the filler content. Bragg's law states that if MMT clay retains its original structure and the original d-spacing when incorporated into the polymer matrix, the position of the Bragg peak that corresponds to the d-spacing in the XRD diffractogram will remain unchanged whereas if the layered structure is maintained and the d-spacing increases, the Bragg peak will be shifted to the lower value. The Bragg's peak disappears altogether when the layered structure is disrupted.

The data obtained showed that pristine PU possessed a visible peak at  $2\theta = 20.99^\circ$  with an angular spacing  $d = 4.23\text{nm}$ . PU-MMT with 1%, 2% and 3% weight percentage showed characteristic diffraction peaks at  $2\theta = 21.03^\circ$  (d-spacing is  $4.22\text{nm}$ ),  $2\theta = 19.96^\circ$  (d-spacing =  $4.44\text{nm}$ ) and  $2\theta = 19.63^\circ$  (d-spacing =  $4.52\text{nm}$ ) respectively. It can be seen from Figure 4.20(a) that PU and 1% PU-MMT appeared as amorphous halo. This could be attributed to the structure of PU which is partially crystalline and partially amorphous. Similar XRD findings of PU were reported by Xiong et al. (2004) who justified that the amorphous component in it gives a very broad peak (halo). It can be observed from Figures 4.20(b) and (c) that there are two visible peaks in the XRD diffractograms for the samples with modified clay with one sharp peak and one broad peak. The sharp peaks obtained are indications that the clay particles functioned as nucleating agents that induced the crystallization of the segments in PU. The peaks attained at angle  $2\theta$  less than  $10^\circ$  is useful in determining the degree of interaction between the polymer and filler as a shift towards the lower angles are associated with the intercalation and exfoliation of the polymer between the clay lamellas (Dias et al., (2010). From the data obtained, PU incorporated with modified clay portrayed a smaller  $2\theta$  value that corresponds to higher angular spacing which indicates that a successful intercalation process has been achieved. PU-MMT Cu demonstrated reflection angles of  $19.5^\circ$  (d-spacing is  $4.57\text{nm}$ ),  $5.89^\circ$  (d-spacing is  $14.99\text{nm}$ ) and  $6.05^\circ$  (d-spacing is  $14.59\text{nm}$ ) in its 1wt%, 2wt% and 3wt% clay loadings whereas PU-MMT Fe had the

lowest reflection angles which was  $6.73^\circ$  with angular spacing 13.13nm in 1wt%,  $5.48^\circ$  with d-spacing 5.48nm in 2wt% and  $5.43^\circ$  with d-spacing 16.20nm in its 3wt%.

The peaks of the modified clay nanocomposites which were seen to shift towards a lower value is an indication that an intercalated clay structure has been created. Xiong et al. (2004) reported in their study that PU incorporated with modified clays shifted towards a smaller angle which has a  $2\theta$  value of  $4.0^\circ$  and d spacing of 2.21nm and they stated that PU was intercalated into the clay's structure. Similar results were obtained in this work. According to Wang and Pinnavaia (1998), the gallery spacing in modified clay becomes larger as a resultant of the longer chain in the clay relative to the conventional clay whereby the extent of gallery expansion is highly dependent on the chain length of the modifier in the interlayer. Barrick et al. (2010) found in their study that the incorporation of Cloisite 15A into PU shows an increase in the d-spacing of the nanocomposites compared to incorporation with pristine nanoclay. They suggested that partially intercalated structure was obtained. According to Barick et al. (2010), the modifiers in Cloisite 15A aided in increasing the gallery height and made the layer separation more as the modifier inside the layer weakens the electrostatic forces between the silicate layers. In this study, the TMI modification process is seen as a method to change the nature of the clay from being hydrophilic to hydrophobic and thus accommodating a higher driving force of the PU into the clay. This resulted in the increase of the d-spacing. The even distribution of the modified MMT clay can be viewed from the FESEM images in Figure 4.4 and SEM micrographs from Figures 4.13 to 4.18 that show the uniform dispersion of the clay into PU with no visible agglomerates. It can be deduced from this that the TMI modification done has promoted an intercalation process in the nanocomposites.

## 4.4 MECHANICAL PROPERTIES

PU is a versatile polymeric material that has been used extensively lately especially in areas such as coatings, adhesives, fibers, foams and insulators. The mechanical properties of PU have a great importance as they are useful in many engineering applications in which strength plays a vital role. In this research, PU-MMT is studied as a thermal insulator and it is important for it to possess excellent characteristics in mechanical properties such as tensile stress and extension at break. In this section, the mechanical properties of polyurethane with pristine clay and modified clay with copper and iron are discussed.

### 4.4.1 Tensile Strength

The tensile strength value of PU-MMT was obtained at the breaking point of the material which was prepared according to ASTM 882. The tests were carried out under a crosshead speed of  $5 \text{ mm min}^{-1}$  on a Universal Testing Machine (UTM) (Carli et al., 2011). In order to avoid factors such as molecular weight and processing history affect the tensile strength values, pure polyurethane (PU) was tested to ensure a more direct comparison with the nanocomposites and by using PU as a reference, the reliability of the data obtained is believed to have been enhanced. The samples that were tested are polyurethane montmorillonite (PU-MMT) without modification and polyurethane montmorillonite clay modified with copper (PU-MMT Cu) and iron (PU-MMT Fe). There were three different weight percentages that were studied in this experiment which were 1%, 2% and 3% clay loading. Six samples were tested for each parameter and average mean value was taken. The results obtained are tabulated in Table 4.5.

**Table 4.5:** Effect of Clay on Tensile Strength

Weight %	Tensile Strength (MPa)			
	PU	PU-MMT	PU-MMT Cu	PU-MMT Fe
1%	0.23	0.30	0.57	0.46
2%	0.23	0.38	0.46	0.42
3%	0.23	0.28	0.56	0.44

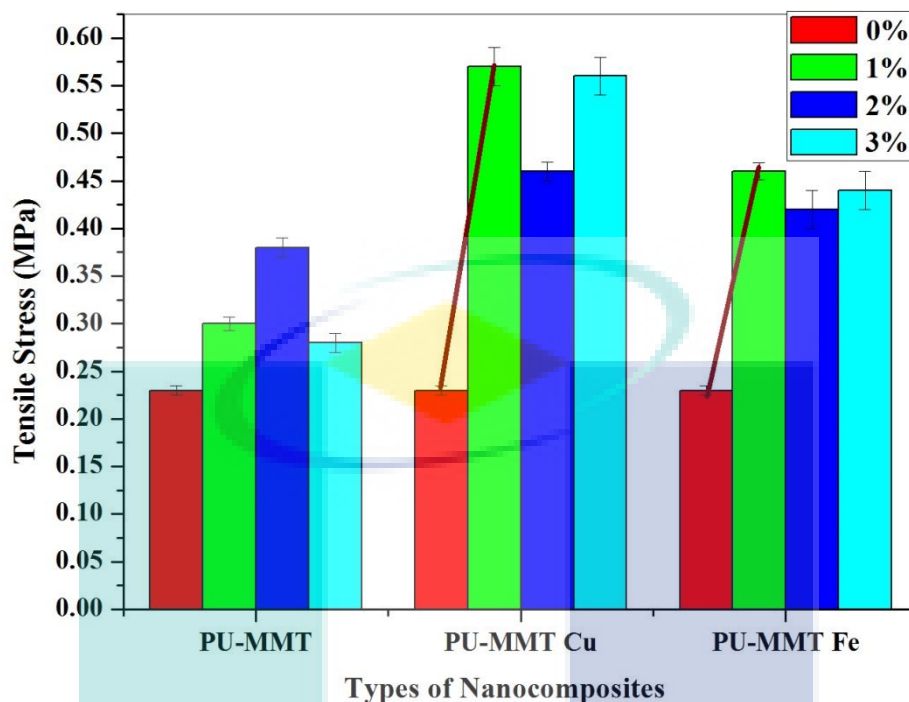


**Figure 4.21: Tensile Stress of Polyurethane Montmorillonite nanocomposite**

From the results obtained, the incorporation of clay in the polymer matrix promoted an increment in the tensile stress as can be seen in Figure 4.21. PU-MMT with 1% clay loading exhibited 65% increment in tensile stress compared to PU. The highest increment among these three different percentages of clay loading was seen on 2% PU-MMT which was 83%. There was not much improvement in the tensile stress of PU-MMT as compared to PU-MMT Cu and PU-MMT Fe due to the clay agglomerations as shown in the Scanning Electron Microscopy (SEM) analysis which is shown in Figures 4.10, 4.11 and 4.12. It can be presumed that the incompatibility of MMT clay with PU was unable to create a good dispersion of these particles in the matrix. Successful strengthening of the interfacial interactions between the dispersed phase and matrix phase could not be achieved in the case of PU-MMT. Dowling et al. (2006) anticipated that the modification of the clay with organic cationic surfactants reduces the agglomerates and helps to intercalate the MMT platelets.

In line with them, the modification done on the clay did indeed result in higher values of tensile stress as compared to PU and PU-MMT. In general, from the results attained it can be seen that the tensile stress of PU-MMT Cu was higher compared to PU-MMT. The highest leap of 148% was seen in 1% and 3% clay loading followed by 100% increase in 2% PU-MMT Cu. The higher increase as compared to PU-MMT is due to lesser clay agglomerates in the structure which is shown in SEM image in Figures 4.12 and 4.13 in which the modification using copper is proven to reduce the agglomerates. Copper has always been of a particular interest due to its catalytic performance in the reactions (Ding and Frost, 2004) and through the incorporation of MMT with modified clay into PU, the strong electrostatic force between the positively charged ions that are attracted to the net negative charge within the clay structure is destroyed and the clay is able to distribute itself evenly in the matrix.

Similar patterns of the result were seen in PU-MMT Fe. A twofold increase was again seen in 1% PU-MMT-Fe. PU-MMT Fe with 2% and 3% clay loading showed 83% and 91% increase respectively. This increment in tensile stress can be attributed to the nature of the iron which has almost similar catalytic performance with than copper. A decrement of tensile stress from 1% clay loading to 2% was observed in both PU-MMT Cu and PU-MMT-Fe. This decrease could be attributed to the high organoclay content in the matrix in which the clay is more prone to settling rather than being distributed evenly in the matrix. Other researchers who found similar results were Isik et al. (2003) and Chang et al. (2003). They argued that at high clay contents, clay particles agglomerates and act as stress concentrators that decrease the impact strength. However, in general, it can be seen that the incorporation of modified clay into polyurethane has brought forth significant improvement in the tensile stress.

#### 4.4.2 Elongation at Break (EB)

The elongation at break (EB) is the increase of percentage in length that occurs before the polymer nanocomposites sample breaks under strain. There were three different weight percentages that were studied in this experiment which were 1%, 2% and 3% clay loading. Six samples were tested for each parameter and average mean value was taken. The results obtained are tabulated as in Table 4.6 below and shown in Figure 4.22.

**Table 4.6:** Effect of Clay on Elongation at Break

Clay %	Elongation at Break (mm)			
	PU	PU-MMT	PU-MMT Cu	PU-MMT Fe
1	1.96	2.95	4.42	3.34
2	1.96	3.25	4.51	4.40
3	1.96	3.41	4.40	4.39

Elongation at break (EB) is highly dependent on the interfacial reactions between the polymer matrix and the clay and from this work; the elongation at break value obtained showed an increasing trend. PU-MMT with 1%, 2% and 3% clay loading showed an increasing pattern in its EB values which were 51%, 65% and 74% respectively. PU-MMT Cu with 1%, 2% and 3% clay incorporation exhibited an increase of 126%, 130% and 124% respectively whereas PU-MMT Fe with the same clay loading increased by 70%, 124% and 124%. The increment observed in PU-MMT Cu is the highest obtained amongst the rest. Abraham et al. (2009) mentioned that the incorporation of fillers to the polymer matrix decreases the EB value however if a good reinforcement can be achieved between the polymer and the filler, the fracture goes from particle to particle rather than following a direct path and the filled polymers have nearly equal EB value with neat polymer. It can be observed from the data obtained that PU with modified clay exhibited higher EB value compared to PU incorporated with conventional clay and it could be deduced that the TMI modification process did improve the dispersion of the filler into the matrix and a good rearrangement of the filler particles were able to be obtained. Increasing trend in EB values may also be an



indicative of a good intercalation and exfoliation phenomena which resulted in high strength reinforcement between the filler and matrix (Varghese et al., 2003).

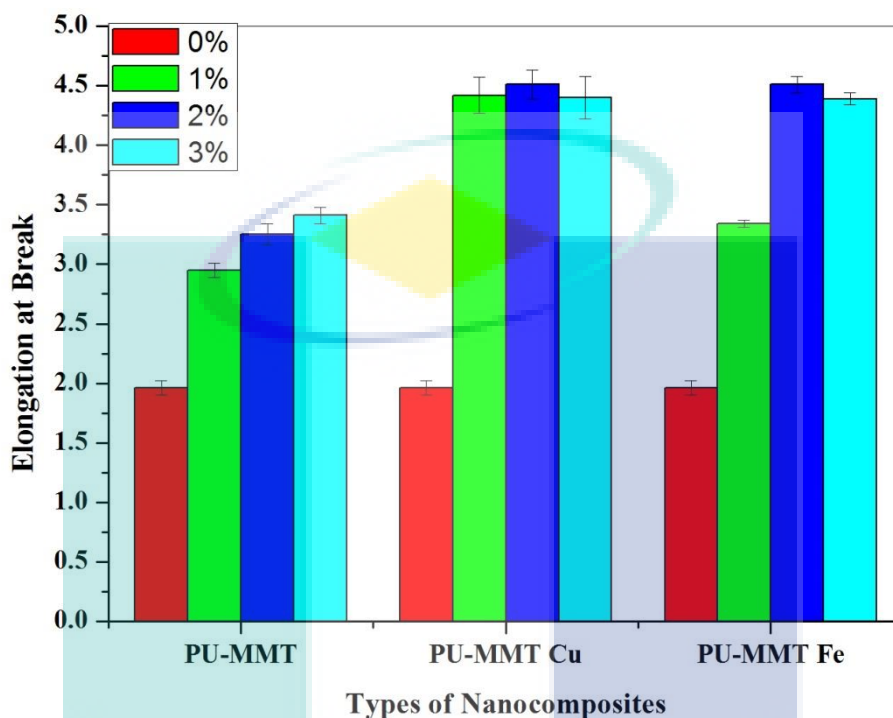


**Figure 4.22: Elongation at Break of Polyurethane Montmorillonite nanocomposite**

Although an increasing trend obtained in this work, there are reports by other authors who obtain a decreasing trend in the EB value with increasing clay loading. Ahmadi et al. (2003) stated that the decrease in the EB values in nanocomposites may be attributed to the fact that ductility decreased when stiffness is increased by reinforcement. Other researches whom reported an increasing and decreasing trend in EB values were Finnigan et al. (2004) and Yao et al. (2002).

## 4.5 PERMEABILITY PROPERTIES

### 4.5.1 Permeability

Permeability properties of materials have attracted significant interest in the past decades especially in applications where transparency and barrier properties are an important carrier. However, it can be seen in literature that the gas and water transport properties of polyurethane nanocomposites have been less thoroughly studied. Osman et al. (2003) claimed that PU adhesives are often of a special interest due to their flexibility and wide application however their overall barrier performance is meager. In order to account to the poor barrier properties of polymeric materials, Moaddeb and Koros (1996) reported in their study that the incorporation of silica particles into the polymer matrix improved the gas separation properties of the polymer-silica membranes. Similar findings were reported in literature by Kusakabe et al. (1996), Kim et al. (2004) and Huang et al. (1994). Generally, permeability is often emphasized on packaging materials and containers however in this study, polyurethane MMT nanocomposites are studied as a thermal insulator and it is equally important for this insulator to possess a good permeability property to allow the smooth transfer of the gases. In this section, the gas and water permeability properties of polyurethane with pristine clay and modified clay with copper and iron are discussed.

### 4.5.2 Gas Permeability Analysis

In this research, the gas permeability properties of PU, PU-MMT, PU-MMT Cu and PU-MMT Fe were tested using the Membrane Separation Unit. Two types of gases were used which were nitrogen and oxygen gases at ambient temperature and three samples were tested for each gas and the average mean value were taken. The gas permeability coefficients ( $10^{-5} \text{ cm}^3 \text{ (STP) cm/cm}^2 \cdot \text{s} \cdot \text{cmHg}$ ) obtained are tabulated in Table 4.7 and depicted in Figure 4.23 and Figure 4.24.

**Table 4.7:** Permeability Coefficients of Polymer Clay Nanocomposites

Sample	Clay Content (wt %)	Permeability Coefficient $10^{-5} \text{ cm}^3 \text{ (STP) cm/cm}^2 \cdot \text{s.cmH}$	
		Nitrogen	Oxygen
PU		3.92	3.13
PU-MMT	1	3.73	3.17
	2	2.83	2.78
	3	2.70	2.86
PU-MMT Cu	1	1.99	2.90
	2	<b>1.84</b>	<b>2.22</b>
	3	1.88	2.44
PU-MMT Fe	1	1.65	2.36
	2	1.53	2.78
	3	<b>1.49</b>	<b>1.83</b>

From the data obtained in the table above, the incorporation of modified clay is seen to remarkably reduce the gas permeability of the polyurethane nanocomposites. In the experiment using nitrogen gas, the highest decrease was seen on 3% PU-MMT Fe which was 62% followed by 2% and 1% clay loading which exhibited a decrease of 61% and 58% respectively. PU integrated with modified copper clay showed a decrease of 52% in 3% clay loading followed by 53% in 2% clay loading and finally 49% in its 1% clay loading. The results gained from PU-MMT did not differ much in both the analysis using the nitrogen and oxygen gas as both permeability coefficients obtained were almost in the same range.

In the gas permeability analysis using oxygen gas the highest decrease was again obtained from 3% PU-MMT Fe which was 42% followed by 2% PU-MMT Cu which was 29%. 1% and 3% PU-MMT Cu portrayed a decrease of 7% and 22% respectively and on the other hand, 1% and 2% of PU-MMT Fe displayed a decrease of 24.6% and 11.2% respectively.

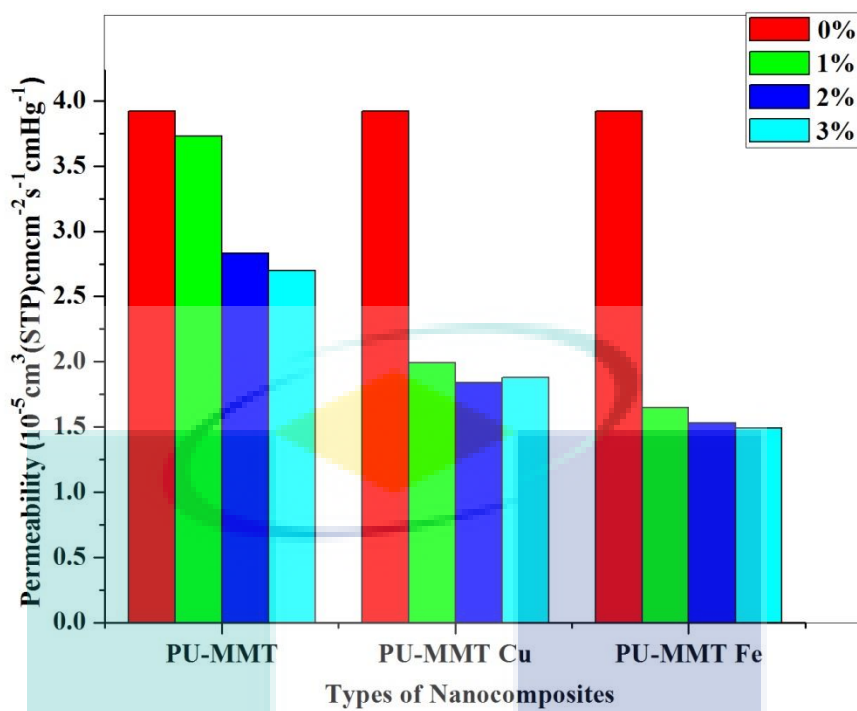


Figure 4.23: Permeability coefficients of PU-Clay Nanocomposites in Nitrogen Gas

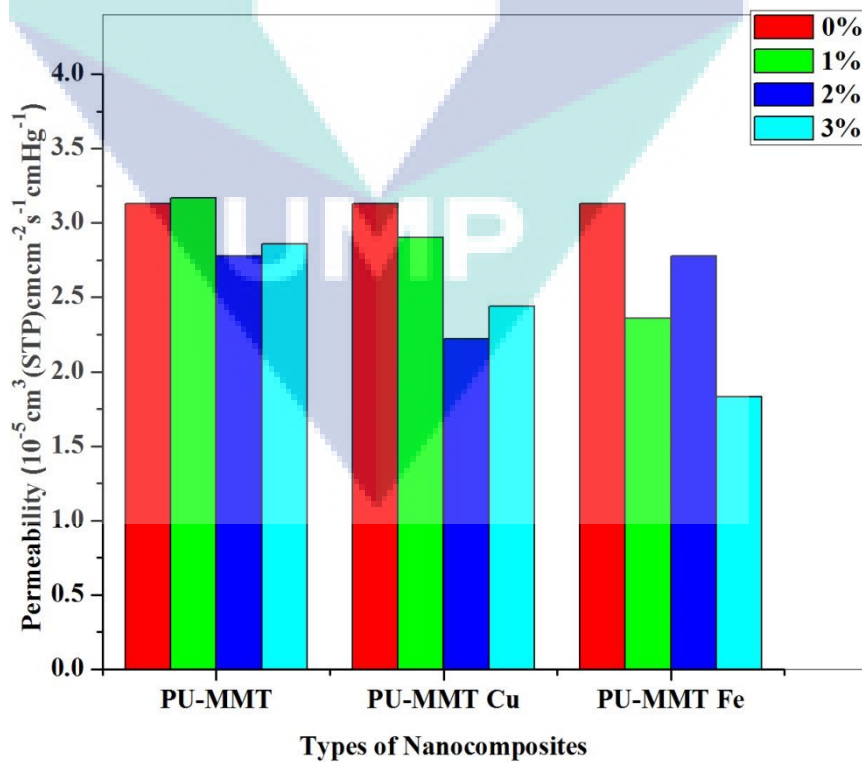
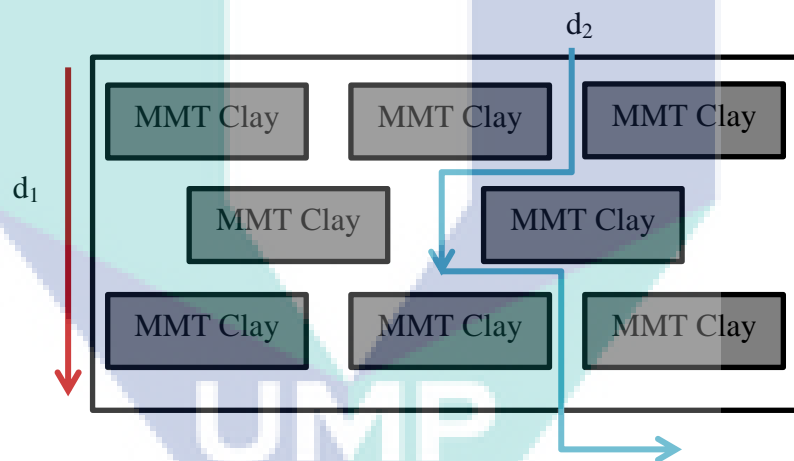


Figure 4.24: Permeability coefficients of PU-Clay Nanocomposites in Oxygen Gas

The incorporation of filler in the polymer matrix has shown a clear decrease in the permeability coefficient values. It is known that the platelet structure of the silicate layers is able to improve the barrier properties of the polymeric material. This has been proved in literature by Chang and Park (2001) whereby in their study, the permeability of the hybrid films decreased with increasing organoclay content. Tortora et al. (2002) also claimed that the permeability of polyurethane nanocomposites decreased up to 20% in their research. Apart from that, Nielsen et al. (1967) proposed in their study that the filler particles incorporated in the polymer matrix are impermeable to the permeant molecules by forming a tortuous path as shown in Figure 4.25 below. In a tortuous path, the distances that the diffusing molecules must travel in a polymer nanocomposite as compared to pristine polymer are maximized as the layered silicates are orientated parallel to the polymer structure. This aids in decreasing the permeability coefficients of the nanocomposites.



**Figure 4.25: Tortuous path in layered silicate nanocomposites;  $d_1$  is the actual distance travelled in the absence of clay and  $d_2$  is the tortuous path length with the presence of clay**

From the results obtained, the permeability coefficient decreased as the clay loading was increased. It was evident from Figures 4.23 and 4.24 that PU incorporated with modified clay showed a greater decline in the permeation values. It can be seen from these decrease that the modification done on the clay via the ion exchange method is seen to have facilitated the penetration of the layered silicates into the polymer matrix and enhanced the intercalation process. However, from Figure 4.24, it can be seen that the permeation coefficient of 2% PU-MMT Fe and 3% PU-MMT Cu showed a slight

increment. It is surmised that the formation of barrier in its structure by LS was not fully achieved as small agglomerates that are presumed to be clay particles can be seen in the SEM micrograph in Figure 4.15 and FESEM micrograph in Figure 4.19.

Nonetheless, successful dispersion of the clay into other fabricated nanocomposites was achieved and this is proven through the coefficients values shown. The polymer clay bond was strengthened in which the layered silicates were able to distribute and arrange themselves evenly in the polymer's structure. Through this, a permeation barrier was able to be formed and the tortuous pathway the gas molecules have to travel during their random motion in the composite are longer and requires a longer period of time. Nielsen (2006) stated that the filler particles in a membrane are impermeable to the permeant molecules since it is uniformly and completely dispersed in the polymer. The hard segment that exists in the nanocomposites on the other hand restricts the chain mobility of the polymer and the space created for diffusion of the permeant molecules. In this study, it can be deduced that the formation of the tortuous path were better in PU-MMT Cu and PU-MMT Fe due to a better interaction between the filler and the matrix. This is supported from the XRD analysis done in the previous section.

In addition, it can be examined from Figure 4.23 and 4.24 that the permeability of oxygen is higher compared to the permeability of nitrogen. Similar results were obtained by Semsarzadeh et al. (2007) and they reported that the permeability of gases is highly dependent on the diffusion coefficient of the gases whereby the order of diffusivity is the reverse of the kinetic diameter for each gas. The kinetic diameter of oxygen and nitrogen is 3.46 Å and 3.64 Å respectively and according to them this justifies the reason on the higher permeation of oxygen compared to nitrogen. The diffusion coefficient of the gases is also dependent on the molecular size of the gas, rigidity, mobility and the condensability of the gases in which oxygen has a higher condensability as compared to nitrogen in which oxygen is able to promote higher solubility in the polymer (Semsarzadeh et al., 2008).

### 4.5.3 Water Permeability Analysis

The water permeability analysis was carried out using a water permeation unit as shown in Figure 3.14. The initial stage required the measurement of flux through the PLSN under ambient temperature and sorbate pressure on the high and low pressure faces. The PLSN membrane was subjected to 3 different pressures from the nitrogen gas and the volume of water permeated through the membrane was kept constant at 10ml. The time taken for the water permeation was recorded and tabulated in Table 4.8. Compared to previous work in this study, only 1% and 2% PU nanocomposites were tested due to the inability of the 3% PU nanocomposites to retain its structure when placed at the water cell under high pressure.

**Table 4.8:** Time recorded for water permeability analysis of PLSN

Sample	Time (s)		
	2 bar	3 bar	4 bar
PU	18.9	14.4	10.0
1wt % PU-MMT	92.4	52.1	23.5
1wt% PU-MMT Cu	253.4	78.3	39.9
1wt% PU-MMT Fe	400.5	172.3	96.7
2wt% PU-MMT	74.2	71.2	40.8
2wt% PU-MMT Cu	250.6	127.6	96.7
2wt% PU-MMT Fe	290.3	99.4	43.0

The results obtained showed that the time taken for water to permeate through PU incorporated with silicate layers increased as compared to pristine PU and the hike were even evident in modified silicate layers. The permeation of water recorded the longest time in PU-MMT Fe followed by PU-MMT Cu. It can be seen that the water molecules took the longest time to permeate through PU-MMT Fe and PU-MMT Cu due to the tortuous path introduced by the LS which results in the permeate to travel a longer distance in PLSN as compared to neat PU. From the results obtained, the flux is determined from the rate of time versus pressure of the permeate gas (Paravar and Hayhurst, 1984) and tabulated in Table 4.9.

**Table 4.9:** Flux values of PU Nanocomposites

Sample	Flux
PU	-4.46
1 wt%	
PU-MMT	-69.49
PU-MMT Cu	-106.73
PU-MMT Fe	-182.07
2 wt%	
PU-MMT	-16.72
PU-MMT Cu	-76.93
PU-MMT Fe	-123.61

The permeation coefficient was obtained from the steady state flux obtained from the graphs above according to Equation 4.2 (Alexandre et al., 2009).

$$P = \frac{J_{st}L}{\Delta a} \quad \text{Equation (4.2)}$$

where  $J_{st}$  is the flux,  $L$  is the thickness of the membrane and  $\Delta a$  is the difference in water activity between the two faces of the film. The permeability coefficients tabulated from the equation above are shown in Table 4.10.

**Table 4.10:** Water Permeability Coefficients

Sample	Permeability Coefficient (bar.mm/s)
PU	-0.1338
1 wt%	
PU-MMT	-2.0847
PU-MMT Cu	-3.2019
PU-MMT Fe	-5.4621
2 wt%	
PU-MMT	-0.5016
PU-MMT Cu	-2.3079
PU-MMT Fe	-3.7083



The permeability coefficients decreased tremendously in the PU incorporated with modified layered silicates. The findings were in line with Mai and Yu (2006) and in their study, they stated that these layered silicates with planar orientations have proved to improve and elevate the barrier properties of the polyurethane nanocomposites by the formation of the tortuous path which increases the water molecule's diffusion distance and indirectly slowing down the permeation of the water molecules. In addition, Gusev and Lusti (2000) reported that a major factor that is accountable for the barrier property is the changes in the local permeability due to transformation of the molecular level in the polymer matrix that is caused by the silicate layers and directly related this to the molecular level interaction between the polymer matrix and the layered silicates.

It can be examined from Table 4.10 that PU-MMT Fe and PU-MMT Cu depicted the lowest permeability coefficient which could be associated to the good interaction level between PU and the LS as the result of the TMI modification done on the clay. The modification process has clearly enhanced the interaction level by creating an intercalated system as supported by the XRD analysis and further proved by the SEM micrographs.

The logo for UMP (Universiti Malaysia Perlis) is a large, downward-pointing arrow shape. It is composed of several overlapping geometric shapes in shades of teal, light blue, and yellow. The letters 'UMP' are written in a bold, white, sans-serif font across the center of the arrow.

UMP

## 4.6 THERMAL PROPERTIES

Thermal properties of PLSN have attracted a significant amount of interest due to the ability of the layered silicates to trigger a tremendous thermal properties' improvement. The improvement in the thermal stability of polymers in the presence of layered silicates can be attributed to the rich intercalation of polymer chains into the lamellae of layered silicates. These layered silicates act as an insulator between the heat source and the surface area of the polymer which is subjected to the heat source (Etmimi, 2012). In this research work, the thermal analyses carried out were the Thermal Gravimetric Analysis (TGA), Differential Scanning Calorimetry (DSC) and thermal conductivity. The sections that follows discusses the results obtained from both the analysis done in order to get a better understanding on the thermal properties of PU nanocomposites prepared in this work.

### 4.6.1 Thermal Gravimetric Analysis (TGA)

Thermogravimetry is used in general to measure the change in mass of a sample as a function of temperature or time. In this work, thermal gravimetric analysis (TGA) was conducted to measure the thermal stability of the prepared polyurethane nanocomposites as a function of temperature. The TGA thermograms of all three different percentages of PU, PU-MMT, PU-MMT Cu and PU-MMT Fe are illustrated in Figures 4.26 and 4.27 whereas Table 4.11 tabulates the thermogravimetric data inclusive of  $T_{10}$  which is the onset temperature at which 10% mass loss of the nanocomposite occurs,  $T_{90}$  which is the temperature at which 90% mass loss occurs, the degradation temperature ( $T_d$ ) and lastly, the remaining fraction of non-volatile material which is the char is also shown.

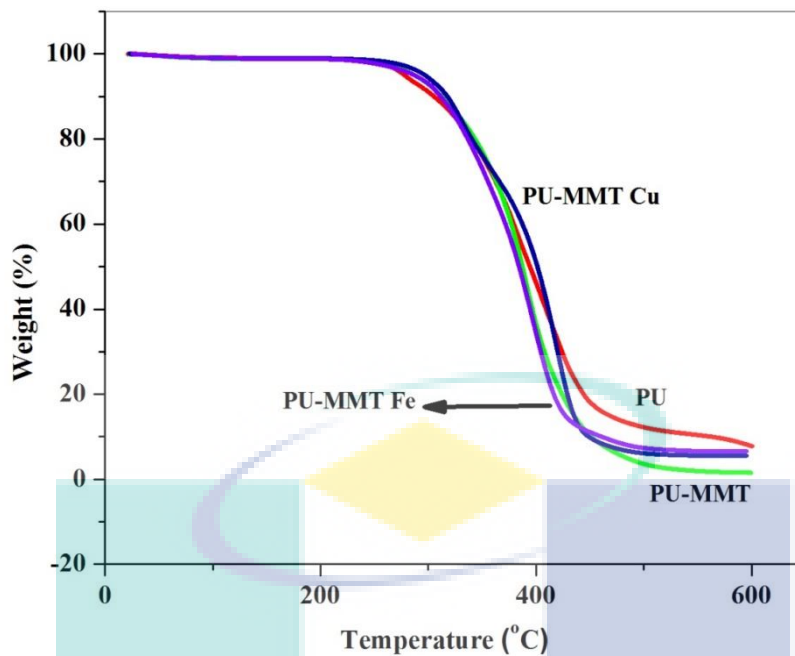
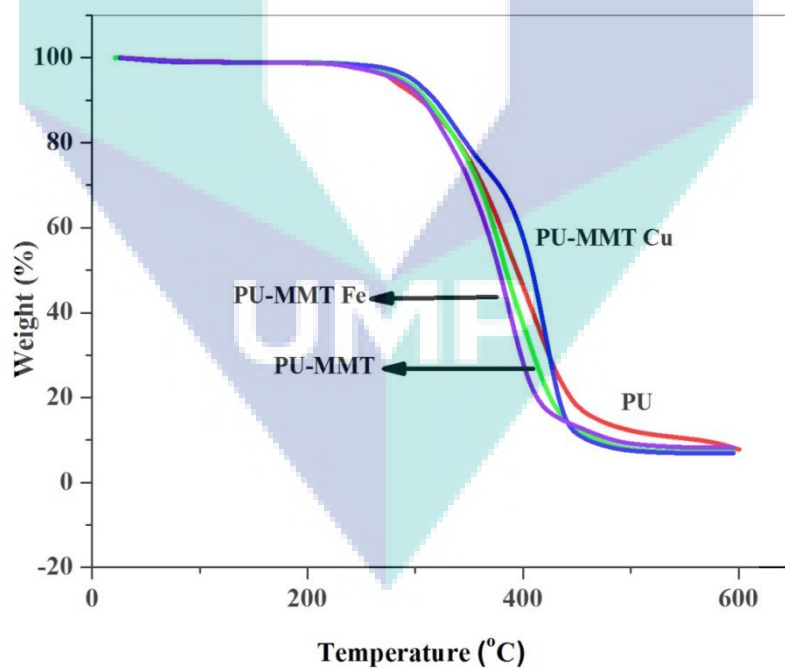


**Figure 4.26 (a):** Thermogravimetric curves of pure PU and 1% modified PU



nanocomposites

**Figure 4.26 (b):** Thermogravimetric curves of pure PU and 2% modified PU nanocomposites

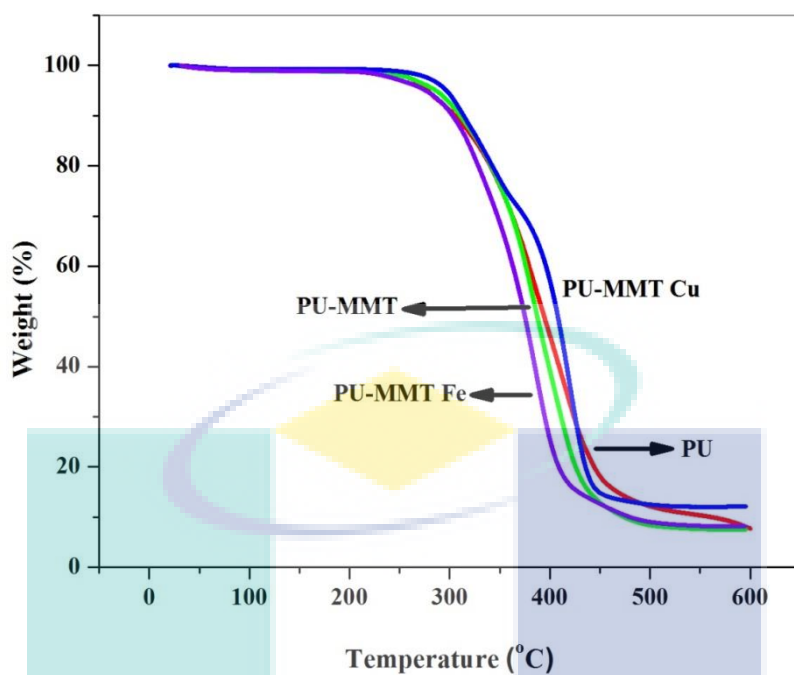


**Figure 4.26 (c):** Thermogravimetric curves of pure PU and 3% PU nanocomposites

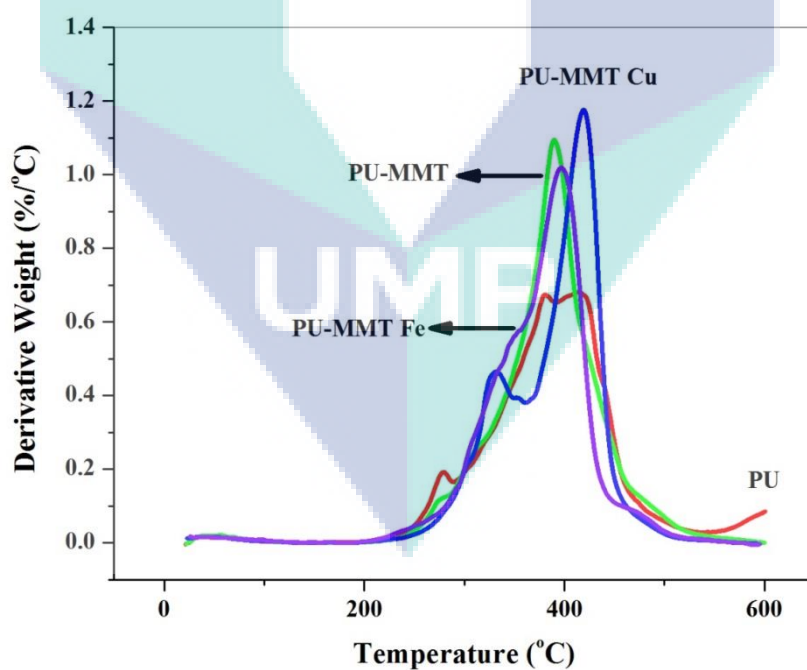


**Figure 4.27 (a):** Derivative thermal gravimetric (DTG) of pure PU and modified 1% PU nanocomposites

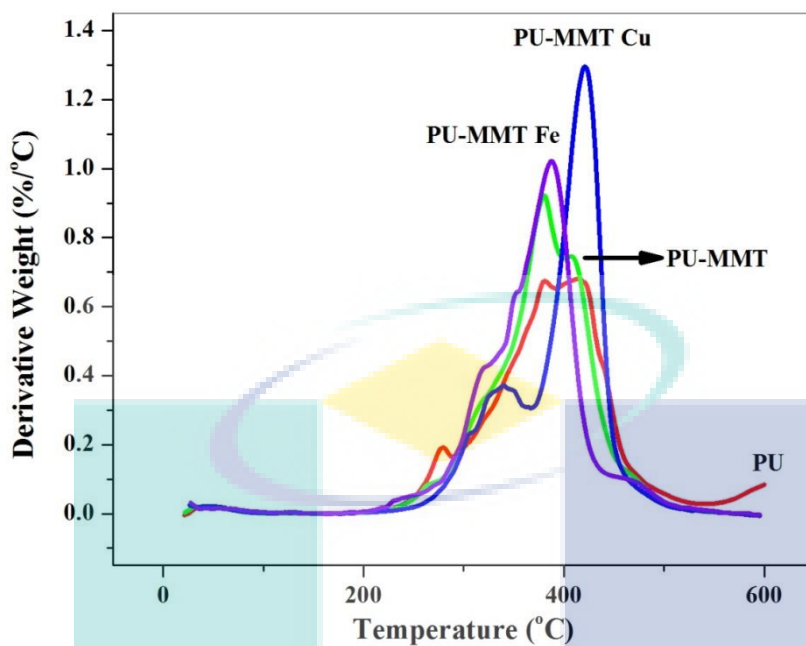


**Figure 4.27 (b):** Derivative thermal gravimetric (DTG) of pure PU and modified 2% PU nanocomposites

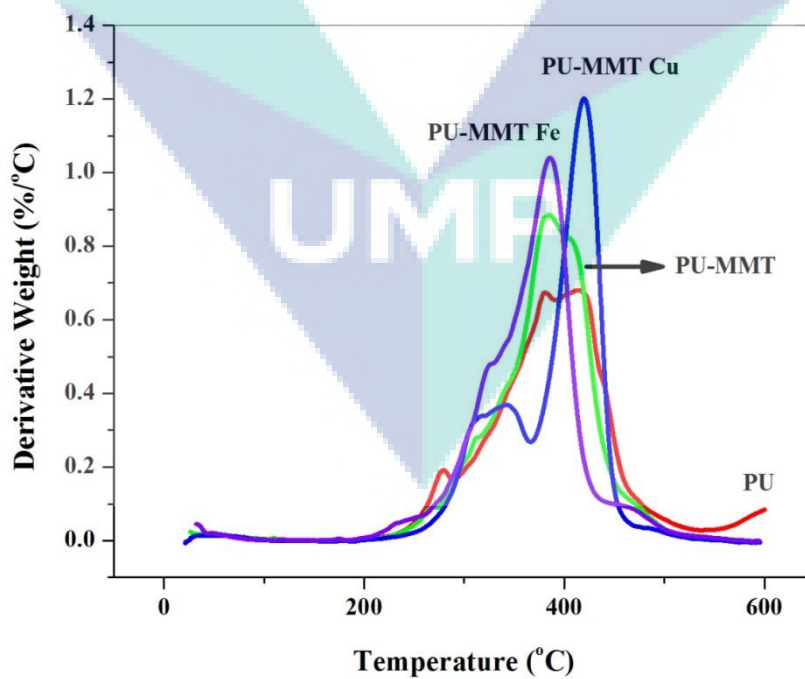


**Figure 4.27 (c):** Derivative thermal gravimetric (DTG) of pure PU and modified 3% PU nanocomposites

**Table 4.11:** Thermogravimetric properties of polyurethane and its nanocomposites with different clay loading (0-3wt %)

Nanocomposite	Clay loading (wt%)	T <sub>10</sub> (°C)	T <sub>90</sub> (°C)	T <sub>d</sub> (°C)	Char (%)
PU	0	460.0	312.6	367.3	0.0
PU-MMT	1	450.0	314.5	386.2	1.5
	2	460.0	318.0	387.0	7.3
	3	470.0	314.3	380.0	7.6
PU-MMT Cu	1	450.4	315.4	382.9	5.5
	2	463.8	319.6	391.7	6.9
	3	508.7	319.2	395.0	12.2
PU-MMT Fe	1	453.2	318.1	381.2	6.6
	2	480.0	315.3	384.1	8.2
	3	499.1	312.0	378.6	8.2

The incorporation of LS into PU has enhanced their thermal stability compared to pristine PU. It can be observed from the data acquired that the onset temperature, T<sub>10</sub> of 2 and 3wt% clay loading of the synthesized nanocomposites increased by 10°C to 48.7°C and T<sub>90</sub> of the nanocomposites increased by 2°C to 6°C. However, T<sub>10</sub> of PU incorporated with MMT appeared to be lower than pristine PU. This could be associated to the early loss of quaternary ammonium ions in the clay which had undergone the Hoffman elimination during the onset degradation. In the cases of PU-MMT Cu and PU-MMT Fe, these temperatures are slightly higher. This might be due to the TMI modification process that has replaced the quaternary ammonium ions in the clay. After the preliminary degradation, the char that is produced acts as a barrier and results in the increase of T<sub>90</sub> and similar results were reported by Saha et al. (2013). The TGA results obtained proved that the enhancement in the thermal stability is more significant with the incorporation of modified clay. At filler loading of 3 wt%, the degradation temperature (T<sub>d</sub>) for PU-MMT, PU-MMT Cu and PU-MMT Fe increased by 3.5%, 7.5% and 3.08% respectively, whereas at 2% clay loading the increase were 5.4%, 6.6% and 4.6%. Mai and Yu (2006) associated this improved stability with the lower thermal

stability of the alkylammonium ions in the layered silicates in their work and this work it could be associated with the lower thermal stability of the TMIs.

It can also be observed from the results that  $T_d$  in general is higher in PU with modified clay compared to conventional clay. This may suggest that the TMI modification done on the clay has played a significant role in exfoliating the layered silicates into the PU matrix with improved thermal stability. The increase in the stability may be a result of the improved barrier properties in the polymer due to the incorporation of the layered silicates whereby it prevents the penetration of oxygen and thus reduces the oxidation of the resin. Similar results were obtained by Baysal et al. (2013). They analysed the thermal properties of polyurethane and polyurethane–organoclay nanocomposites and they found that the introduction of organoclays into polymer backbones increased its thermal stability. They suggested that the nanocomposites displayed higher thermal resistance than pristine polymer due to the decomposition of the intercalated polymers present in the interlayers of the clay.

From the data gained according to Table 4.11, it can be observed that there are no residue or char for PU however the charred residue of the nanocomposites increased at increasing clay loading of the layered silicates. The highest char was produced by 3wt% PU-MMT Cu with 12.19% followed by 2 and 3 wt% of PU-MMT Fe which showed 8.2%. The introduction of layered silicates in PU is seen to enhance the formation of char in the polymer which indirectly reduces the rate of decomposition of the polyurethane nanocomposites. PU-MMT, PU-MMT Cu and PU-MMT Fe with 1wt% clay loading of layered silicates portrays a weight loss of 98.5%, 94.5% and 93.4% respectively whereas the same nanocomposites with 3wt% of clay loading exhibited less weight loss which were 92.4%, 87.8% and 91.8%. The dispersion of clay particles is seen as a heat barrier that enhances the thermal stability of the system as well as forming char residues after thermal decomposition and during the initial stage of the thermal decomposition, the clay is able to shift the decomposition temperature higher (Okamoto, 2003).

The amounts of char in modified layered silicates were lesser in 1 and 2 wt% of PU-MMT Cu and 3 wt% of PU-MMT Fe compared to conventional clay incorporated into the matrix however the rest of the nanocomposites exhibited a slight increase in the

weight percentage. It is known generally that layered silicates consist of stacking layers and it does not burn easily. This in return results in high char residue however in the case of 1 and 2 wt% of PU-MMT Cu and 3 wt% of PU-MMT Fe, the clay is seen to have intercalated perfectly into the structure of the nanocomposites as supported by the XRD analysis. This justifies the lesser amount of the char produced by these nanocomposites.

Derivative thermal gravimetric (DTG) was further employed to study the thermal stability of the nanocomposites which was expected to shed some light on the chemical structure of the nanocomposites. Figure 4.30 delineated the DTG of the different types of nanocomposites analyzed in this study. In the case of PU, three steps of the weight loss may be observed. The weight residues from 260°C can be related to the thermal dissociation of the ester bonds whereas the peak at 400°C shows the decomposition of the isocyanurate rings which are more thermostable. The urethane bonds formed through the reaction of aromatic diisocyanate with polyols are characterized by the temperature of thermal dissociation around 630°C.

Vitkauskiene et al. (2011) reported similar thermal profiles of polyurethane-polyisocyanurate foams in their study. The incorporation of MMT clay is seen to shift the peak temperature to slightly high values and this shows that the clay has a contribution in the decomposition rate. PU incorporated with MMT showed a visible peak at around 400°C where this occurrence can be related to the decomposition of the silica particles. However, with the addition of clay modified with copper and iron ions, two peaks may be observed especially in the case of PU-MMT Cu. The first peak may be attributed to the decomposition of the PU's matrix whereas the second peak which appeared at a higher temperature is due to the PU physicochemical attachment to the nanoparticle's surface. Similar results were reported by Guo et al. (2007) and they claimed that this phenomenon is an indication of strong chemical bonding between the nanoparticles and the Pu's matrix.



#### 4.6.2 Differential Scanning Calorimetry (DSC)

Differential Scanning Calorimetry (DSC) is a technique used to study the thermal transitions of a substance when it is being heated. Thermal transitions are the changes that take place in a polymer such as the melting of the crystalline and the glass transition of the substance. The changes in the enthalpy are measured using a calorimeter which records the displacement of heat flux,  $Q$ , from the baseline. All the nanocomposites studied in this section of the report are polyurethane incorporated with 1% clay loading of pristine MMT and MMT modified with copper and iron ions. Figure 4.28 illustrates the graph plot of the data obtained from the analysis.

Polymeric materials are known to melt over a relatively broad range due to its semi crystalline behavior and the melting range is governed by the structure of the polymer. From Figure 4.27, four different types of data were obtained which are the temperatures in which the less perfect crystallites in the semi crystalline polymers begin to melt ( $T_{im}$ ), the onset temperature which is the intersection of the extrapolated linear section of the falling peak edge with the baseline extrapolated from temperatures below the peak ( $T_{eim}$ ), the melting peak temperature ( $T_{pm}$ ), and the end melting temperature at which all the crystallites have melted and the crystalline order has been destroyed ( $T_{efm}$ ). The acquired data were then tabulated in Table 4.12.

**Table 4.12:** Characteristic temperatures of PU nanocomposites' melting curve

Nanocomposites	$T_{im}$	$T_{eim}$	$T_{pm}$	$T_{efm}$
PU	350	375	390	398
PU-MMT	368	354	380	398
PU-MMT Cu	346	348	372	388
PU-MMT Fe	340	350	370	384

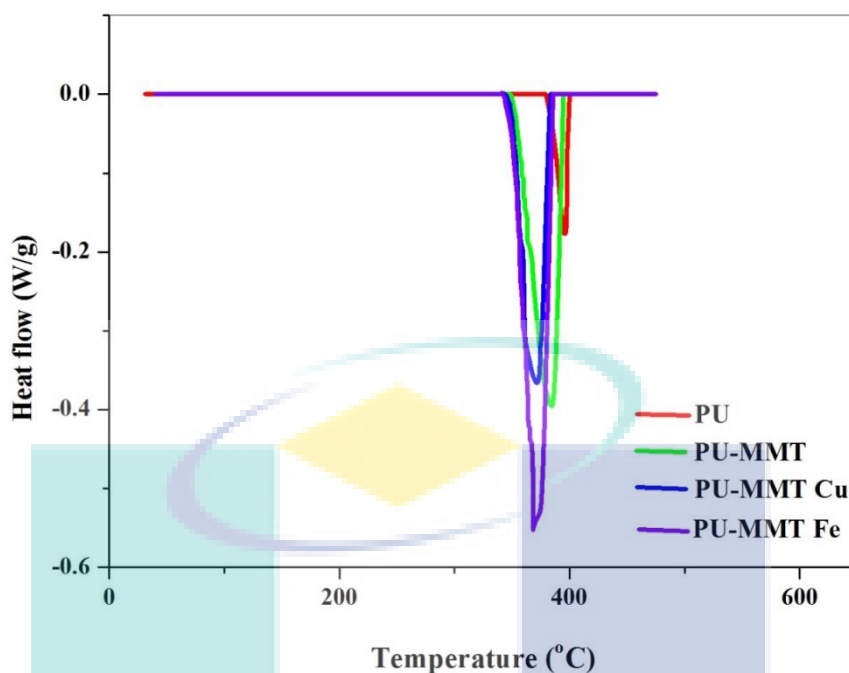
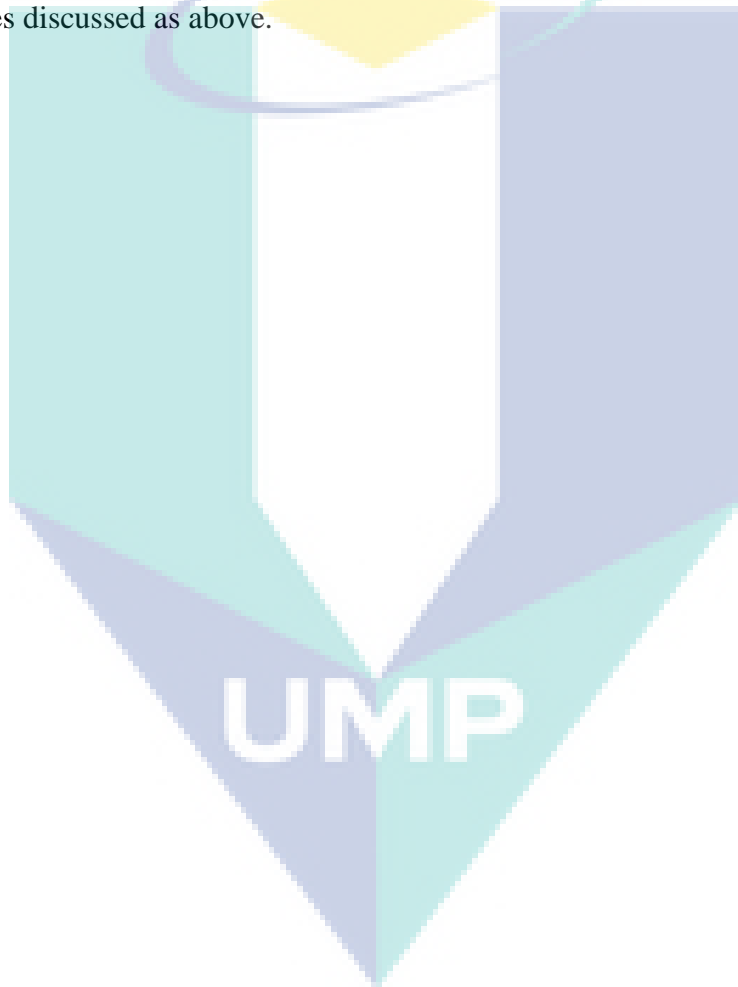


**Figure 4.28:** Heating curve for 1% clay loading of PU nanocomposites (Melting transitions)

From the results obtained, it can be observed that the  $T_{im}$  of the nanocomposites were almost in the same range and this can be attributed to the backbone structure of PU that is consisted of soft segment (SS) and hard segment (HS). PU is well known to exhibit phase separation in which the SS units confer elastomeric behavior whereas the HS provides physical cross linking. In the initial melting state of the polymer, the semi crystallites in the SS stage tend to melt which is then followed by the melting of the microphase in HS. It can be noted from the temperatures obtained that the incorporation of clay into the polymer matrix did not significantly shift the temperature to a higher or lower value. This indicates that the clay incorporated was predominantly confined to the amorphous phase without significantly affecting the development of crystals in the copolymer matrix. The melting temperature ( $T_{pm}$ ) of the nanocomposites showed a decreasing trend as shown in Table 4.13. It can be presumed that the addition of LS into the PU's matrix has disrupted the formation of crystallites due to the polarity in the clay's structure. Similar results were obtained by Naguib et al. (2013). In their study, they reported a declining trend in the melting and crystallinity of Poly(3-hydroxybutyrate) with an increasing amount of C30B clay. Apart from them, Panupakorn et al. (2013) justified in their work that there was no significant change in

the melting temperature of polyethylene with the addition of nanoclay due to the decrease of the nature of crystallization. The insignificant change was attributed to the large amount of clay particles locating themselves in the interlamellar spaces and leaving little room for additional crystallization. It can be assumed from this study that the hard segments in the PU nanocomposites were unable to form crystal structures as they were prepared through solvent intercalation and this is in line with a study conducted by Seymour and Cooper (1973). A perfect phase separation could not be achieved thus the addition of MMT clay in the structure did not affect the range of temperatures discussed as above.



#### 4.6.4 Thermal Conductivity

Thermal conductivity is the measure of the capacity of a material to conduct heat through its mass. In this work, PU nanocomposites prepared are studied as a thermal insulation material and the main function of an insulation material is to reduce the transmission of heat through the material. A good insulation material is expected to have a low thermal conductivity value in order to reduce the total coefficient of heat transmission. In this part of the research, the thermal conductivity of each sample was obtained through the average of three specimens. Figure 4.29 depicts the thermal conductivity of PU and PU nanocomposites whereas Table 4.13 summarizes the data obtained.

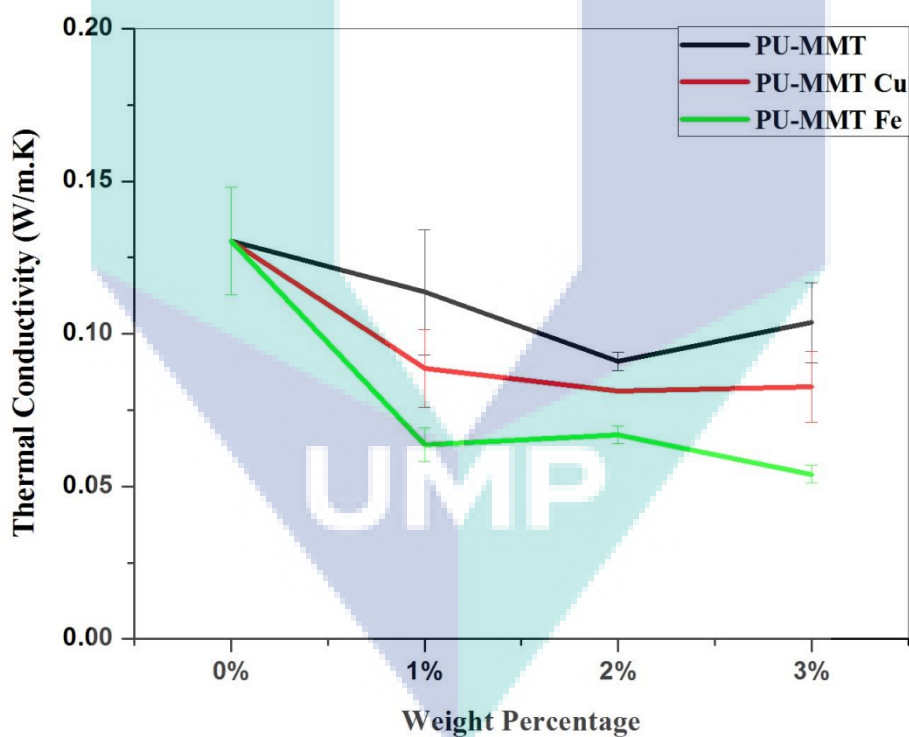


Figure 4.29: Thermal Conductivity of Polyurethane Nanocomposites

**Table 4.13:** Thermal conductivity data of polyurethane nanocomposites

Sample	Clay Content (wt %)	Thermal Conductivity (W/m.K)
PU	0	0.13
PU-MMT	1	0.11
	2	0.09
	3	0.10
PU-MMT Cu	1	0.09
	2	<b>0.08</b>
	3	<b>0.08</b>
PU-MMT Fe	1	0.06
	2	0.07
	3	<b>0.05</b>

From the data obtained, a decrease in thermal conductivity as a function of increasing concentration of modified clay can be observed. The highest thermal conductivity was shown by PU followed by PU-MMT, PU-MMT Cu and PU-MMT Fe. According to Fourier's Law, thermal conductivity ( $k$ ) is defined as below and expressed in reduced units of W/mK.

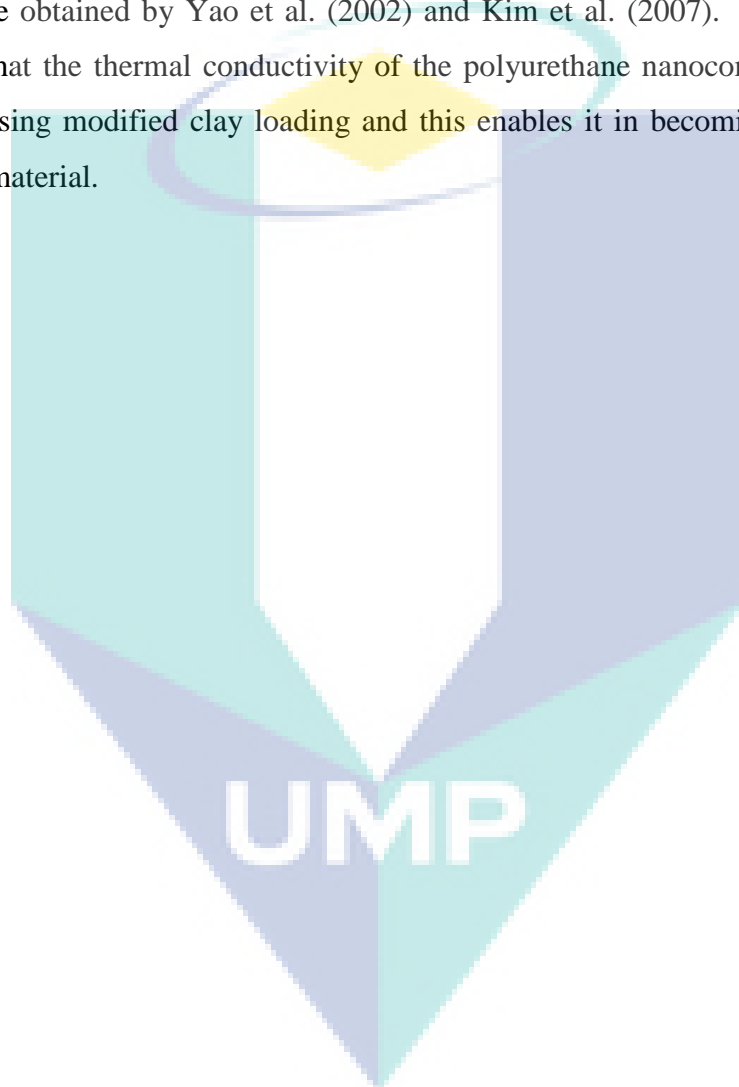
$$k = \frac{q \cdot t}{A \cdot \Delta T} \quad (\text{Equation 4.3})$$

where:

- $q$  = heat flow in Watts
- $t$  = length of heat path (interface thickness)
- $A$  = area in meters
- $\Delta T$  = temperature difference across the interface

The decrease in the thermal conductivity of the nanocomposites may be attributed to the large surface area of the intercalated clay layers in polyurethane matrix. It can be seen from the Equation 4.3 that the area of the material is reciprocal to thermal conductivity. When the layered silicates are intercalated in the matrix, a larger surface area of the

material is obtained and reduces the conductivity. It is also to be noted that PU with modified clay showed good intercalation through the XRD analysis and this intercalation has lowered the conductivity values even more. In addition, the incorporation of clay in the polyurethane will result in a distribution of small nano-sized grain in its structure and due to the grain boundary scattering effects (Zink et al., 2006), the heat path taken will be shorter which reduces the thermal conductivity. Similar results were obtained by Yao et al. (2002) and Kim et al. (2007). It can be deduced from this that the thermal conductivity of the polyurethane nanocomposites decreased with increasing modified clay loading and this enables it in becoming a good thermal insulation material.



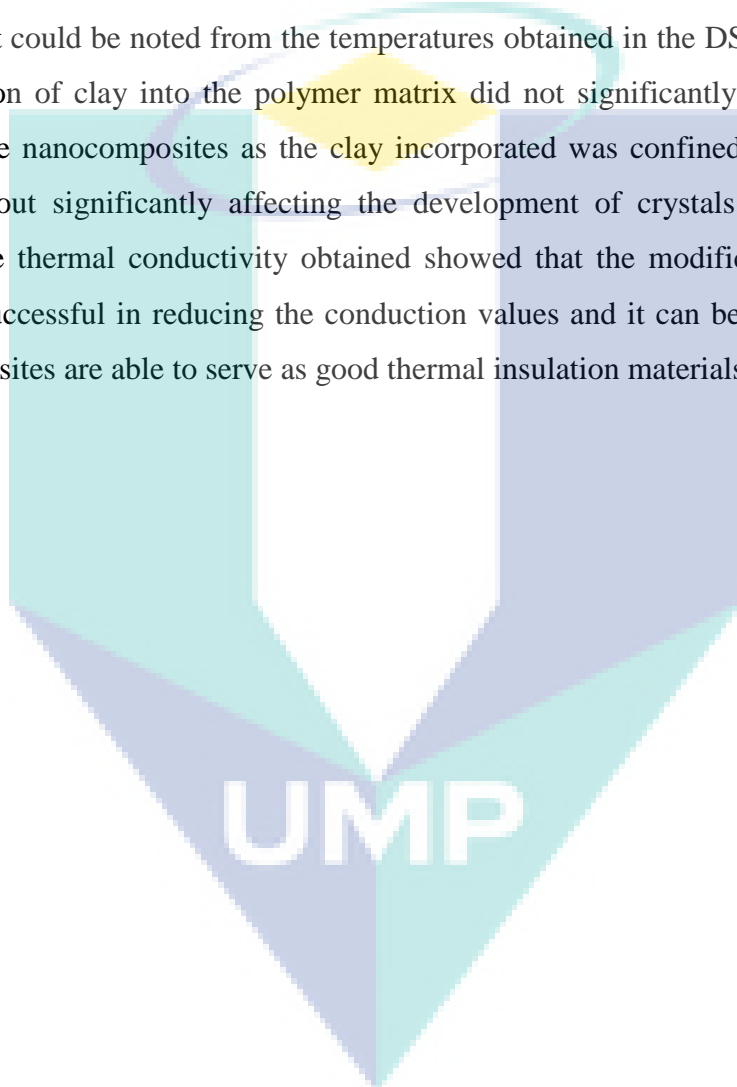
#### 4.7 SUMMARY

The incorporation of clay into PU was confirmed through the presence of peak obtained in the FTIR analysis. ICP-MS was employed in the study to affirm the modification process done was successful in depicting the presence of the copper and iron ions in the clay. The increase in the interlayer spacing of the modified PU nanocomposites relative to PU incorporated with conventional MMT clay confirmed the insertion of the MMT between the PU's structure was better with the TMI modification process and affirmed the intercalation of the clay. SEM and FESEM were used to visualize the structure of the nanocomposites. Results obtained showed the presence of large agglomerates in the PU-MMT were due to poor distribution of the clay in the matrix and the intrinsic incompatibility of hydrophilic layered silicates and hydrophobic polymers, however, with the incorporation of modified clay into the matrix, lesser agglomerates were present due to the ion exchange between inorganic sodium cations on the clay surface with the copper and iron ions. Presence of smaller agglomerates were however visible in higher clay percentage and this was attributed to the tendency of the clay that is unable to distribute itself evenly at high clay loading as the clay particles are more prone to settling and unable to create a uniform dispersion.

The mechanical testing showed an increasing trend in the tensile stress of PU incorporated with modified clay. Incorporation of clay enhanced the mechanical properties of the polyurethane as it is known to have a surface area and external surfaces of nanomaterial has less defect compared to the polymer materials. The modified organoclay is seen to increase the interfacial interaction between the filler and the PU matrix which enables the nanoparticle agglomerates to break down. This enhances the dispersion of the nanoparticles filler, strengthens the clay composite bond and elevates the mechanical properties of the nanocomposites. For the water and gas permeability analysis, the incorporation of clay was seen to create a tortuous path in the structure of the nanocomposites. This path restricts the passage of gases and liquid through them. In general, the weaker force in the polymer chains usually move aside to allow the permeation of the gases and liquid, however with the addition of clay, the forces were held stronger and the permeation coefficients obtained were lesser as increasing clay loading. The decreases in permeation values were even more evident in the modified

clay nanocomposites due to the strong interaction between the polymer matrix and the clay.

The thermal analysis employed which were the TGA and DTG indicated that the polymer nanocomposites prepared with modified clay had better thermal stability compared to neat polymer as the thermal degradation temperature of the nanocomposites shifted to higher temperature in the presence of modified clay. However, it could be noted from the temperatures obtained in the DSC analysis that the incorporation of clay into the polymer matrix did not significantly affect the melting range of the nanocomposites as the clay incorporated was confined to the amorphous phase without significantly affecting the development of crystals in the copolymer matrix. The thermal conductivity obtained showed that the modification done on the clay was successful in reducing the conduction values and it can be presumed that the nanocomposites are able to serve as good thermal insulation materials.





## CHAPTER 5

### CONCLUSION AND RECOMMENDATIONS

#### 5.1 CONCLUSIONS

All the objectives in this study were successfully achieved. The first objective was the preparation of the nanocomposites through solution intercalation and it was successfully done by using chloroform as the solvent. The second objective which was the modification process was successful as the transition metal ions which were copper and iron ions were detected in the modified clay and it was in abundance when compared to the pristine clay. After the modification process, the distribution of the clay was even and this was depicted in the FESEM micrographs. The following objective was the incorporation of the pristine and modified clay into the polyurethane and studying its morphology. After the fabrication process, the presence of the clay was confirmed through the peaks that appeared in the Fourier Transform Infrared Spectroscopy (FTIR). Further analysis of the morphology was carried out using Scanning Electron Microscope (SEM) and FESEM. Images obtained showed that the incorporation of pristine clay into PU created large agglomerates in its structure. This problem was anticipated as clay has the tendency to agglomerate due to its stacked layer structure and hydrophilic nature and the modification process was intended to decrease these agglomerations. The modification proved to be successful as there were almost no agglomerates present in the micrographs of polyurethane with modified copper and iron in both the SEM and FESEM analysis. This also confirmed that solution intercalation method was rewarding in fabricating the polyurethane nanocomposites with lesser agglomerations.

Major improvements on the mechanical properties of the PU nanocomposites were observed in PU-MMT Cu and PU-MMT Fe whereby the tensile stress and

elongation at break of the modified PU nanocomposites showed a significant increase compared to incorporation with MMT clay. 1% and 3% clay loading of PU-MMT Cu and PU-MMT Fe were the dominant of all samples tested. The barrier properties of the polyurethane clay nanocomposites were tested via two different approaches which was the gas permeability properties and water permeations. In both the barrier test, PU-MMT Cu and PU-MMT Fe depicted the best improvements. The decrease in the polymer coefficients can be attributed to the formation of the tortuous path in the polymer nanocomposites which increases the gas and water diffusion distance. The ability of the silicates to arrange themselves evenly in the polymer's structure is associated with the modification process that creates a good interaction between the clay and the polymer matrix. Following that, improved thermal stability in the polyurethane with modified clay could be seen from the TGA and DTG analysis as higher thermal degradation temperature were obtained in the presence of polyurethane modified clay nanocomposites. From the DSC results attained, it can be observed that the degree of crystallinity was not affected by the incorporation of the clay as decreases in the melting temperature's peak of the PU nanocomposites were noticed.

In summary, this work has established a good understanding on the use of layered silicate as a filler material for fabricating advanced polyurethane clay nanocomposites. The intercalation of clay into the polyurethane is crucial in order to achieve great advancements in the properties. It was clearly demonstrated that the transition metal modifications on the clay played a vital role in achieving a good intercalation between the filler and the polymer host. Significant improvements in the mechanical, barrier and thermal properties were gained in the polyurethane with modified clay nanocomposites.

## 5.2 RECOMMENDATIONS FOR FUTURE WORK

In order to have a better understanding on the influence of the incorporation of conventional clay and modified clay on the properties of polymer clay nanocomposites, different polymers could be used as the polymer matrix. For instance, polymer such as polyamide 6 (PA6) and polylactic acid (PLA) could be used and the property studies could be widened even further to biodegradability studies and rheological studies.

Apart from that, methods on sample preparation may be improved by employing different kinds of approaches such as melt processing. It is important that the new approach used is able to produce good intercalated polymer nanocomposites in a big amount in order to be more time and cost efficient. In addition, varying clay weight percentages should be done to understand more on the impact of the concentrations on the properties tested. The 3% volume fraction used in this study should be made the lowest starting point of the further study. In this work, the MMT clay was modified using copper and iron ions. It is recommended that other types of transition metal ions such as Titanium and Zinc are used to modify the clay to get a better understanding on the catalytic performance that this metal brings upon the clay.

The morphological study of the polymer nanocomposites can be expanded even further by employing analysis such as Transmission Electron Microscopy (TEM) to gain a better understanding on the structure of the nanocomposite formed. In addition to the mechanical tests formed in this work, other mechanical tests such as hysteresis and Dynamic Mechanical Analysis (DMA) can be carried out to study the viscoelastic properties of the nanocomposites. The gas permeability analysis may be varied by using different kinds of gases such as methane and carbon dioxide. In addition, the recovery of the chloroform used in this work could be studied to minimize environmental effect and to reduce health hazards to the surrounding people. It is expected that these recommendations will be able to give a wider understanding on polymer nanocomposites and its properties.

## REFERENCES

- Abdou, A.A and Budaiwi, I.M. 2005. Comparison of thermal conductivity measurements of insulation materials under various operating temperatures. *Journal of Building Physics*. **29**:171.
- Abraham, R., Thomas, S.P., Kuryan, S., Isac, J., Varughese, K.T. and Thomas, S. 2009. Mechanical properties of ceramic-polymer nanocomposites. *Express Polymer Letters*. **3**: 177-189.
- Ahmadi, S.J., Yudong, H. and Li, W. 2004. Synthesis of EPDM/organoclay nanocomposites: Effect of the clay exfoliation on structure and physical properties. *Iranian Polymer Journal*. **13**(5): 415-422.
- Alam, M., Rahman, S., Halder, P.K., Raquib, A. and Hasan, M. 2012. Lee's and Charlton's method for investigation of thermal conductivity of insulating materials. *IOSR Journal of Mechanical and Civil Engineering*. **3**(1): 53-60.
- Alexander, M. and Dubois, P. 2000. Polymer layered silicate nanocomposites: preparation, properties and uses of a new class of materials. *Mater Sci Eng R*. **28**: 1-63.
- Alix, S., Follain, N., Tenn, N., Alexandre, B., Bourbigot, S., Soulestin, J., Marais, S. 2012. Effect of highly exfoliated and orientated organoclays on the barrier properties of polyamide 6 based nanocomposites. *The Journal of Physical Chemistry*. **116**: 4937-4947.
- Alvarez, V.A. and Vazquez, A. 2008. Biodegradable nanocomposites based on starch, pcl and their blends in *Nanocomposites: Preparation, Properties and Performance*. Mancini, L.H. and Esposito, C.L. Nova Science Publishers, Inc: New York.
- Assanpanel. 2009. Polyurethane (online). <http://www.assanpanel.com.tr/en/urunler/sandvic-paneller/cati-sistemleri>. Retrieved on 20<sup>th</sup> November 2013.
- Asim, P. and Sadhan, C.J. 2005. Synthesis of thermoplastic polyurethane nanocomposites of reactive nanoclay by bulk polymerization methods. *Polymer*. **46**: 3275-3288.
- Aviv, O., Laout, N., Ratner, S., Harik, O., Kunduru, K.R. and Domb, A.J. 2013. Controlled iodine release from polyurethane sponges for water decontamination. *Journal of Controlled Release*. **172**: 634-640.
- Barick, A.K. and Tripathy, D.K. 2011. Effect of organically modified layered silicate nanoclay on the dynamic viscoelastic properties of thermoplastic polyurethane nanocomposites. *Applied Clay Science*. **52**(3): 312-321.

- Baroi, N.G. 2006. *Continuous leaching ICP-MS for the study of metal speciation in sediments*. Master's Thesis. Chalmers University of Technology, Sweden.
- BASF Polyurethane GmbH. 2011. Thermoplastic polyurethane elastomers (TPU) Material Properties (online). (19<sup>th</sup> November 2013).
- Baysal, G., Aydin, H., Koytepe, S. and Seckin, T. 2013. Comparison dielectric and thermal properties of polyurethane/organoclay nanocomposites. *Thermochimica Acta*. **566**: 305-313.
- Becker, O. and Simon, G.P. 2006. *Polymer Nanocomposites*. Mai, Y.W. and Yu, Z.Z. England; Woodhead Publishing Limited.
- Berta, M., Lindsay, C., Pans, G. and Camino, G. 2006. Effect of chemical structure on combustion and thermal behaviour of polyurethane elastomer layered silicate nanocomposites. *Polymer Degradation and Stability*. **91**: 1179-1191.
- Bhattacharya, S.N., Gupta, R.K. and Kamal, M.R. 2008. *Polymeric Nanocomposites Theory and Practice*. Carl Hanser Verlag; Germany.
- Biswas, M. and Sinha, R.S. 2001. Recent progress and synthesis in evaluation of polymer montmorillonite nanocomposites. *Advanced Polymer Science*. **155**: 167-221.
- Blumstein, A. 1965. Polymerization of adsorbed mono-layers. I. Preparation of the clay-polymer complex. *Journal of Polymer Science: Part A*. **3**: 2653-2664.
- Caraculacu, A.A., Agherghinei, I., Prisacariu, C. and Cozan, V. 1990. Dibenzyl structures in a macromolecular chain III dibenzyl diisocyanates reactivity. *Journal of Macromolecular Science, Part A: Pure and applied chemistry*. **27**(12): 1547.
- Carli, L.N., Crespo, J.S. and Mauler, R.S. 2011. PHBV nanocomposites based on organomodified montmorillonite and halloysite: The effect of clay type on the morphology and thermal and mechanical properties. *Composites Part A: Applied Science and Manufacturing*. **42**(11): 1601-1608.
- Castro, R.H.R. and Benthem, K. 2013. *Sintering: Mechanisms of convention nanodensification and field assisted processes*. London. Springer-Verlag Berlin Heidelberg.
- Chang, H. and Wu, H. 2013. Graphene-based nanocomposites: preparation, functionalization, and energy and environmental applications. *Energy and Environmental Science*. **6**: 3483-3507.
- Chang, J.H., An, Y.U., Cho, D. and Giannelis, E.P. 2003. Poly(lactic acid) nanocomposites: comparison of their properties with montmorillonite and synthetic mica (II). *Polymer*. **44**(13): 3715-3720.

- Chang, J.H. and Park, K.M. 2001. Polyimide nanocomposite: comparison of their properties with precursor polymer nanocomposites. *Polymer Engineering and Science*. **41**(12): 2226-2230.
- Chou, C.W., Hsu, S.H., Chang, H., Tseng, S.M. and Lin, H.R. 2006. Enhanced thermal and mechanical properties and biostability of polyurethane containing silver nanoparticles. *Polymer Degradation and Stability*. **91**: 1017-1024.
- Cervantes, J.M., Espinosa, J.I., and Roman, J.S. 2009. TGA/FTIR studies of segmented aliphatic polyurethanes and their nanocomposites prepared with commercial montmorillonites. *Polymer Degradation and Stability*. **94**:1666-1677.
- Chattopadhyay, D.K. and Raju, K.V.S.N. 2007. Structural engineering of polyurethane coatings for high performance applications. *Progress in Polymer Science*. **3**: 352-418.
- Chen, Y., Zhou, S., Yang, H., Gu, G. and Wu, L. 2004. Preparation and characterization of nanocomposite polyurethane. *Journal of Colloid and Interface Science*. **279**(2): 370-378.
- Chen, Z. and Gong, K. 2002. Preparation and dynamic mechanical properties of poly(styrene-b-butadiene)-modified clay nanocomposites. *Journal of Applied Polymer Science*. **84**(8): 1499-1503.
- Ciobanu, G., Carja, G. and Ciobanu, O. 2008. Structure of mixed matrix membranes made with SAPO-5 zeolite in polyurethane matrix. *Microporous and Mesoporous Materials*. **115**(1-2): 61-68.
- Clemiston, I.R. 2008. *Castable Polyurethane Elastomers*. Boca Raton. Taylor & Francis Group.
- Davis, C.H., Mathias, L.J., Gilman, J.W., Schiraldi, D.A., Shields, J.R., Trulove, P., Sutto, T.E. and DeLong, H.C. 2002. Effects of melt-processing conditions on the quality of poly(ethylene terephthalate) montmorillonite clay nanocomposites. *Journal of Polymer Science Part B: Polymer Physics*. **40**(23): 2661-2666.
- Dias, R.C.M., Goes, A.M., Serakides, R., Ayres, E. and Orefice, R.L. 2010. Porous biodegradable polyurethane nanocomposites: preparation, characterization, and biocompatibility tests. *Material Research*. **13**(2): <http://dx.doi.org/10.1590/S1516-14392010000200015>.
- Ding, Z. and R.L. Frost. 2004. Thermal study of copper adsorption on montmorillonites. *Thermochimica Acta*. **416**(1-2):11-16.
- Demharter, A. 1998. Polyurethane rigid foam, a proven thermal insulating material for applications between +130°C and -196°C. *Cryogenics*. **38**(1): 113-117.

- Dennis, H.R., Hunter, D.L., Chang, D., Kim, S., White, J.L., Cho, J.W. and Paul, D.R. 2001. Effect of melt processing conditions on the extent of exfoliation in organoclay-based nanocomposites. *Polymer*. **42**(23): 9513-9522.
- Dong, Y. and Bhattacharyya, D. 2008. Effects of clay type, clay/compatibiliser content and matrix viscosity on the mechanical properties of polypropylene/organoclay nanocomposites. *Composites*. **39**: 1177-1191.
- Dowling, A.H., Stamboulis, A. and Fleming, G.J.P. 2006. The influence of montmorillonite clay reinforcement on the performance of a glass ionomer restorative. *Journal of Dentistry*. **34**(10): 802-810.
- Ebdon, L., Fisher, A. and Hill, S.J. 1998. *An introduction to analytical atomic spectrometry*. Evans, E.H. Chichester; Wiley.
- Elder Rubber Company. 2013. Properties of Rubber Compounds (online). <http://www.elderrubber.com/resources/product-properties.htm> (24 October 2013).
- Etmimi, H.M. 2012. *New approaches to the synthesis and exfoliation of polymer/functional graphene nanocomposites by miniemulsion polymerization*. PhD. University of Stellenbosch, South Africa.
- Fabris, H.J. 1976. Thermal and oxidative stability of urethanes in *Advances in urethane science and technology*. Frisch, C., Reegen, S.L. and Klempner, D. **4**. Technomic Publishing Company; United Kingdom.
- Fischer, H. 2003. Polymer nanocomposites: From fundamental research to specific application. *Material Science Engineering*. **23**: 763-772.
- Finnigan, B., Martin, D., Halley, P., Truss, R. and Campbell, K. 2004. Morphology and properties of thermoplastic polyurethane nanocomposites incorporating hydrophilic layered silicates. *Polymer*. **45**(7): 2249-2260.
- Fornes, T.D., Yoon, P.J., Hunter, D.L., Keskkula, H. and Paul, D.R. 2002. Effect of organoclay structure on nylon 6 nanocomposite morphology and properties. *Polymer*. **43**(22): 5915-5933.
- Frisch, K.C. and Dieter, J.A. 1975. An overview of polyurethane elastomers. *Polymer Plastics and Technology*. **4**(1): 1-21.
- Fukushima, K., Tabuani, D. and Camino, G. 2012. Poly(lactic acid)/clay nanocomposites: effect of nature and content of clay on morphology, thermal and thermo-mechanical properties. *Materials Science and Engineering: C*. **32**(7): 1790-1795.
- Giannelis, E.P. 1996. Polymer layered silicate nanocomposites. *Advanced Materials*. **8**(1): 29-35.

- Giannelis, E.P., Krishnamoorti, R. and Manias, E. 1999. Polymer silicate nanocomposites: modeled systems for confined polymer and polymer brushes in Polymers in confined environments. *Advanced Polymeric Science*. Springer Berlin Heidelberg. **138**: 107-147.
- Guo, Z., Park, S., Wei, S., Pereira, T., Moldovan, M., Karki, A.B., Young, D.P. and Hahn, H.T. 2007. Flexible high-loading particle-reinforced polyurethane magnetic nanocomposite fabrication through particle-surface-initiated polymerization. *Nanotechnology*. **18** 335704: 1-8.
- Hasegawa, N., Okamoto, H., Kato, M., Usuki, A. and Sato, N. 2003. Nylon 6/Na-montmorillonite nanocomposites prepared by compounding Nylon 6 with Na-montmorillonite slurry. *Polymer*. **44**(10): 2933-2937
- Hepburn, C. 1992. *Polyurethane Elastomers*. 2<sup>nd</sup> Edition. Elsevier Science Publishers Ltd; England.
- Hohne, G.W.H., Hemminger, W.F. and Flammersheim, H.J. 2003. *Differential Scanning Calorimetry*. 2. Germany; Springer-Verlag Berlin Heidelberg.
- Huang, S.L. and Lai, J.Y. 1994. On the gas permeability of hydroxyl terminated polybutadiene. *Journal of Membrane Science*. **105**: 137-145.
- Huskic, M., Zigon, M. and Ivankovic, M. 2013. Comparison of the properties of clay polymer nanocomposites prepared by montmorillonite modified by silane and by quaternary ammonium salts. *Applied Clay Science*. **85**: 109-115.
- Hussain, F., Hojjati, M., Okamoto, M., and Gorga, R.E. 2006. Review article: Polymer-matrix nanocomposites, processing, manufacturing, and application: an overview. *Journal of Composite Materials*. **17**: 1511-1575.
- Hwang, S.S., Park, J.S. and Namkoong, W. 2007. Ultrasonis-assisted extraction to release heavy metals from contaminated soil. *J.Ind. Eng. Chem*. **4**: 650-656.
- Isik, I., Yilmazer, U. and Bayram, G. 2003. Impact modified epoxy/montmorillonite nanocomposites: synthesis and characterization. *Polymer*. **44**(20): 6371-6377.
- Ismail, Z. 2013. *Study the effect of screw speed and temperature profile on structure, thermal and physical properties of melt blended polyamide 6/MMT nanocomposites*. Master. Universiti Malaysia Pahang, Malaysia.
- Jeon, H.G., Jung, H.T., Lee, S.W. and Hudson, S.D. 1998. Morphology of polymer/silicate nanocomposites: High density polyethylene and a nitrile copolymer. *Polymer Bulletin*. **41**: 107-113.
- Jianqi, W. and Zhidong, H. 2006. The combustion behavior of polyacrylate ester/graphite oxide composites. *Polymers for Advanced Technologies*. **17**(4): 335-340.



- Jiawen, X., Yunhang, L., Xiaohui, Y. and Xinling, W. 2004. Thermal and mechanical properties of polyurethane/montmorillonite nanocomposites based on a novel reactive modifier. *Polymer Degradation and Stability*. **86**: 549-555.
- Jordan, J., Jacob, K.I., Tannenbaum, R., Sharaf, M.A. and Jasiuk, I. 2005. Experimental trends in polymer nanocomposites: A review. *Materials Science and Engineering A*. **393**: 1-11.
- Kapteijn, F., Bakker, W.J.W., Zheng, G., Poppe, J. and Moulijn, J.A. 1995. Permeation and separation of light hydrocarbons through a silicalite-1 membrane: Application of the generalized Maxwell-Stefan equations. *The Chemical Engineering Journal and the Biochemical Engineering Journal*. **57**(2): 145-153.
- Khudyakov, I.V., Zopf, R.D. and Turro, N.J. 2009. Polyurethane Nanocomposites. *Designed Monomers and Polymers*. **12**: 279-290.
- Kim, B.K., Seo, J.W. and Jeong, H.M. 2002. Morphology and properties of waterborne polyurethane/clay nanocomposites. *European Polymer Journal*. **39**: 85-91.
- Kim, Y.H., Choi, S.J., Kim, J.M., Han, M.S. and Kim, W.N. Effects of Organoclay on the Thermal Insulating Properties of Rigid Polyurethane Foams Blown by Environmentally Friendly Blowing Agents. *Macromolecular Research*. **15**(7): 676-681.
- Kim, J.K., Hu, C., Woo, R.S.C. and Sham, M.L. 2004. Moisture barrier characteristics of organoclay-epoxy nanocomposites. *Composites Science and Technology*. **65**: 805- 813.
- Kojima, Y., Usuki, A., Kawasumi, M., Okada, A., Fukushima, Y., Kurauchi, T.T. and Kamigaito, O. 1993. Swelling behavior of montmorillonite cation exchanged for  $\alpha$ -amino acids by  $\epsilon$ -caprolactam. *Material Research*. **8**:1174-1178.
- Koo, J.H. 2006. *Polymer nanocomposites: Processing, characterization and applications*. United States of America; McGraw-Hill.
- Koo, J.H., Pilato, L.A. and Wissler, G.E. 2007. Polymer nanostructured materials for propulsion systems. *Journal of Spacecraft and Rockets*. **44**: 1250-1262.
- Krishnamoorti, R., Vaia, R.A. and Giannelis, E.P. 1996. Structure and Dynamics of Polymer-Layered Silicate Nanocomposites. *Chem Mater*. **8**: 1728-1734.
- Kusakabe, K., Ichiki, K., Hayashi, J.I., Maeda, H. and Marooka, S. 1995. Preparation and characterization of silica-polyimide composite membranes coated on porous tubes CO<sub>2</sub> separation. *Journal of Membrane Science*. **115**: 65-75.
- Kusmono, Wildan, M.W. and Mohd Ishak, Z.A. 2013. Preparation and properties of clay- reinforced epoxy nanocomposites. *International Journal of Polymer Science*. **2013**.

- LeBaron, P.C., Wang, Z. and Pinnavaia, T.J. 1999. Polymer layered silicate nanocomposites: An overview. *Applied Clay Science*. **15**(1): 11-29.
- Lee, H.T. and Lin, L.H. 2006. Waterborne polyurethane/clay nanocomposites: novel effects of the clay and its interlayer ions on the morphology and physical and electrical properties. *Macromolecules*. **39**: 6133-6141.
- Li, Y., Pan, D., Chen, S., Wang, Q., Pan, G. and Wang, T. 2013. In situ polymerization and mechanical, thermal properties of polyurethane/graphene oxide/epoxy nanocomposites. *Materials & Design*. **47**: 850-856.
- Liu, L., Jia, D., Luo, Y. and Guo, B. 2006. Preparation, structure and properties of nitrile-butadiene rubber-organoclay nanocomposites by reactive mixing intercalation method. *Journal of Applied Polymer Science*. **100**: 1905-1913
- Luo, T. and Lloyd, J.R. 2012. Enhancement of thermal energy transport across graphene/graphite and polymer interfaces: A molecular dynamics study. 2012. *Advanced Functional Materials*. **22**(12): 2495-2502.
- Maurizio Galimberti, Rubber Clay Nanocomposites, Wiley, 2011, pp. 2066.
- Materials Evaluation and Engineering, Inc. 2009. Handbook of analytical methods for materials (online). <http://mee-inc.com/thermal-analysis.html>.
- Michael, A. and Philippe, D. 2000. Polymer-layered silicate nanocomposites:preparation, properties and uses of a new class of materials. *Materials Science and Engineering*. **28**: 1-63.
- Moaddeb, M. and Koros, W.J. 1996. Gas transport properties of thin polymeric membranes in the presence of silicon dioxide particles. *Journal of Membrane Science*. **125**: 143-163.
- Moghaddam, L., Martin, D.J., Halley, P.J. and Fredericks, P.M. 2009. Vibrational spectroscopic studies of laboratory scale polymer melt processing: Application to a thermoplastic polyurethane nanocomposite. *Vibrational Spectroscopy*. **51**(1): 86-92.
- Moniruzzaman, M. and Winey, K.I. 2006. Polymer Nanocomposites Containing Carbon Nanotubes. *Macromolecules*. **39**(16): 5194-5205.
- Montaser, A. and Golightly, D.W. 1992. *Inductively Coupled Plasmas in Analytical Atomic Spectrometry*, 2<sup>nd</sup> Revised and Enlarged Edition. New York; Wiley-VCH.
- Naguib, H.F., Abdel Aziz, M.S. and Saad, G.R. Synthesis, morphology and thermal properties of polyurethanes nanocomposites based on poly(3-hydroxybutyrate) and organoclay. *Journal of Industrial and Engineering Chemistry*. **19**: 56-62.

- Nan, C.W., Birringer, R., Clarke, D.R., and Gleiter, H. 1997. Effective thermal conductivity of particulate composites with interfacial thermal resistance. *Journal of Applied Physic.* **81**: 6692-6699.
- Nielson, L.E. 1967. Models for the permeability of filled polymers. *Journal of Macromolecular Science.* **A1**(5): 929-949.
- Oguzlu, H. 2011. *Water vapor and gas barrier properties of biodegradable polymer nanocomposites film.* Master Thesis. Izmir Institute of Technology, Turkey.
- Okamoto, M. 2003. Polymer/Layered Silicate Nanocomposites. *Rapra Review Reports.* **14**(7): 36.
- Okamoto, M. 2004. Polymer/clay nanocomposites. *Encyclopedia of Nanoscience and Nanotechnology.* 1<sup>st</sup> Edition. Nalwa, H.S. American Scientific Publishers; California.
- Okamoto, M. 2006. Recent advances in polymer/layered silicate nanocomposites: an overview from science to technology. *Materials Science and Technology.* **22**(7):756-779.
- Olphen, H.V. 1963. An introduction to clay colloid chemistry. *Journal of Pharmaceutical Sciences.* **53**(2): 230.
- Olphen, H.V. 1977. *An Introduction to Clay Colloidal Chemistry.* New York. Wiley.
- Osman, M.A., Mittal, V., Morbidelli, M. and Suter, U.W. 2003. Polyurethane adhesive nanocomposites as gas permeation barrier. *Macromolecules.* **36**: 9851-9858.
- Osman, M.A., Mittal, V., Morbidelli, M. and Suter, U.W. 2004. Epoxy-Layered Silicate Nanocomposites and Their Gas Permeation Properties. *Macromolecules.* **37**:7250-7257.
- Panupakorn, P., Chaichana, E., Prasrthdam, P. and Jongsomjit, B. Polyethylene/Clay Nanocomposites Produced by In Situ Polymerization with Zirconocene/MAO Catalyst. *Journal of Nanomaterials*: **2013**.
- Parfitt, R.L. and Greenland, D.J. 1970. The adsorption of poly(ethylene glycols) on clay minerals. *Clay Minerals.* **8**:305-315.
- Pattanayak and Jana, S.C. Synthesis of thermoplastic polyurethane nanocomposites of reactive nanoclay by bulk polymerization methods. *Polymer.* **46**(10): 3275-3288, A.
- Paul, D.R. and Robeson, L.M. 2008. Polymer nanotechnology: Nanocomposites. *Polymer.* **49**(15): 3187-3204.
- Pavlicevic, J., Sprikova, M., Jovicic, M., Bera, O. and Poreba, R. The structure and thermal properties of novel polyurethane/organoclay nanocomposites obtained by pre-polymerization. *Composites Part B: Engineering.* **45**(1): 232-238.

- Pavlidou, S. and Papaspyrides, C.D. 2008. A review on polymer-layered silicate nanocomposites. *Progress in Polymer Science*. **33**(12): 1119-1198.
- PhotoMetrics. 2012. Field Emission Scanning Electron Microscope (online). <http://www.photometrics.net/feSEM.html> (24th November 2013).
- Pinto, F.C.H., Cunha, A.S., Pianetti, G.A., Ayres, E., Orefice, R.L., Silva, G.R.D. 2011. Montmorillonite clay based polyurethane nanocomposite as local triamcinolone acetone delivery system. *Journal of Nanomaterial*. 1-11.
- Polyurethane Technologies. 2009. Mechanical properties (online). [http://www.purelast.com.ua/about\\_polyurethanes/mechanical\\_properties.html](http://www.purelast.com.ua/about_polyurethanes/mechanical_properties.html) (19th November 2013)
- Potts, J.R., Dreyer, D.R., Bielawski, C.W. and Ruoff, R.S. 2011. Graphene-based polymer nanocomposites. *Polymer*. (52): 5-25
- Prisacariu, C. 2011. *Polyurethane Elastomers: From morphology to mechanical aspects*. Springer-Verlag Wien; New York
- Prisacariu, C., Scortanu, E. and Agapie, B. 2011. New insights into polyurethane elastomers obtained by changing the polyaddition procedures. Proceedings of the World Congress on Engineering. London. 6 – 8 July.
- Potts, J.R., Dreyer, D.R., Bielawski, C.W. and Ruoff, R.S. 2011. Graphene-based polymer nanocomposites. *Polymer*. **52**: 5-25
- Ray, S.S. and Bousmina, M. 2006. *Polymer nanocomposites and their applications*. California; American Scientific Publishers.
- Ray, S.S. and Okamoto, M. 2003. Polymer/layered silicate nanocomposites: a review from preparation to processing. *Prog. Polym. Sci.* **28**: 1539-1641.
- Reddy, B. 2011. *Advances in diverse industrial applications of nanocomposites*. InTech.
- Rludson. 2011. Polyurethane (online). [http://www.rludson.com/material\\_profiles/polyurethane.htm](http://www.rludson.com/material_profiles/polyurethane.htm) (08th November 2013).
- Rodriguez, J.V.C., Chan, L.H.C., Sanchez, F.H. and Cervantes, J.M. 2013. *Advances in biomaterials science and biomedical applications*. Rosario Pignatello. InTech.
- Roytech. 2013. Thermal Insulation (online). [www.roytech.co.uk/Related/Thermos/Thermos\\_insulation.html](http://www.roytech.co.uk/Related/Thermos/Thermos_insulation.html) (08th November 2013).
- Saha, M.C., Kabir, M.E. and Jeelani, S. 2008. Enhancement in thermal and mechanical properties of polyurethane foam infused with nanoparticles. *Materials Science and Engineering A*. **479**: 213-222.

- Sahoo, N. G., Rana, S., Cho, J. W., Lin, L. and Chan, S. W. Polymer nanocomposites based on functionalized carbon nanotubes. *Progress in Polymer Science*. **35**: 837-867.
- Sakai, T., McCurdy, E. and Wilbur, S. 2005. Ion chromatography (IC) ICP-MS for chromium speciation in natural samples. Agilent Technologies (online). (22 September 2013).
- Salahuddin, N., Abo-El-Enein, S.A., Selim, A. and El-Dien, O.S. 2010. Synthesis and characterization of polyurethane/organo-montmorillonite nanocomposites. *Applied Clay Science*. **47**(3-4): 242-248.
- Sarier, N., Onder, E. and Ersoy, S. 2010. The modification of Na-montmorillonite by salts of fatty acids: An easy intercalation process. *Colloids and Surfaces A: Physicochemical and Engineering Aspects*. **371**(1-3):40-49.
- Saunders, J.H. and Frisch, K.C. 1964. *Polyurethanes chemistry and technology*. **2**. Interscience Publishers.
- Seefried, C.G., Koleske, J.V. and Critchfield, F.E. 1975. Thermoplastic urethane elastomers. III. Effects of variations in isocyanate structure. *Journal of Applied Polymer Science*. **19**(12): 3185-3191.
- Semsarzadeh, M.A., Sadeghi, M., Barikani, M. and Moadel, H. 2007. The effect of hard segments on the gas separation properties of polyurethane membranes. *Iranian Polymer Journal*. **16**(12): 819-827.
- Semsarzadeh, M.A., Sadeghi, M. and Barikani, M. 2008. Effect of chain extender length on gas permeation properties of polyurethane membranes. *Iranian Polymer Journal*. **17**(6): 431-440.
- Seymour, R.W. and Cooper, S.L. 1973. Thermal analysis of polyurethane block copolymers. *Macromolecules*. **6**(1): 48-53.
- Shahryar, P., Siddaramaiah and Akheel, A.S. 2011. Thermal Characteristics of Nanostructured Filler incorporated Polyvinyl Ester Nanocomposites. *International Journal of ChemTech Research*. **3**: 94-103.
- Shelley, J.S., Mather, P.T. and Devries, K.L. 2001. Reinforcement and environmental degradation of nylon-6/clay nanocomposites. *Polymer*. **42**(13): 5849-5858.
- Silva, M.J.D., Kanda, D.H.F. and Nagashima, H.N. 2012. Mechanism of charge transport in castor oil-based polyurethane/carbon black composite. *Journal of Non-Crystalline Solids*. **358**(2): 270-275.
- Soilweb. 2014. Retrieved from <http://wiki.ubc.ca/LFS:SoilWeb> (13<sup>th</sup> March 2014).

- Song, M., Xia, H.S., Yao, K.J. and Hourston, D.J. 2005. A study on phase morphology and surface properties of polyurethane/organoclay nanocomposite. *European Polymer Journal*. **41**: 259-266.
- Sozer, N. and Kokini, J.L. 2009. Nanotechnology and its applications in the food sector. *Trends in Biotechnology*. **27**(2):82-89.
- Sreedar, B., Chattopadhyay, D.K. and Swapna, V. Thermal and surface characterization of polyurethane-urea clay nanocomposite coatings. *Journal of Applied Polymer Science*. **100**: 2393-2401.
- Stockon, G.R. 2011. Methodologies for finding, analyzing and prioritizing moisture problems in roofing materials using infrared thermal imaging (online). <http://www.stocktoninfrared.com/ir-info-2013/>. (8<sup>th</sup> November 2013).
- Strawhecker, K.E. and Manias, E. 2006. Nanocomposites based on water soluble polymers and unmodified smectite clay. *Polymer Nanocomposites*. 2<sup>nd</sup> Edition. Mai, Y.W. and Yu, Z.Z. Woodhead Publishing; New York.
- Subrata, M. and Darren, M. 2012. Hydrolytic degradation of segmented polyurethane copolymers for biomedical applications. *Polymer Degradation and Stability*. **97**: 1553-1561.
- Suin, S., Maiti, S., Shrivastava, N.K. and Khatua, B.B. 2014. Mechanically improved and optically transparent polycarbonate/clay nanocomposites using phosphonium modified organoclay. *Materials & Design*. **54**: 553-563.
- Szycher, M. 1999. *Szycher's Handbook of Polyurethane*. CRC Press INC. Florida.
- Theng, B.K.G. 1979. *Formation and properties of clay-polymer complexes*. Elsevier:Amsterdam.
- Theng, B.K.G. 1982. Clay-polymer interactions: Summary and perspectives. *Clay and clay minerals*. **30**(1): 1-10.
- Theng, B.K.G. 2012. *Formation and properties of clay-polymer complexes*. 2<sup>nd</sup> Ed. Elsevier; United Kingdom.
- Theron, J.P., Knoetze, J.H., Sanderson, R.D., Hunter, R., Mequanint, K., Franz, T., Zilla T. and Bezuidenhout, D. 2010. Modification, crosslinking and reactive electrospinning of a thermoplastic medical polyurethane for vascular graft applications. *Acta Biomaterialia*. **6**(7): 2434-2447.
- Tien, Y.I. and Wei, K.H. 2002. The effect of nano-sized silicate layers from montmorillonite on glass transition, dynamic mechanical and thermal degradation properties of segmented polyurethane. *Journal of Applied Polymer Science*. **86**:1741-1748.
- Todokoro, H., Ezumi, M. and Mito. 1999. Scanning electron microscope. *United States Patent*.

- Tortora, M., Gorassi, G., Vittoria, V., Galli, G., Rotrovati, S. and Chiellini, E. 2002. Structural characterization and transport properties of organically modified montmorillonite/polyurethane nanocomposites. *Polymer*. **43**: 6147-6157.
- Tjong, S.C. 2006. Carbon Nanotube Reinforced Composites: Metal and Ceramic Matrices. *Mater*. **53**:73-197.
- Usuki, A., Kawasumi, M., Kojima, Y and Okada, A. 1993. Swelling behavior of montmorillonite cation exchanged for  $\omega$ -amino acids by  $\epsilon$ -caprolactam. *Mater*. **8**:1174-1178.
- Usuki, A., Kojima, Y., Kawasumi, M., Okada, A., Fukushima, Y., Kurauchi, T. and Kamigaito, O. Synthesis of nylon 6-clay hybrid. *Journal of Materials Research*. **8**: 1179-1184.
- Usuki, A., Hasegawa, N., Kato, M. and Kobayashi, S. 2005. Polymer-Clay Nanocomposites. *Inorganic Polymeric Nanocomposites and Membranes Advances in Polymer Science*. **179**: 135-195.
- Utracki, L.A. 2004. *Clay-containing polymeric nanocomposites*, Rapra Technology Limited.
- Vaia, R.A. and Giannelis, E.P. 1997. Lattice model of polymer melt intercalation in organically-modified layered silicates. *Macromolecules*. **30**(25): 7990-7999.
- Vaia, R.A., Price, G., Ruth, P.N., Nguyen, H.T. and Lichtenhan, J. 1999. Polymer/layered silicate nanocomposites as high performance ablative materials. *Applied Clay Science*. **15**: 67-92.
- Varghese, S., Kocsis, J.K. and Gatos, K.G. 2003. Melt compounded epoxidised natural rubber/layered silicate nanocomposites: Structure-properties relationships. *Polymer*. **44**: 3977-3983.
- Venkataraman, A. and Lagashetty, A. (2005). Polymer nanocomposites. *Resonance*. 49-60.
- Vilar, W.D. 2002. Chemistry and technologies of polyurethanes (online). <http://web.cip.com.br/vilar/Ingles/Chapter1/17Correlations.htm> (19th November 2013).
- Vitkauskiene, I., Makuska, R., Stirna, U. and Cabulis, U. 2011. Thermal properties of polyurethane-polyisocyanurate foams based on Poly(ethylene terephthalate) waste. *Materials Science*. **17**(3): 249-253.
- Wang, S.K. and Sung, C.S.P. 2002. Spectroscopic characterization of model urea, urethane compound, and diamine extender for polyurethane-urea. *Macromolecules*. **35**: 877-882.

- Wang, X.P., Huang, A.M., Jia, D.M. and Li, Y.M. 2008. From exfoliation to intercalation – Changes in morphology of HNBR/organoclay nanocomposites. *European Polymer Journal*. **44**: 2784-2789.
- Wang, Z., Massam, J. and Pinnavaia, T.J. 2000. Epoxy clay nanocomposites in *Polymer clay nanocomposites*. Pinnavaia, T.J. and Beall, G.W. John Wiley and Sons; New York: 127-149.
- Wang, Z., Wang, X., Li, G. and Zhang, Z. 2008. Enhanced exfoliation of montmorillonite prepared by hydrothermal method. *Applied Clay Science*. **42**: 146-150.
- Wang, Z. and Pinnavaia, T.J. 1998. Nanolayer reinforcement of elastomeric polyurethane. *Chemistry of Materials*. **10**: 3769-3771.
- Xie, W., Gao, Z., Liu, K., Pan, W.P., Vaia, R., Hunter, D. and Singh, A. 2000. Thermal characterization of organically modified montmorillonite. *Thermochimica Acta*. **367-368**: 339-350.
- Xiong, J., Liu, Y., Yang, X. and Wang, X. 2004. Thermal and mechanical properties of polyurethane/montmorillonite nanocomposites based on a novel reactive modifier. *Polymer Degradation and Stability*. **86**(3): 549-555.
- Xu, R., Manias, E., Alan, J.S., James, R., 2002. Low permeability biomedical polyurethane nanocomposites. *Journal of Biomedical Materials Research*. **64A**:114-119.
- Yao, K.J., Song, M. Hourston, D.J. and Luo, D.Z. 2002. Polymer/layered clay nanocomposites: 2 polyurethane nanocomposites. *Polymer*. **43**: 1017-1020.
- Yano, K., Usuki, A. and Okada, A. 1997. Synthesis and properties of polyamide-clay hybrid films. *Journal of Polymer Science Part A: Polymer Chemistry*. **35**(11): 2289-2294.
- Yapar, S. 2009. Physicochemical study of microwave-synthesized organoclays. *Colloid Surface A*. **345**: 75-81.
- Yeh, S.K. and Gupta, R.K. 2010. Nanoclay-Reinforced, Polypropylene-based wood-plastic composites. *Polymer Engineering and Science*. **50**(10):2013-2020.
- Yusoh, K., Jin, J. and Song, M. 2010. Subsurface mechanical properties of polyurethane/organoclay nanocomposite thin films studied by nanoindentation. *Progress in Organic Coatings*. **67**(2): 220-224.
- Zaspalis, V.T., Kikkinides, E.S., Kolenbrander, M. and Mauczok, R. 2003. Method for the morphological characterization of powder raw materials for the manufacturing of ceramics. *Journal of Materials Processing Technology*. **142**(1):267-274.



- Zheng, J., Ozisik, R. and Siegal, R.W. 2006. Phase separation and mechanical responses of polyurethane nanocomposites. *Polymer*. **47**(22): 7786-7794.
- Zilg, C., Thomann, R., Mulhaupt, R. and Finter, J. 1999. Polyurethane Nanocomposites Containing Laminated Anisotropic Nanoparticles Derived from Organophilic Layered Silicates. *Advanced Materials*. **11**(1): 49-52.
- Zhu, Y., Wang, M., Du, H., Wang, F., Mou, S. and Haddad, P.R. 2002. Organic analysis by ion chromatography determination of aromatic amines and aromatic diisocyanates by cation-exchange chromatography with amperometric detection. *Journal of Chromatography A*. **956** (1-2): 215-220.



## APPENDIX A

MODIFICATION OF MMT CLAY AND FABRICATION OF PU  
NANOCOMPOSITES

## A1 ICP-MS DATA

CENLAB/F/007

Universiti  
Malaysia  
PAHANG  
Engineering • Technology • Creativity

**CENTRAL LABORATORY**  
Universiti Malaysia Pahang, Lebuhraya Tun Razak,  
26300 Kuantan, Pahang Darul Makmur.  
Tel: 09-5493344/8097 Fax: 09-5493353  
E-mail: ucl@ump.edu.my

**CERTIFICATE OF ANALYSIS (COA)**

To :	Shamini Gunaseelan	Attn :	-
Address :	FKKSA, UMP		
c.c. :		Page :	2 pages
Fax No : 09-5492766	Tel No : 013-9221487	Sample Lab No: 2013/106	

Sample description : 3 samples of solid powder in plastic bag

Sample marking : Refer Below

Date of sample received : 06-03-2013

Date reported : 22-03-2013

**RESULTS:**

1. SAMPLE: 1 (Cu)

No	Parameter	Results	Unit	Test Method
1.	Copper (Cu)	56012.0	ppm	In-house Method CENLAB/WI/CHEM-TM/002 Based on AOAC999.10

2. SAMPLE: 2 (Zn)

No	Parameter	Results	Unit	Test Method
1.	Zinc (Zn)	389896.7	ppm	In-house Method CENLAB/WI/CHEM-TM/002 Based on AOAC999.10


**Figure A1-1:** ICP-MS data for pristine clay and modified clay with Cu<sup>2+</sup> and Fe<sup>3+</sup>

## 3. SAMPLE: 3 (Fe)

No	Parameter	Results	Unit	Test Method
1.	Iron (Fe)	114005.9	ppm	In-house Method CENLAB/WI/CHEM-TM/001 Based on AOAC999.10

The certificate shall not be reproduced except in full without the written approval of the laboratory.

The above analysis is based on the sample submitted by the customer.

  
MOHD RAFIE BIN ROSLY  
AMIC NO: A/3476/6363/12  
PEGAWAI SAINS  
MAKAMAL BERPUSAT  
UNIVERSITI MALAYSIA PAHANG  
LEBUHRAYA TUN RAZAK  
26300 GAMBANG, KUANTAN  
PAHANG DARUL MAKRUR

UMP

**Figure A1-1:** ICP-MS data for pristine clay and modified clay with  $\text{Cu}^{2+}$  and  $\text{Fe}^{3+}$   
(continued)

CENLAB/F/007


  
**Universiti  
Malaysia  
PAHANG**  
Engineering • Technology • Growth

**CENTRAL LABORATORY**  
 Universiti Malaysia Pahang, Lebuhraya Tun Razak,  
 26300 Kuantan, Pahang Darul Makmur.  
 Tel: 09-5493344/8097 Fax: 09-5493353  
 E-mail: ucl@ump.edu.my

**CERTIFICATE OF ANALYSIS (COA)**

To:	Shamini Cunaseelan	Attn:	
Address:	FKSA, UMP	Page:	1 page
c.c.:		Ter No.:	019-2056039
Fax No.:		Sample Lab No.:	2014/146

Sample description : One powder sample in plastic bag  
 Sample marking : Pure Mati  
 Date of sample received : 12/03/2014  
 Date reported : 20/03/2014

**RESULTS:**

No	Parameter	Results	Unit	Test Method
1.	Iron (Fe)	1801.66	ppm	In-house Method CENLAB/WI/CHEM-TM/001 Based on AOAC992.10
2.	Copper (Cu)	0.0371	ppm	In-house Method CENLAB/WI/CHEM-TM/002 Based on AOAC992.10

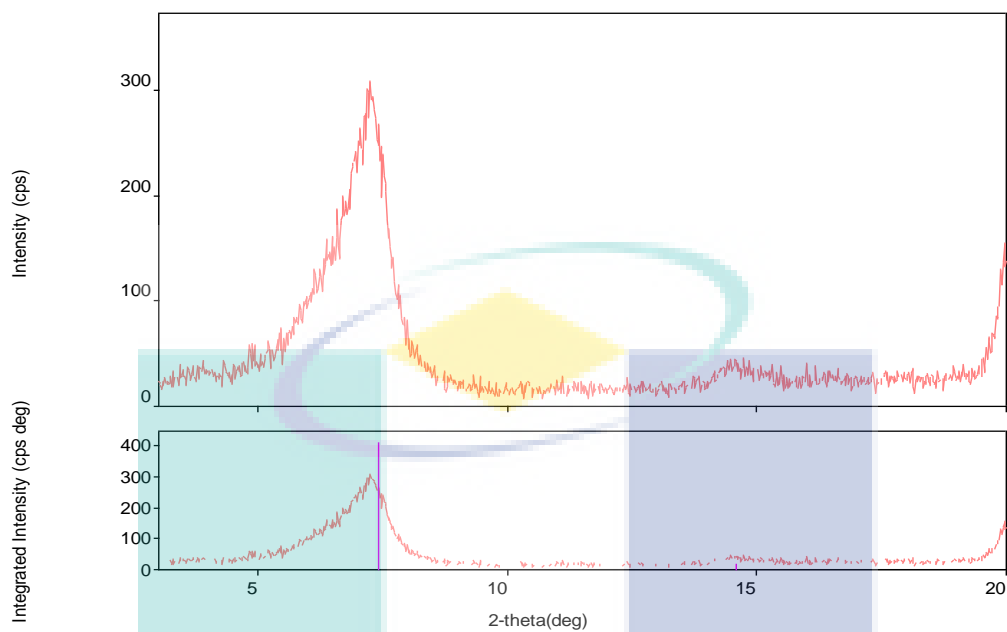
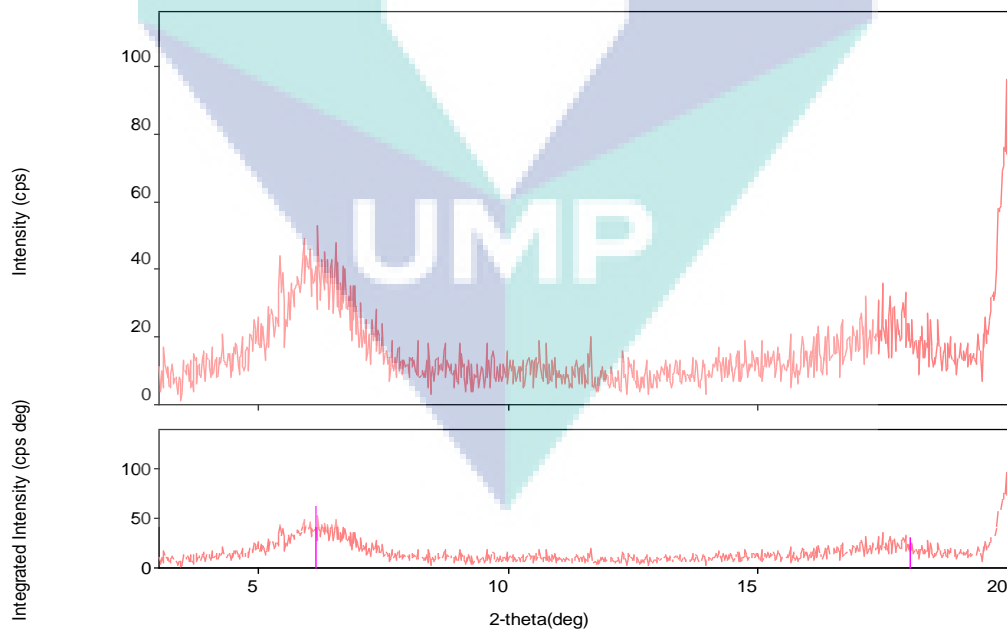
The certificate shall not be reproduced except in full without the written approval of the laboratory.  
 The above analysis is based on the sample submitted by the customer.

UMP

MOHD RAFIE BIN ROSLY  
 AMIC NO: A/3476/363/12  
 PEGAWAI SAINS  
 MAKMAL BERPUSAT  
 UNIVERSITI MALAYSIA PAHANG  
 LEBUHRAYA TUN RAZAK  
 26300 GAMBANG, KUANTAN  
 PAHANG DARUL MAKMUR

2014/146  
 Page 1 of 1

**Figure A1-1: ICP-MS data for pristine clay and modified clay with  $\text{Cu}^{2+}$  and  $\text{Fe}^{3+}$**   
(continued)

**A2 X-RAY DIFFRACTION****Figure A2.1:** X-RAY Diffraction of pristine MMT clay**Figure A2.2:** X-RAY Diffraction of MMT clay modified with copper

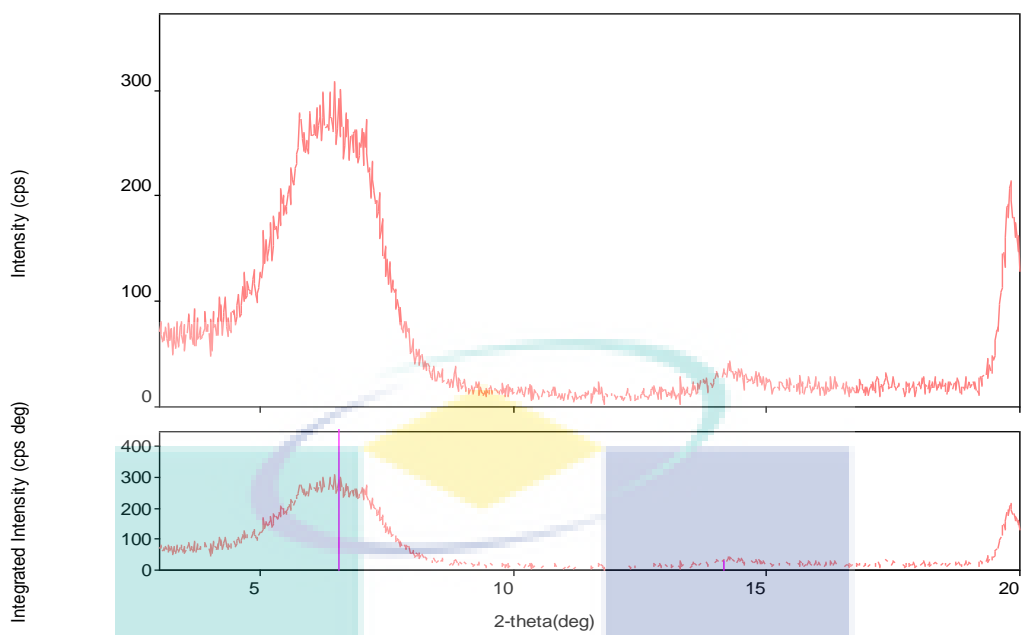


**Figure A2-3:** X-RAY Diffraction of MMT clay modified with iron

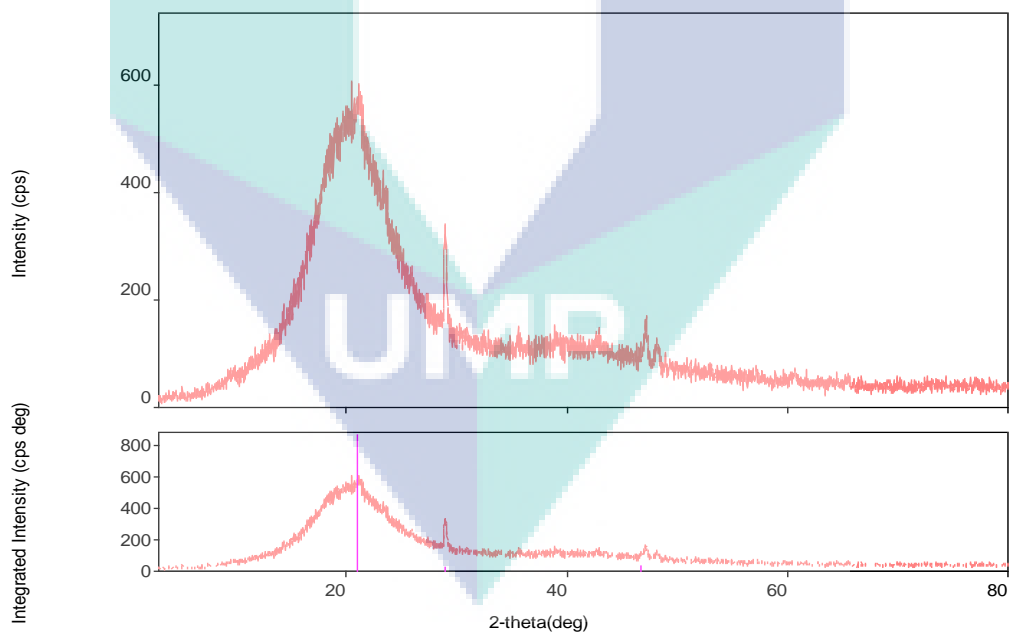


**Figure A2-4:** X-RAY Diffraction of PU

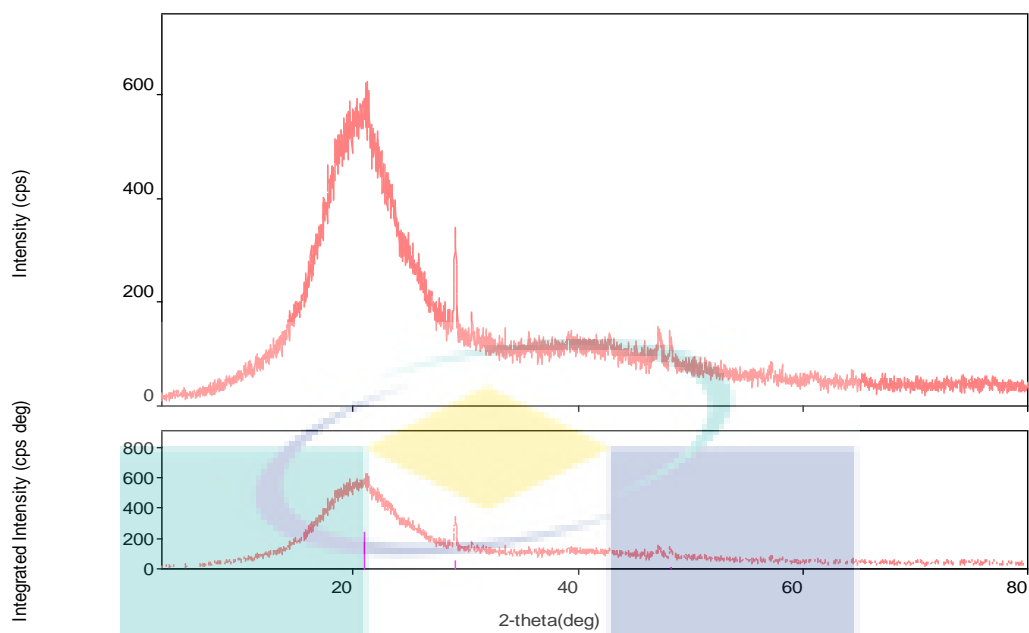


**Figure A2-5: X-RAY Diffraction of 1% PU-MMT**

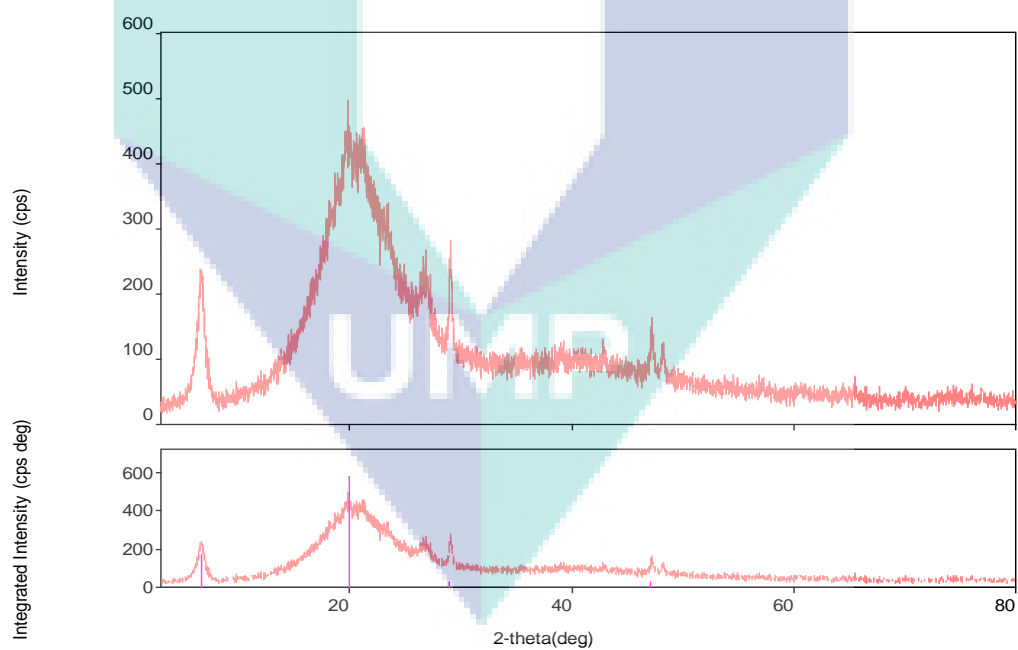


**Figure A2-6: X-RAY Diffraction of 2% PU-MMT**

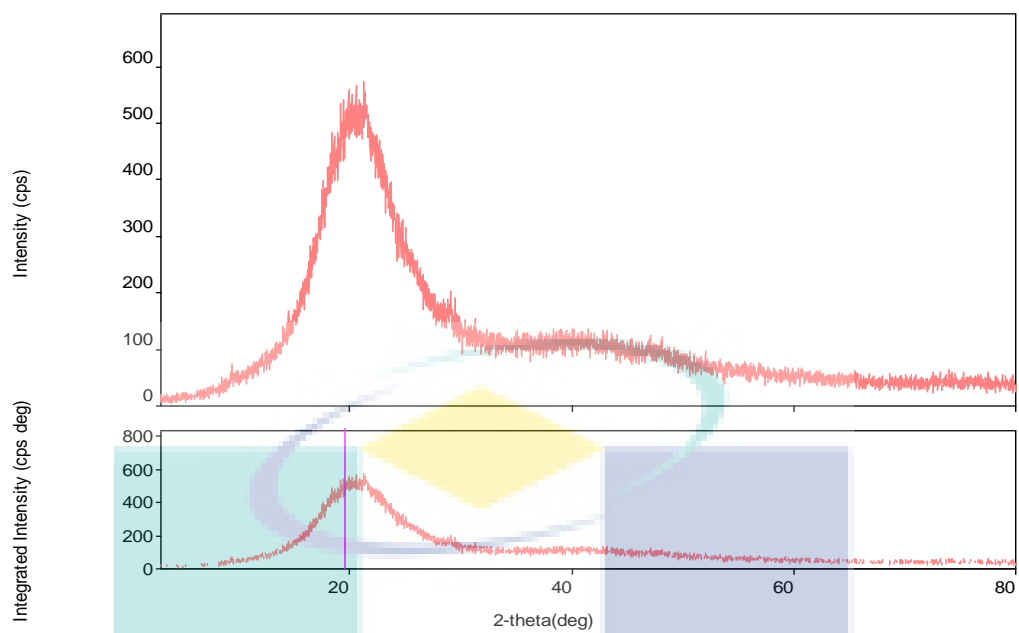


**Figure A2-7: X-RAY Diffraction of 3% PU-MMT**

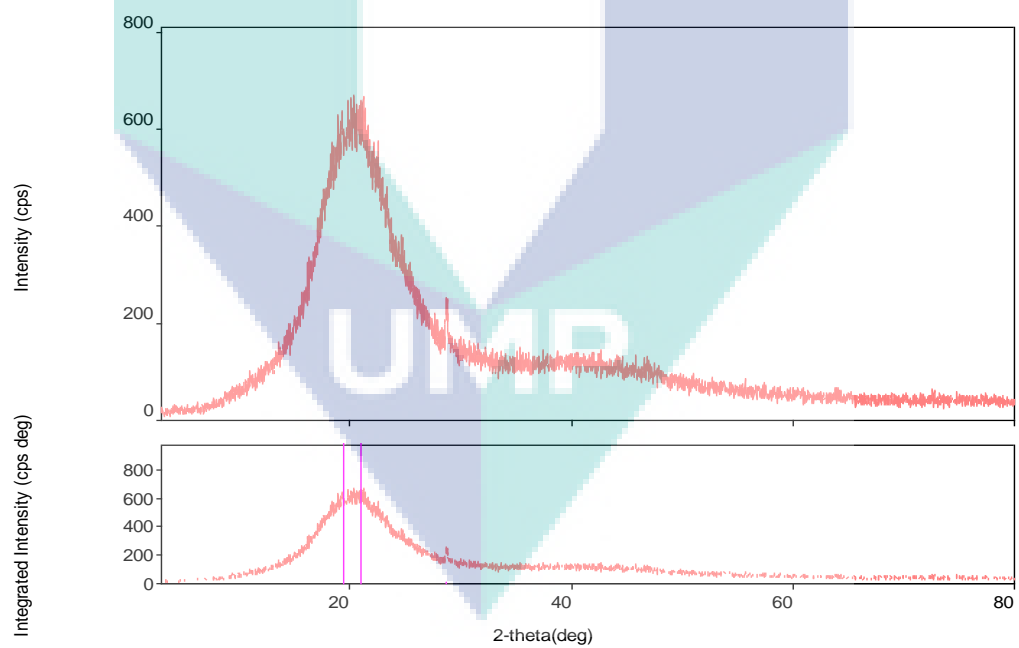


**Figure A2-8: X-RAY Diffraction of 1% PU-MMT Cu**



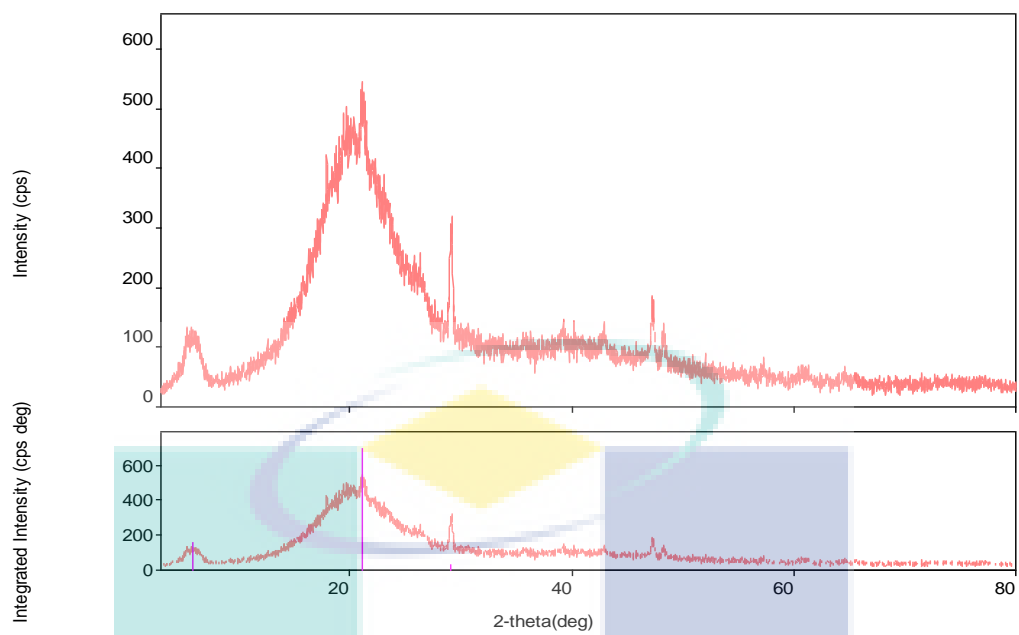


**Figure A2-9: X-RAY Diffraction of 2% PU-MMT Cu**

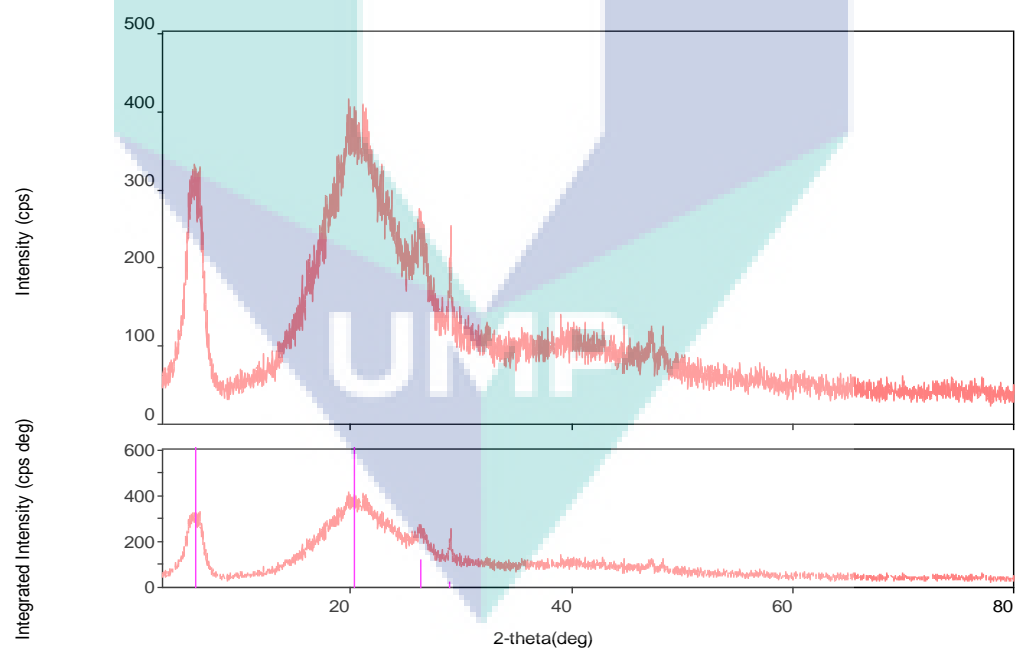


**Figure A2-10: X-RAY Diffraction of 3% PU-MMT Cu**

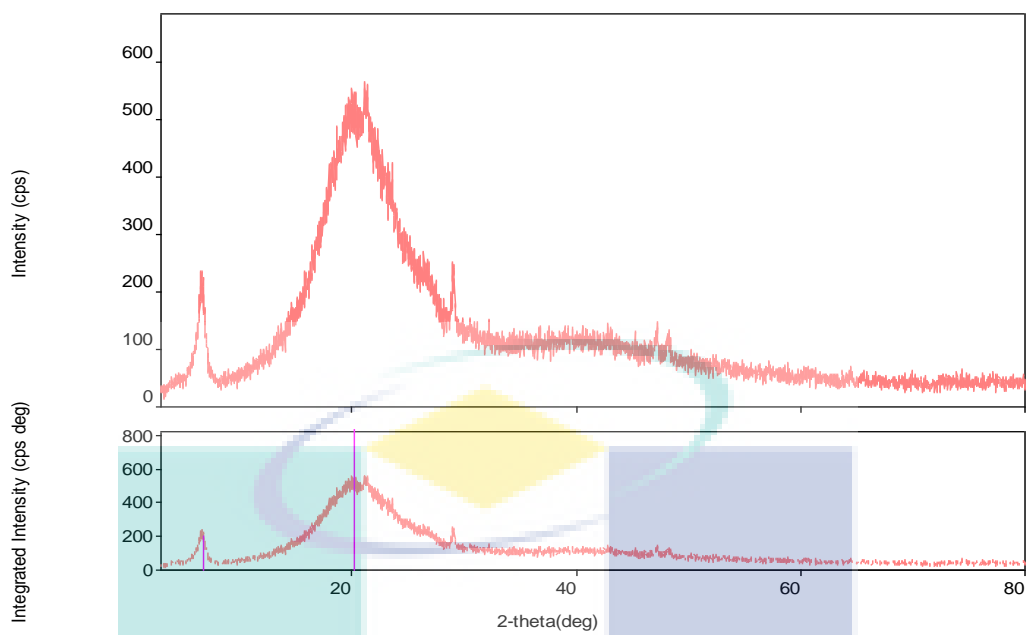


**Figure A2-11: X-RAY Diffraction of 1% PU-MMT Fe**

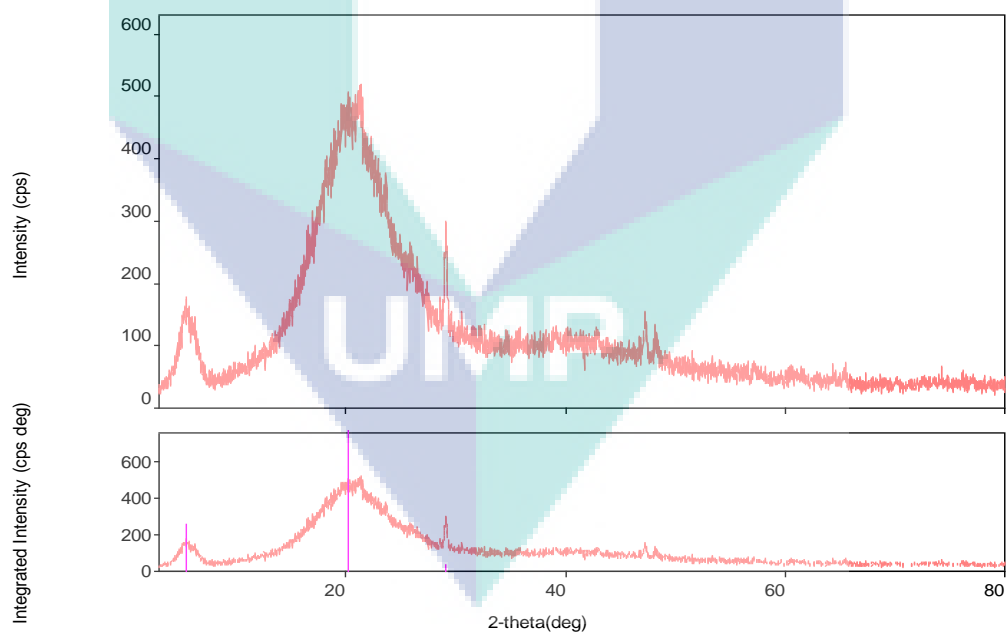


**Figure A2-12: X-RAY Diffraction of 2% PU-MMT Fe**

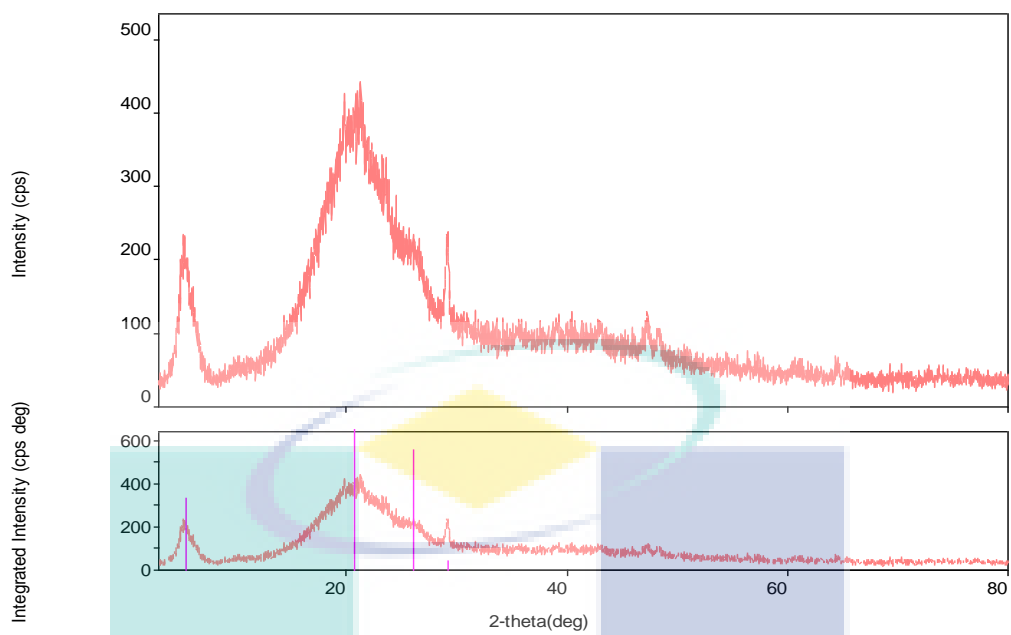


**Figure A2-13: X-RAY Diffraction of 3% PU-MMT Fe**

UMP

### A3 FOURIER TRANSFORM INFRARED SPECTROSCOPY

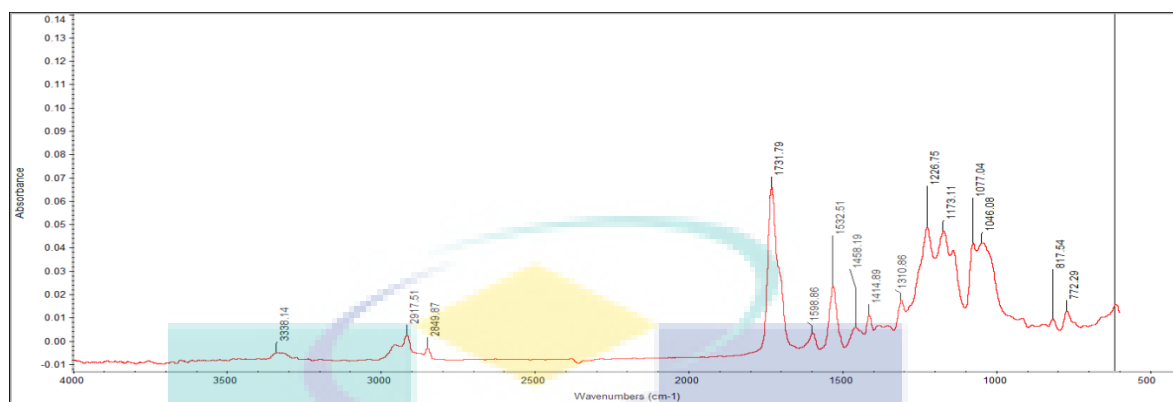


Figure A3-1: FTIR Spectroscopy of 1% PU-MMT

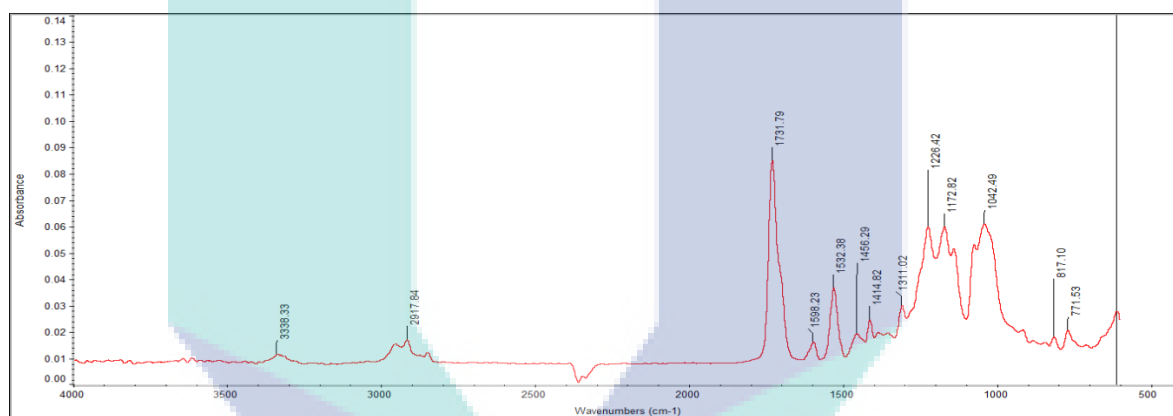


Figure A3-2: FTIR Spectroscopy of 2% PU-MMT

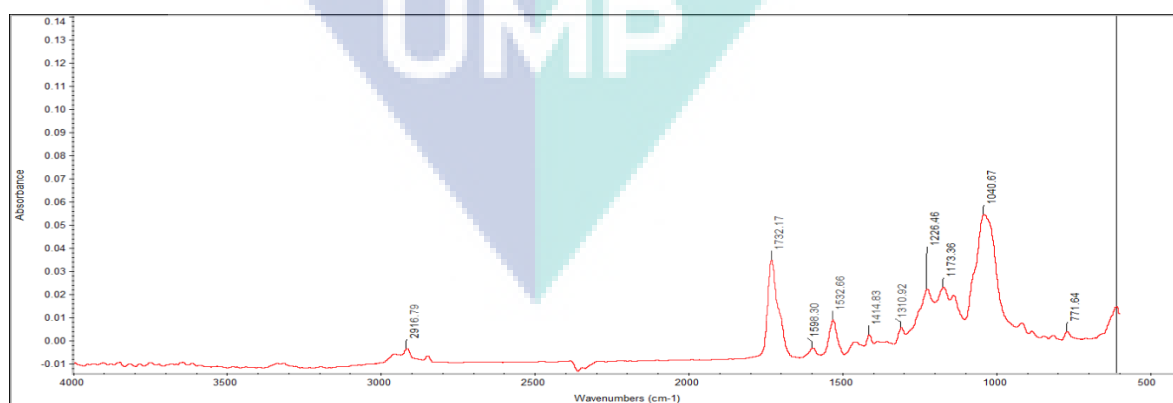


Figure A3-3: FTIR Spectroscopy of 3% PU-MMT

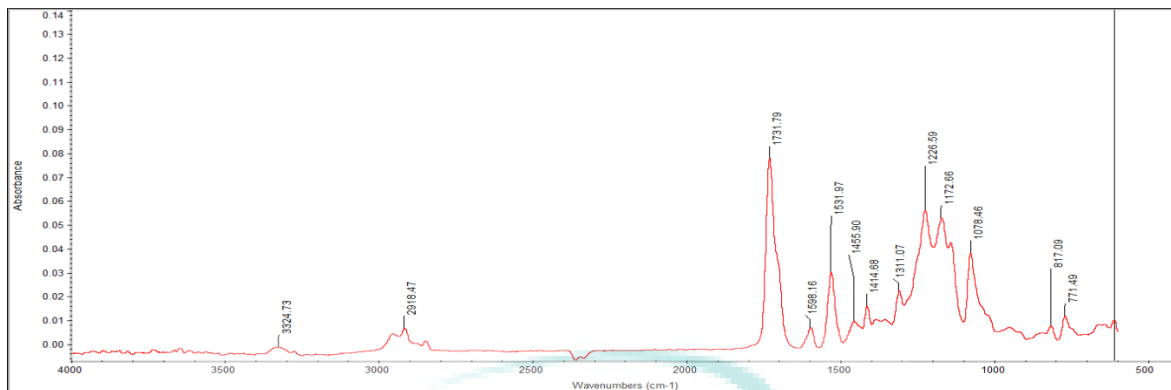


Figure A3-4: FTIR Spectroscopy of 1% PU-MMT Cu

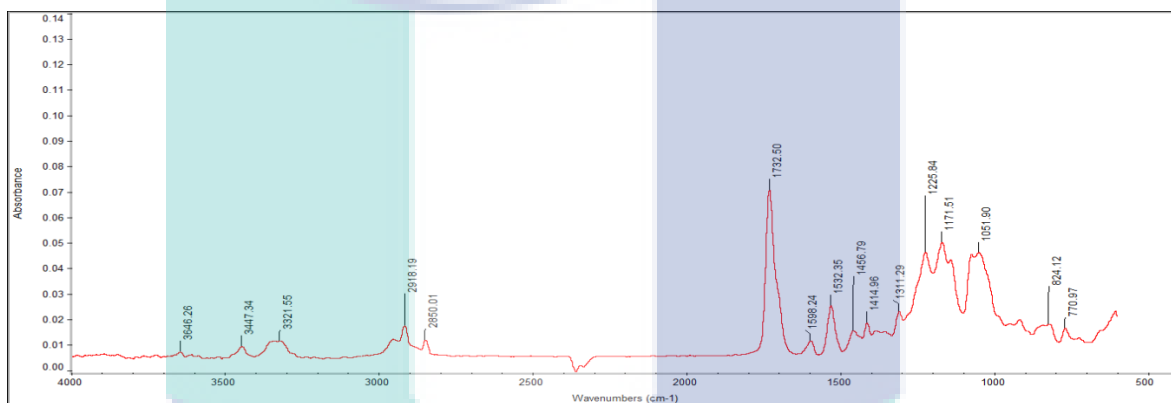


Figure A3-5: FTIR Spectroscopy of 2% PU-MMT Cu

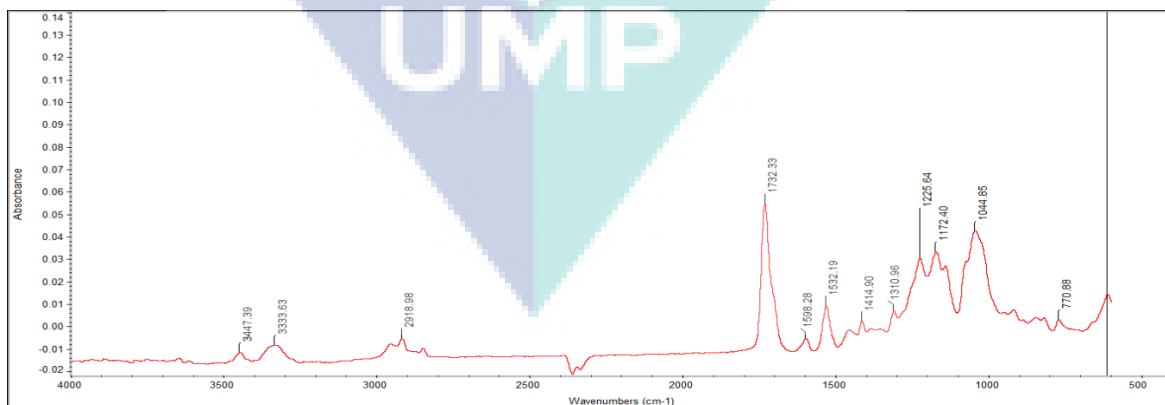


Figure A3-6: FTIR Spectroscopy of 3% PU-MMT Cu

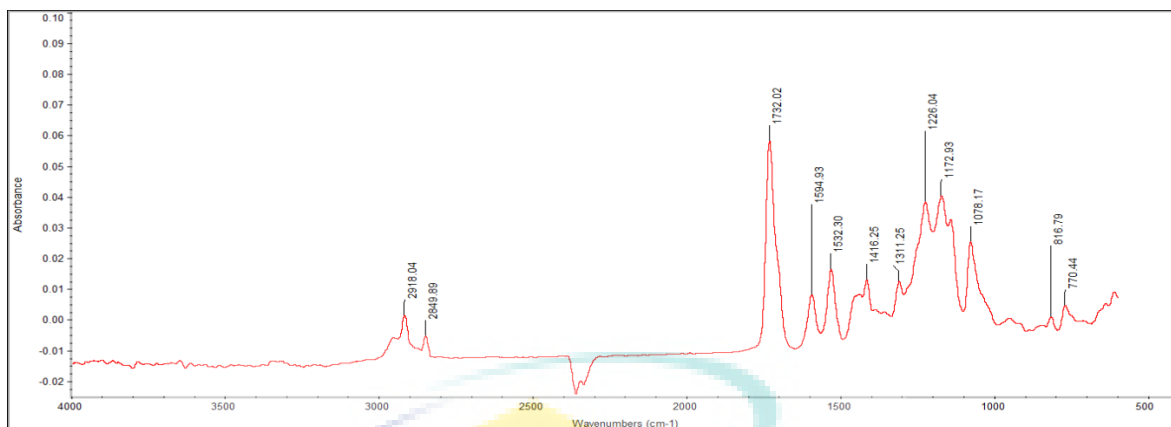


Figure A3-7: FTIR Spectroscopy of 1% PU-MMT Fe

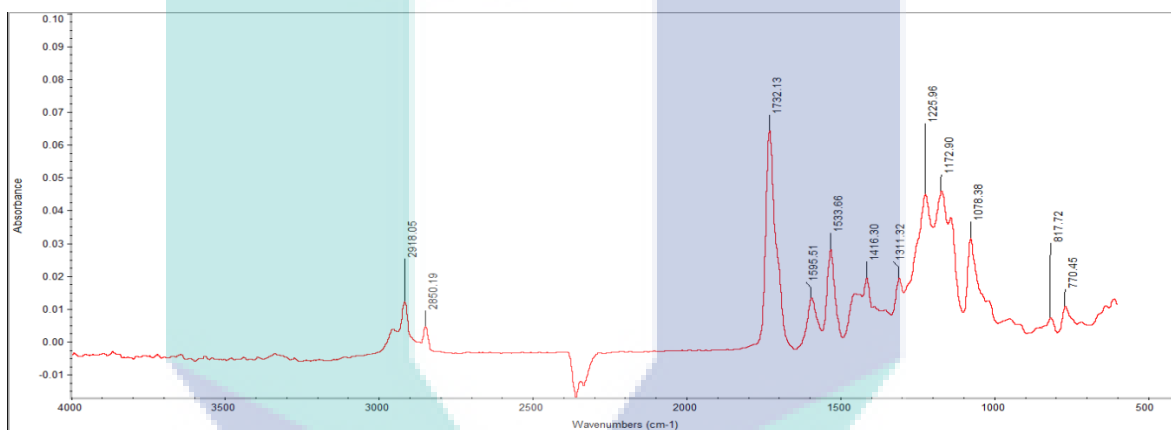


Figure A3-8: FTIR Spectroscopy of 2% PU-MMT Fe

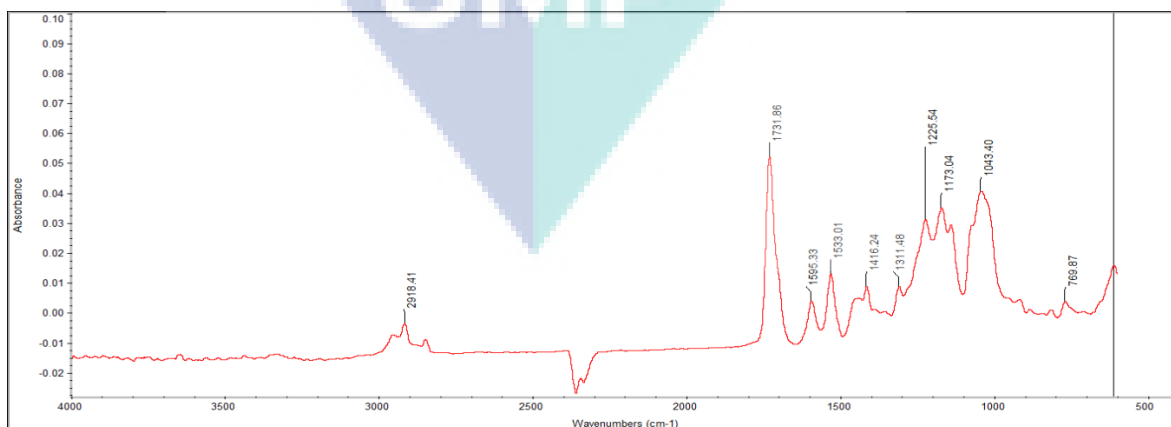
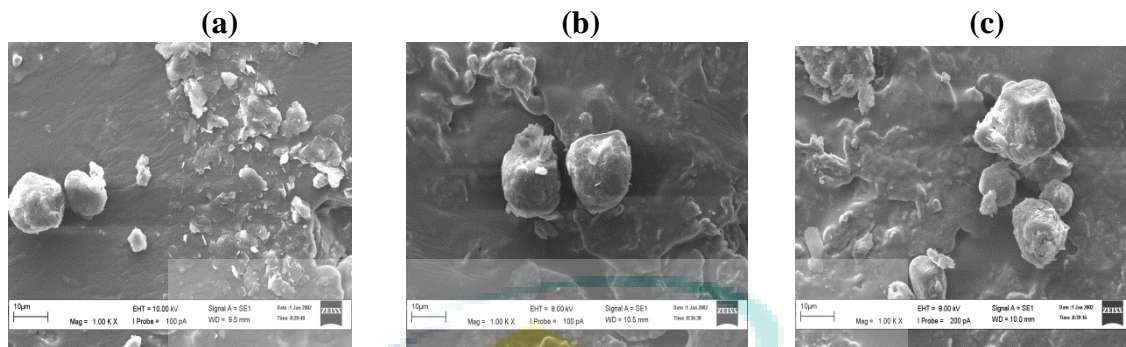
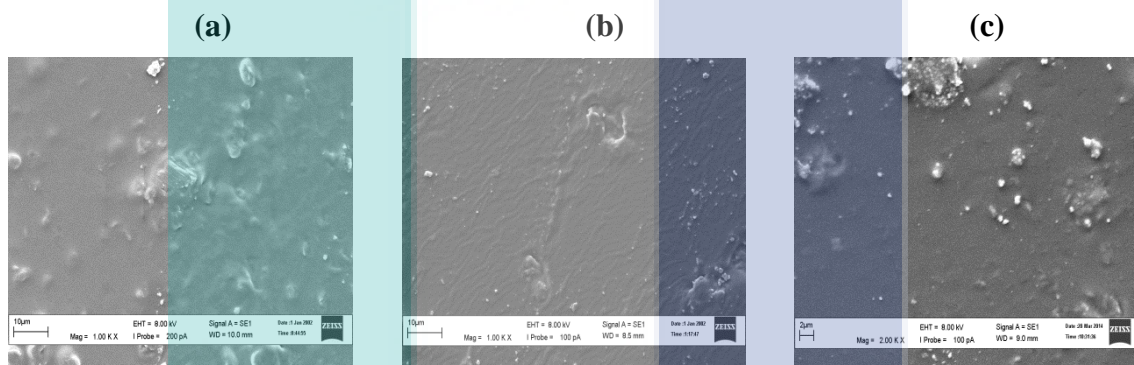


Figure A3-9: FTIR Spectroscopy of 3% PU-MMT Fe

**A4 SCANNING ELECTRON MICROSCOPE (SEM)**



**FIGURE A4-1: SEM Micrographs OF 1% (a) PU-MMT (b) PU-MMT Cu (c) PU-MMT Fe**



**FIGURE A4-2: SEM Micrographs OF 2% (a) PU-MMT (b) PU-MMT Cu (c) PU-MMT Fe**

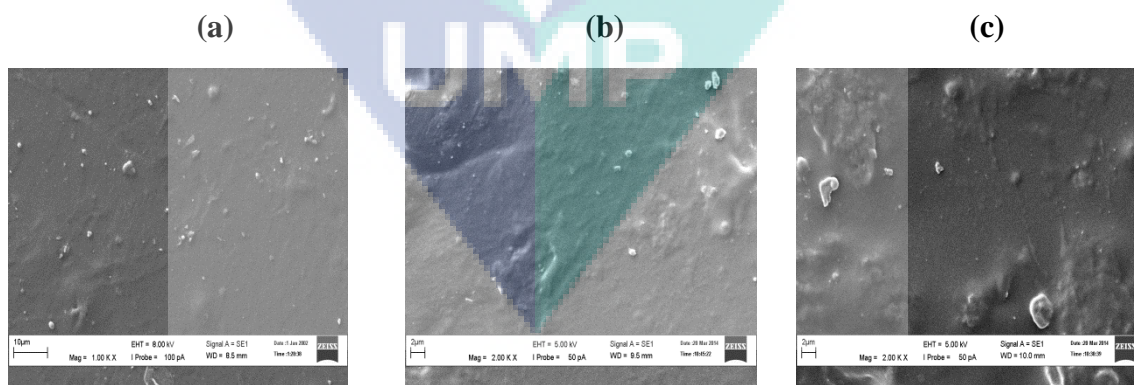


**FIGURE A4-3: SEM Micrographs OF 3% (a) PU-MMT (b) PU-MMT Cu (c) PU-MMT Fe**

**APPENDIX B**  
**MECHANICAL PROPERTIES**

**Table B-1:** Tensile stress values of the nanocomposites

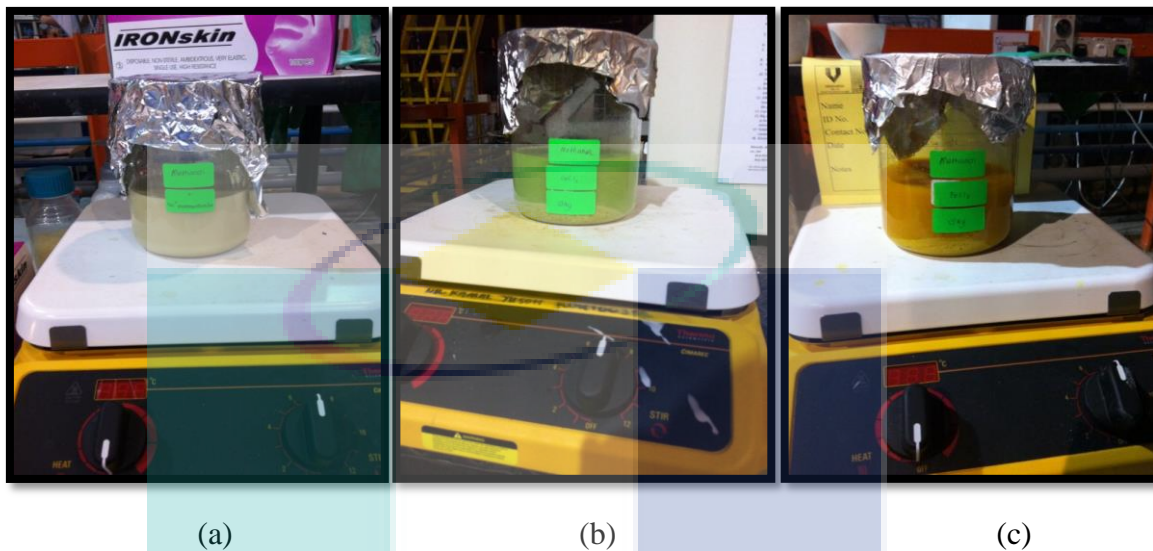
Sample	Tensile Stress (MPa)					
	1	2	3	4	5	6
PU	0.18	0.19	0.26	0.26	0.22	0.25
1% PU-MMT	0.27	0.26	0.29	0.31	0.27	0.38
2% PU-MMT	0.39	0.22	0.32	0.34	0.38	0.38
3% PU-MMT	0.41	0.23	0.31	0.43	0.27	0.28
1% PU-MMT Cu	0.62	0.45	0.64	0.67	0.45	0.30
2% PU-MMT Cu	0.35	0.42	0.58	0.52	0.43	0.44
3% PU-MMT Cu	0.62	0.66	0.64	0.45	0.42	0.42
1% PU-MMT Fe	0.44	0.42	0.41	0.52	0.53	0.29
2% PU-MMT Fe	0.31	0.48	0.32	0.34	0.66	0.43
3% PU-MMT Fe	0.40	0.32	0.53	0.45	0.48	0.44

**Table B-2:** Extension at break of the nanocomposites

Sample	Tensile Stress (MPa)					
	1	2	3	4	5	6
PU	1.72	2.14	1.56	1.80	2.67	1.89
1% PU-MMT	3.05	2.22	3.18	3.32	3.09	2.86
2% PU-MMT	3.03	3.76	2.37	3.51	3.01	3.82
3% PU-MMT	3.46	4.18	3.32	3.26	3.05	3.17
1% PU-MMT Cu	3.59	5.82	4.71	4.33	3.69	3.08
2% PU-MMT Cu	4.83	3.25	5.23	4.51	4.28	4.96
3% PU-MMT Cu	3.59	4.33	4.71	5.81	3.57	2.75
1% PU-MMT Fe	3.26	3.57	3.46	3.28	3.12	2.82
2% PU-MMT Fe	4.62	4.98	4.06	4.06	4.33	5.03
3% PU-MMT Fe	4.58	4.32	4.08	4.71	4.61	4.04



## APPENDIX C

MODIFICATION METHOD AND FABRICATION OF PU  
NANOCOMPOSITES

**Figure C-1:** (a) Washing process of MMT clay prior to TMI modification  
(b) TMI modification with copper (II) chloride  
(c) TMI modification with iron (III) chloride



**Figure C-2:** Filtration of clay using centrifugal pump



**Figure C-3:** Clay after being dried in oven following the TMI modification process

UMP



(a)



(b)



(c)



(d)

**Figure C-4:** (a) Mixing of pristine PU for 5 hours  
(b) Mixing of PU and MMT for 5 hours  
(c) Mixing of PU and MMT Cu for 5 hours  
(d) Mixing of PU and MMT Fe for 5 hours



(a)

(b)

**Figure C-5:** (a) Drying process of the PU nanocomposites (b) Films obtained

UMP

**APPENDIX D****LIST OF PUBLICATIONS****(a) Proceeding Papers**

Shamini Gunaseelan and Kamal Yusoh. 2013. Modification of montmorillonite using ion exchange method in polyurethane clay nanocomposites: Mechanical properties study. *8<sup>th</sup> CUTSE International Conference 2013*, 3 December 2013-4 December 2013.

Yusoh, K., Azizi, N. and Shamini, G. 2014. Mechanical and barrier properties of thermoplastic polyurethane clay nanocomposites for thermal insulation roofing materials. *International Conference on Nanotechnology, Nanomaterials and Thin Films for Energy Applications*. 19 February 2014-21 February 2014.

**(b) Journal Papers**

Shamini, G and Yusoh, K. 2013. Gas Permeability Properties of Thermoplastic Polyurethane Modified Clay Nanocomposites. *International Journal of Chemical Engineering and Applications*. 5(1): 64-68.

Shamini Gunaseelan and Kamal Yusoh. 2014. Mechanical and barrier properties of polyurethane modified nanoclay. *Iranian Polymer Letter* (in progress).



UMP